

Mechanical Engineering Department

NAAC-IQAC Contributions "Inculcation of Research Culture amongst the Students"

Academic Year	Number of students participated in National Conferences	Number of students participated in International Conferences	Number of papers published in peer reviewed journals by students	Number of students filed/published patents	Number of students participated in Project Exhibition	Achievement/Award
2018-2019	--	24	19	--	--	01
2019-2020	25	04	14	05	06	02

Number of students participated in International Conferences

A.Y. – 2018-19

Sr. No.	Name of the teacher	Title of the paper	Name of the conference	National / International	ISBN/ISSN number of the proceeding
1.	Nikhil V. Chavan, Rushikesh M. Bhagwat, Suraj S. Gaikwad, Shivam S. Shete	Fabrication & Characterization of Micro features on PMMA Using CO2 Laser Machining	International Conference on Budding Trends in Engineering and Technology	International	ISSN: 2349-9303
2.	Rahul C Kambale, Shubham Shahane Shriyash Patange, Makarand Burud	Design Development of Parabolic Trough Solar Concentrator for Water Heating	International Conference on Budding Trends in Engineering and Technology	International	ISSN: 2349-9304
3.	Hrushikesh Dhananjay Kulkarni Ashish Bhaskar Rasal Onkar Hemant Bidkar	Fabrication of Micro-Textures on Conical Shape Hydrodynamic Journal Bearing	International Conference on Budding Trends in Engineering and Technology	International	ISSN: 2349-9305
4.	Rupesh Bandgar, Sagar Bagewadi Sachin Kumbhare, Pravin Kachare	Fabrication of Compliant Mechanism for Micro Gripper using Photo Chemical Machining	International Conference on Budding Trends in Engineering and Technology	International	ISSN: 2349-9306
5.	RAakash Bawale, Somesh Burande Rajkumar Bile, Akash Jagtap	Fabrication and Characterization of Micro Channel Mold using CO2 LASER Machining	International Conference on Budding Trends in Engineering and Technology	International	ISSN: 2349-9307
6.	Rohan D. Gaikwad, Prashant N. Pawar, Kiran G. Gaikwad	Fabrication of Gear Lever Locker for Side Stand	International Conference on Budding Trends in Engineering and Technology	International	ISSN: 2349-9307

Fabrication & Characterization of Microfeatures on PMMA Using CO2 Laser Machining

**NIKHIL V. CHAVAN¹, RUSHIKESH M. BHAGWAT²,
SURAJ S. GAIKWAD³, SHIVAM S. SHETE⁴**

Department of Mechanical Engineering
SVERI's College of Engineering

SANDEEP S. WANGIKAR⁵

Department of Mechanical Engineering
Associate Professor,
SVERI's College of Engineering

Abstract— The micro-features are employed in a wide range of applications like Lab on a chip (LOC), micro Total Analytic Systems (μ TAS), Textured hydrodynamic bearings, Micro Heat Sinks, etc. The fabrication of microfeatures is a critical task. This paper focuses on the fabrication and characterization of micro features using CO2 Laser machining. The three micro feature shapes are considered in the study viz. circular, square, and hexagonal. The size of the microfeatures has been varied from 300 μ m to 1000 μ m with an interval of 100 μ m. The micro-features have been fabricated on polymethylmethacrylate (PMMA) material. The experiments have been performed to study the effect of process parameters (power, scanning speed) on the surface roughness and the dimensions. The characterization has been performed using RAPID I Vision 5 Microscope and Mitutoyo surface roughness tester.

Further, the straight channels also have been fabricated with a width varying from 300 μ m to 1000 μ m with an interval of 100 μ m. The characterization of the straight channels has been carried out. The fabricated channels are observed to be in agreement with the required dimensions. Thus, CO2 laser machining is capable of fabrication the straight channels and micro features which have a significant application for the fabrication of mold in soft lithography.

Index Terms— ADXL335, MAX30100, ARDUINO UNO, DHT11, ESP8266 Node MCU.

1.Introduction

The microfluidics has been evolved as a key technology in the areas like bio-engineering and analytical chemistry, etc. A microchannel is an essential and decisive component in Lab on a chip (LOC) LOC system. The microchannels are employed for mixing of reagents, delivery of reactant, fluidic control, physical particle separation, and cooling of computer chips. The microchannels when used for mixing generally termed as micromixers. The micromixers are of two types - active and passive. Active micromixers utilize external energy source for the mixing enhancement while in passive micromixers, different geometric shapes and fluid characteristics are effectively used (No external energy source). The flow in the microchannels is laminar, and hence the mixing depends upon diffusion only. Thus, the use of obstacles in the microchannels has significantly improved the mixing characteristics of microchannels. The obstacles are nothing but the micro-features provided along the length of the microchannel. The obstacles may be of various shapes viz. triangular, rectangular, square, circular, J shape, etc. [1],[2],[3]. The microfeatures are also useful in micro-texturing of a hydrodynamic journal bearing [4].

The microchannels are fabricated using different materials. One of the suitable and straightforward method of microchannels fabrication is soft lithography. For the soft lithography process, molds are required to be fabricated.

The most used materials in soft lithography are PMMA (Polymethylmethacrylate) and PDMS (Polydimethylsiloxane). The molds can be fabricated using different methods like wire-cut electric discharge machining, photochemical machining CO2 laser machining, etc. [5],[6],[7],[8]. Each approach has some advantages and limitations. Amongst these, CO2 laser machining is one of the easy and suitable methods for fabrication of microchannels molds on PMMA material. Laser cutting technology employs a laser to cut the materials. The laser beam is focused on the material, which then either burns, melts, or vaporizes away by a jet of gas, leaving an edge with a high-quality surface finish. In industries, the laser cutters are employed to cut different types of sheet material, structural and piping materials. The different studies on laser machining of polymer materials have been reported by various researchers for studying the machining performance [9],[10],[11].

The fabrication of micro-features is very critical. There is a good scope for fabrication of micro-features and channels using any non-conventional process. The fabrication of micro-features and straight channels on PMMA material using CO2 laser machining and its characterization is presented in this paper. The straight channels and microfeatures with eight different sizes from 300 μ m to 1000 μ m have been fabricated using CO2 laser machining.

2 MATERIAL AND METHODS

The material selected for fabrication of microchannel is Polymethylmethacrylate (PMMA) also called as Acrylic. This material is durable and stiff with excellent weather resistance, and the chemical formula is $C_5H_8O_2$. It has higher tensile and flexural strength. Its impact strength is about ten times more than glass [11]. PMMA has the highest surface hardness of all common thermoplastics and is also highly scratch resistant. PMMA is transparent, and it has good scope in microfluidic applications. Also, it is compatible with the soft lithography process. Therefore, for the fabrication of microfeatures and microchannels, PMMA material is suitable.

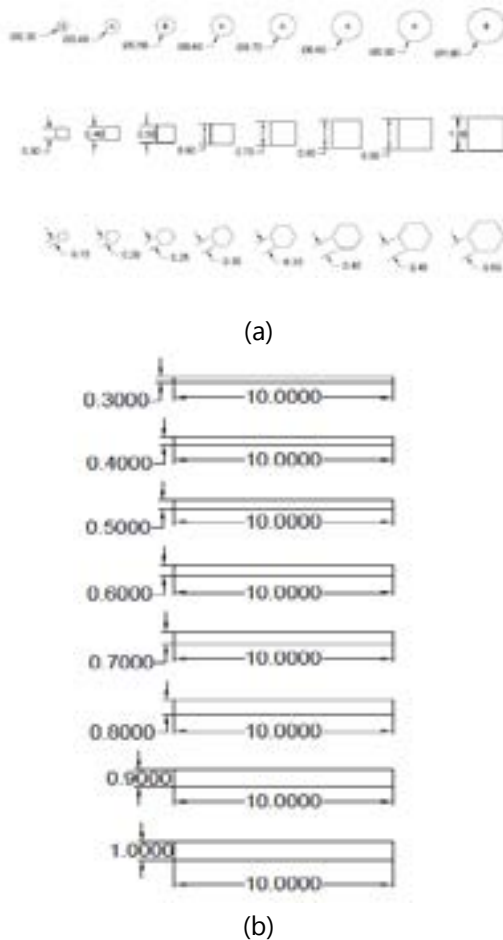


Figure 1: CAD Geometry for (a) Microfeatures (b) Straight channels

The design of the microfeatures and straight channels is made ready with the help of AutoCAD software. The different drawings for the straight microfeatures and microchannel geometries with different widths are depicted in Figure 1 (a). The size of the microfeatures is varied from 300 μm to 1000 μm with an interval of 100 μm . The width of the straight channels is also changed the same as for microfeatures. The geometries for straight channels is depicted in Figure 1 (b). These drawings are imported in the LASER cutting machine database. The laser cutting machine photograph is shown in Figure 2. The microfeatures and channels have been fabricated by varying the two process parameters, i.e. laser power and laser speed.

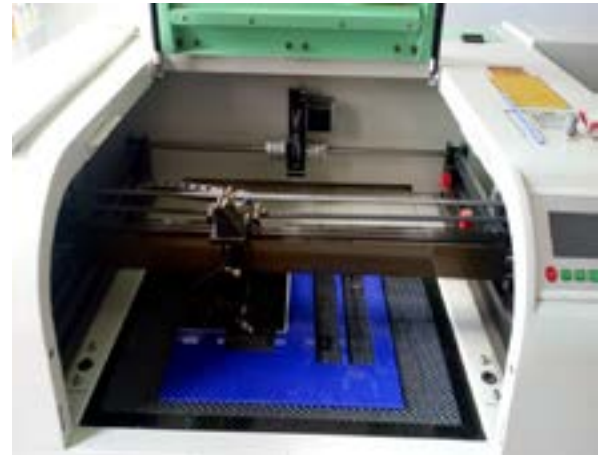


Figure 2: Laser Cutting Machine

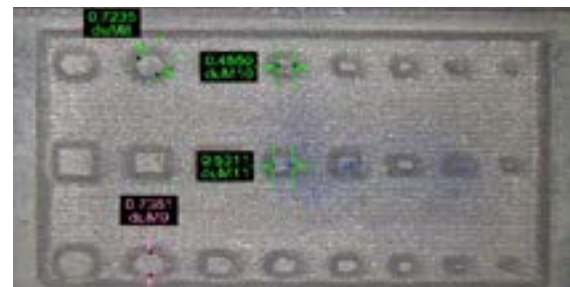
3 RESULT AND DISCUSSION

The laser machining has been performed on PMMA material for two different conditions for achieving different depths and surface conditions. The fabricated microfeatures on PMMA material are shown in Figure 3. The characterization for dimensions has been performed using RAPID I Vision 5 Microscope. The desired aspects for microfeatures are achieved using CO₂ Laser machining. It is observed that the microfeatures having a size greater than 500 μm are more accurate in dimensions as compared to the smaller ones.

The straight channels have also been fabricated using CO₂ Laser machining. The fabricated straight channels are shown in Figure 4. The characterization for dimensions has been performed using RAPID I Vision 5 Microscope. The required width has been achieved for straight channels.



(a)

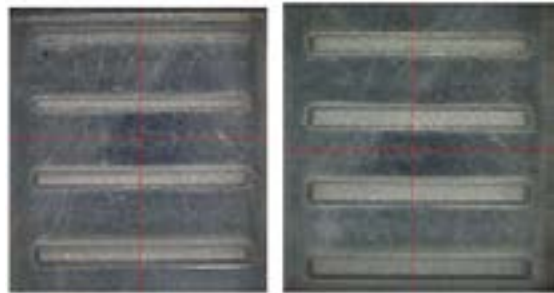


(b)

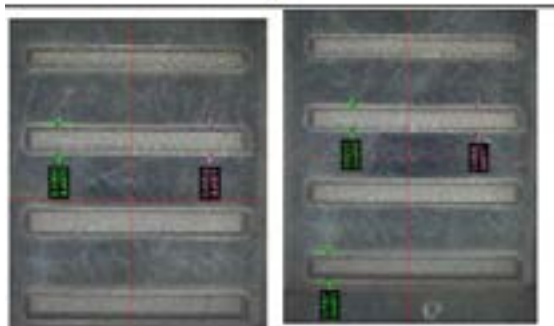


(c)

Figure 3: Fabricated Microfeatures



(a)



(b)



(c)

Figure 4: Fabricated Straight Channels

4. Conclusion:

The microfeatures and straight channels have been fabricated using CO₂ laser machining on the PMMA material. The three shapes of microfeatures as circular, square and hexagonal with different sizes from 300 μm to 1000 μm with a variation of 100 μm . The microfeatures are having a size greater than 400 μm are observed to be fabricated as per the required dimensions. The straight channels with a width from 300 μm to 1000 μm with a variation of 100 μm have been fabricated and are found to as per the required sizes. Thus, CO₂ laser machining is a good candidate for fabrication of microfeatures and straight channels on PMMA (acrylic) material.

5. References

- [1] S. S. Das, S. D. Tilekar, S. S. Wangikar, and P. K. Patowari, "Numerical and experimental study of passive fluids mixing in micro-channels of different configurations", *Microsystem Technologies*, Vol. 23(12), pp. 5977-5988, 2018.
- [2] S. S. Wangikar, P. P. Patowari, and R. D. Misra, "Numerical and experimental investigations on the performance of a serpentine microchannel with semicircular obstacles", *Microsystem Technologies*, vol 24, pp. 3307-3320, 2018.
- [3] R. R. Gidde, P. M. Pawar, B. P. Ronge, A. B. Shinde, N. D. Misal, and S. S. Wangikar, "Flow field analysis of a passive wavy micromixer with CSAR and ESAR elements", *Microsystem Technologies*, vol. 25, 2019.
- [4] A. Shinde, P. Pawar, P. Shaikh, S. Wangikar, S. Salunkhe, and V. Dhamgaye, "Experimental and Numerical Analysis of Conical Shape Hydrodynamic Bearing With Partial Texturing" *Procedia Manufacturing*, vol. 20, pp. 300-310, 2018.
- [5] S. S. Wangikar, P. P. Patowari, and R. D. Misra, "Parametric Optimization for Photochemical Machining of Copper Using Grey Relational Method", In *Techno-Societal 2016, International Conference on Advanced Technologies for Societal Application*, pp. 933-943, 2016.
- [6] S. S. Wangikar, P. P. Patowari, and R. D. Misra, "Effect of process parameters and optimization for photochemical machining of brass and German silver" *Materials and Manufacturing Processes*, vol. 32 no. 15, pp.1747-1755, 2017.
- [7] S. S. Wangikar, P. P. Patowari, and R. D. Misra, "Parametric optimization for photochemical machining of copper using overall evaluation criteria" *Materials Today: Proceedings*, vol. 5, no. 2, pp. 4736-4742, 2018.
- [8] S. S. Wangikar, P. P. Patowari, R. D. Misra, and N. D. Misal, "Photochemical Machining: A Less Explored Non-Conventional Machining Process", . In *Non-Conventional Machining in Modern Manufacturing Systems*, pp. 188-201, 2018.
- [9] S. Prakash and S. Kumar, "Pulse smearing and profile generation in CO₂ laser micromachining on PMMA via raster scanning," *Journal of Manufacturing Processes*, vol. 31, pp. 116-123, 2018.
- [10] H. Qi, T. Chen, L. Yao, and T. Zuo, "Micromachining of microchannel on the polycarbonate substrate with CO₂ laser direct-writing ablation," vol. 47, pp. 594-598, 2009.
- [11] I. A. Ā. Choudhury and S. Shirley, "Optics & Laser Technology Laser cutting of polymeric materials: An experimental investigation," *Optics and Laser Technology*, vol. 42, no. 3, pp. 503-508, 2010.

Design Development of Parabolic Trough Solar Concentrator for Water Heating

**RAHUL C KAMBALE¹, SHUBHAM SHAHANE²
SHRIYASH PATANGE³, MAKARAND BURUD⁴**

Department of Mechanical Engineering
SVRI's College of Engineering

BHASKAR D. GAIKWAD⁵

Department of Mechanical Engineering
Associate Professor,
SVRI's College of Engineering

Abstract— In this paper a survey of parabolic trough solar concentrator and its application for heating water is provided. Initially, an overview of environmental related problems to the use of conventional sources of energy is presented and benefits offered by renewable energy systems are outlined. An introduction of flat-plate collector and its characteristics are compared with parabolic trough solar collector, and the corresponding results are obtained for PTC. This is followed by an optical, thermal and thermodynamic analysis of the collectors and description of the methods used to evaluate their performance. A tracking system is used to track the sun rays so as to get the maximum intensity which would be used for a wide range of application and provide significant benefits, therefore, they should be used wherever possible.

Index Terms— Solar Energy, Parabolic Collector, Solar Collector.

1. Introduction

There are various renewable energy sources available like wind energy, solar, tidal, etc. Each of the energy source has its advantages and limitations. The use of wind energy using vertical axis and horizontal wind turbine for mechanical or electrical energy generation has been reported by many researchers [1-3]. The use of a solar thermal system for heating application is becoming popular day by day. The rising prices of fuel, as well as the effects of its usage on the environment, are the main concerns nowadays.

Parabolic trough collectors (PTCs) are currently the most feasible solar thermal technology for fluid heating since high temperature can be obtained without any decrease of the collector efficiency. The parabolic trough concentrator (PTC) converts solar energy into thermal energy in its linear receiver [4].

Flat-plate collector, Evacuated tube collector, Linear Fresnel reflector, cylindrical trough collector, parabolic trough collector have temperature application range of 30 – 800 C, 50 – 2000 C, 60 – 2500 C, 60 – 3000 C, 60 – 4000 C respectively [5].

PTC is contributing the 90% of the solar concentrators because this technology is the most usable among the concentrating collectors; it leads to lightweight structure systems and high-temperature range [6].

Htun et al. [7] designed a parabolic trough collector system for electricity generation through steam turbines. It is designed for 1 MVA capacity. Design calculation of absorbed flux, useful heat gain, and exit temperature are described. Sintali et al. [8], development of energy equations for computation of the efficiency of Parabolic-Trough Collector (PTC) using solar coordinates. The thermal efficiency of the PTC considered both the direct and reflected solar energy incident on the glass-cover

as well as the thermal properties of the collector and the total energy losses in the system. The developed energy equations can be used to predict the performance of any PTC using the meteorological and irradiative data of any particular location.

Figure 1 shows the different configurations of the solar collectors.

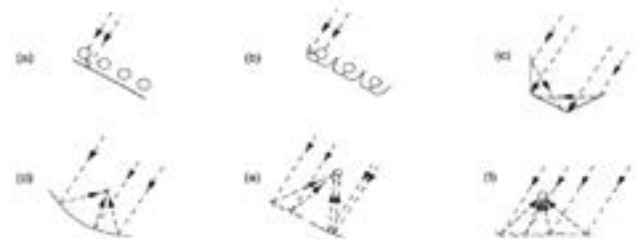


Figure 1 - Possible concentrating collector configurations: (a) tubular absorbers with diffuse back reflector; (b) tubular absorbers with specular cusp reflectors; (c) plane receiver with plane reflectors; (d) parabolic concentrator; (e) Fresnel reflector; (f) array of heliostats with central receiver [3].

Yaseen [9], performed an experimental and theoretical study has been conducted to determine the thermal efficiency of a parabolic trough solar collector. It has been found the experimental thermal efficiency of the collector is less than the theoretical one.

2 Terminologies in Parabolic Trough Collector

2.1 Concentration Ratio

It is the ratio of surface area of the collector to the surface area of the receiver tube.

2.2 Rim Angle

The angle between the optical axis and the line between the focal point and the mirror rim

2.3 Focal Length

The distance between the focal point and the vertex of a parabola is a parameter that determines the parabola completely.

3 Design and Specifications of Collector

This topic includes the selection of local and operating parameters, geometrical parameters, selection of rim angle, and construction of parabola and fabrication of parabolic trough collector. Table 1 shows the factors considered for parabolic trough collector design.

Table1
Factors considered for PTC design

Sr. No.	Parameters	Values
1	Average beaminsolation for a day	744W/m ²
2	Wind velocity	3 m/s
3	Flow rate of water	0.0013 kg/s
4	Average ambient temperature	30 °C
5	Area of the collector	0.5 m ²
6	Outlet water temperature required	65 °C
7	Orientation	N-S horizontal

Table 2 gives information about parameters selected for the construction of PTC. It includes a selection of the length of the trough, the width of a trough, rim angle, and receiver diameter. Parabolic trough collector with frame support

Table 2
Specifications of PTC

Sr.No.	Parameters	Value
1	Width of Aperture	600 mm
2	Length of Aperture	1 m
3	Focal Length	134 mm
4	Rim angle	90°
5	Outer Receiver Diameter	12.5 mm
6	Concentration Ratio	13.33
7	The material used for trough	M.S. sheet of 2mm thick coated with Aluminum foil.
8	Receiver	Copper tube
9	Rotameter	0 – 10 LPH

Figure 2 shows the geometrical construction of the parabola.

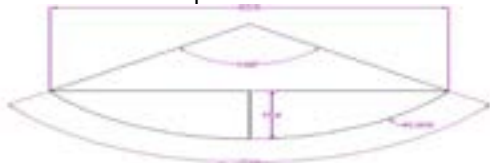


Figure 2 - Construction of Parabola.

The analytical relation between the focal length of the parabola and the width of the parabola is given by the below equation.

$$F / W = (1 + \cos Q) / (4 \sin Q)$$

Where F is the focal length of the parabola and width of the parabola. The geometrical concentration ratio is given by the following relation,

$$CR = (\sin Q) / \pi \sin Q$$

Q is the rim angle of the parabola. Figure 3 shows the variation of concentration ratio with the rim angle of the parabola.

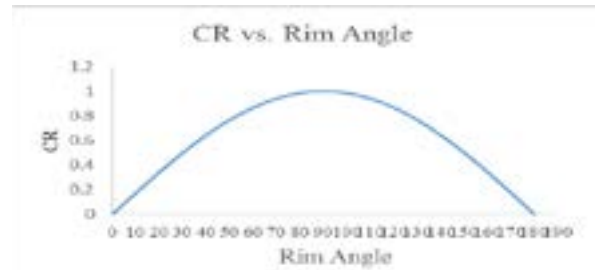


Figure 3 – Concentration Ratio vs. Rim Angle

It is desired to have higher concentration ratio for the collector. From figure 3 it can be observed that the rim angle of 90° has maximum concentration ratio. Therefore rim angle of 90° is selected for a parabola

4. Experimental Analysis

Figure 4 shows the schematic model of the parabolic trough with a uniform diameter for better performance. It consists of absorber pipe with uniform diameter & parabolic trough. The absorber is a copper pipe with a uniform diameter.



Figure 4 – Experimental Setup

5. Result and Discussion

This section discusses the results of parabolic trough solar collector with a uniform tube copper receiver and its characteristics. Readings were taken between 12.00 pm to 2.00 pm.

5.1 Effect of Mass Flow Rate on outlet Temperature

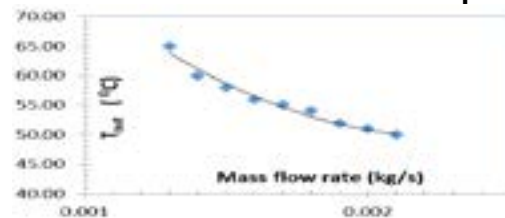


Figure 5 – Mass Flow Rate vs. Temperature

From figure 5 it can be observed that the mass flow rate of water is increased, the outlet temperature of the water is decreased. The maximum temperature of the water is found to be 65°C when the mass flow rate of water was 0.0013 kg/s.

5.2 Time versus outlet Temperature

The mass flow rate of the water was kept constant while conducting this test. The flow rate of 0.0013 kg/s. has given maximum outlet temperature of the water, therefore flow rate was kept equal to 0.0013 kg/s during the entire test. The performance of the collector depends on the time slot of the day, as the radiation from the sun to earth varies from time to time.

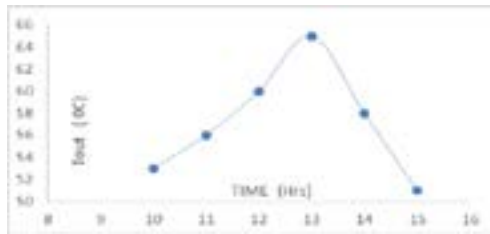


Figure 6 – Time hours vs. outlet temperature

From figure 6 it can be observed that the peak performance is achieved during the time period of 12 pm to 2 pm. It is obvious as during this period the light intensity is the highest.

5.3 Pipe Diameter vs. Outlet Temperature

Figure 7 shows the effect of the pipe diameter on the outlet temperature of the water. The pipes are available in standard size. 12 mm pipe has given the highest temperature when the flow rate was kept constant at 0.0013 kg/s.

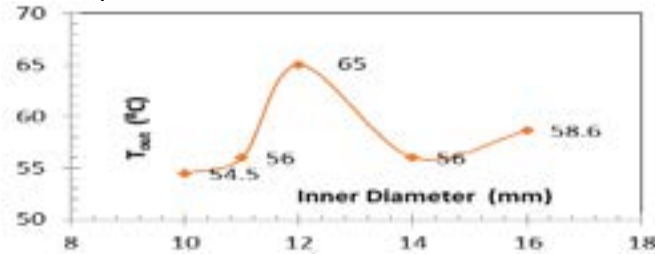


Figure 7 – Pipe diameter vs. outlet temperature

The output temperature of water first increases and then decreases. The maximum output temperature of the water is found to be 65 °C for absorber tube of inner diameter 12 mm and then correspondingly goes on reducing with an increase in diameter of the inner tube. The heat losses in the form of convection and radiation affected by the pipe size.

5.4 Temperature distribution along the length of the pipe.

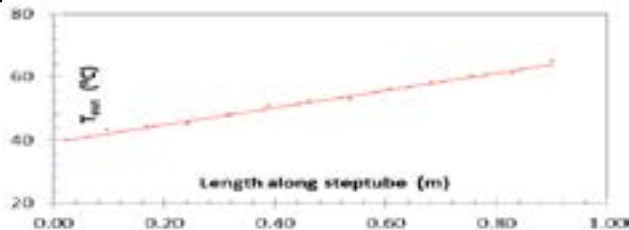


Figure 8 – Temperature of water along the length of the pipe

From figure 8, it is observed that the temperature of the water is increasing linearly along the length of the pipe.

7 Conclusion

In this study, a solar concentrator design has been installed. This equipment is based on a reflector plate and an absorber tube. The working fluid has achieved maximum temperature when the mass flow rate is kept as minimum as possible. While pipe size has a significant effect on the outlet temperature of the working fluid as the heat losses are governed by the size of the pipe.

Here the environmental factors are not taken into considerations as these are non-controllable factors. In reference to the various results and conclusion made above it is clear that by increasing the parabolic area the temperature of the fluid can be increased to a certain desired level

Acknowledgment

The authors wish to thank Dr. B. P. Ronge the principal of College of Engineering Pandharpur and Prof. B. D. Gaikwad the guide of the work to support this work.

References

- [1]S. S. Wangikar and N. D. Misal, "Effect of some design parameters on performance of a shutter type vertical axis wind turbine", In ASME 2012 Gas Turbine India Conference, GTINDIA 2012, 2012.
- [2]S. S. Wangikar, S. U. Jagtap, A. B. Tarmude, A. S. Pore, and S. P. Shinde, "Performance analysis of casement type vertical axis wind turbine," Inn ASME 2013 Gas Turbine India Conference, GTINDIA 2013, 2013.
- [3]V. R. Muttagi, S. S. Wangikar, S. S. Bhosale, and S. B. Bhosale, "Optimization of Process Parameters for Shutter Type Vertical Axis Wind Turbine" In Techno-Societal 2016, International Conference on Advanced Technologies for Societal Applications, Techno Societal 2016, 2016.
- [4]C. Tzivanidis, E. Bellos, D. Korres, K. A. Antonopoulos, and G. Mitsopoulos, "Thermal and optical efficiency investigation of a parabolic trough collector," Case Studies in Thermal Engineering, vol. 6, pp. 226-237, 2015.
- [5]S. A. Kalogirou, "Solar thermal collectors and applications", Progress in energy and combustion science, vol 30, no. 3, pp.231-295, 2004.
- [6]J. A. Duffie and W. A. Beckman, Solar engineering of thermal processes, John Wiley & Sons , 2013.
- [7]T. Htun, and M. T. Tun, "Design Calculation of Parabolic Trough Solar Thermal System and Three-phase Turbo Alternator", International Journal of Electrical and Computer Engineering vol. 5, no. 5, pp. 939-947, 2015.
- [8]I. S. Sintali, G. Egbo, and H. Dandakouta, "Energy equations for computation of parabolic-trough collector efficiency using solar position coordinates", American Journal of Engineering Research, vol. 3, no. 10, pp. 25-33, 2014.
- [9]T. A. Yassen, "Experimental and theoretical study of a parabolic trough solar collector", Anbar Journal for Engineering Sciences, vol. 5, no. 1, pp. 109-125, 2012.

Fabrication of Micro-Textures on Conical Shape Hydrodynamic Journal Bearing

HRUSHIKESH DHANANJAY KULKARNI¹, ASHISH BHASKAR RASAL²
ONKAR HEMANT BIDKAR³, VISHAL HANUMANT MALI⁴

SAGAR AUDUMBAR ATKALE⁵

Department of Mechanical Engineering
SVERI's College of Engineering

DR. SANDEEP S. WANGIKAR⁶

Department of Mechanical Engineering
SVERI's College of Engineering

Abstract—Hydrodynamic journal bearings are used for various applications in industries. These bearings are used to reduce the coefficient of friction and increase the load carrying capacity. For this, there is need to develop modified configurations of journal bearing to improve performance of bearing for high speed applications. The hydrodynamic bearings are of cylindrical or conical shape out of which the conical journal bearing is a good alternative. The micro irregularities on the surface of bearing are able to develop sufficient fluid film pressure and hence load carrying capacity. In this paper, an attempt has been made for fabrication of the micro textures (i.e. grooves) on the inner surface of the bearing using chemical machining process. The grooves are made on 90-degree portion on inner surface of the bearing. The radium paper is used as a maskant. The required grooves are made on radium paper and it is fixed on the bearing at the appropriate position. Ferric Chloride is used as etchant. The grooves are generated by chemical etching process. Further, the surface roughness is measured at the groove location. From the study, it is concluded that the micro textures on the inner surface of the bearings can be manufactured using chemical machining.

Index Terms— Conical hydrodynamic bearing, Micro-texturing, fabrication, chemical machining, radium paper.

1. Introduction

Hydrodynamic lubrication principle of hydrodynamic lubrication mechanism that is essential to the efficient functioning of the hydrodynamic journal bearings, which are used for various applications. The behavior of the contact is governed by the bulk physical properties of the lubricant, notably viscosity, and the frictional characteristics arise purely from the shearing of the viscous lubricant. Therefore, it becomes important to study the rheological properties of lubricants under various operating conditions such as temperature, pressure and shear rate. It is also important to understand tribology under various operating conditions and operating geometric arrangements. Bearing qualification is very much important before its use in the practical applications. However, in practice all standard journal bearings are tested for its dimensional accuracy and alignments during assembly, due to its simple construction. If the bearing is with complex geometry, it is difficult to measure dimensional accuracy and its need to study functional characteristics. Indirect way of measuring the bearing parameters are frictional coefficient and heat generation.

The performance of hydrodynamic journal bearing lubrication was analyzed by Hamilton et al. [1] and suggested that micro irregularities on the surface were able to develop sufficient fluid film pressure and hence load carrying capacity. The effect of cylindrical texture shape location on the performance characteristics of the hydrodynamic journal bearing was reported by Tala et al.

[3], [4], [5], [6], [7] have reported the work related to performance analysis of journal bearing, its optimization, use of micro texturing, etc. The fabrication of micro texturing on the inner surface of the bearing is also a crucial task. The micro texturing includes grooves, dimples or any other micro geometry on the inner surface. The micro texturing can be accomplished by different non-conventional machining processes. Photochemical machining and chemical machining are one of the most suitable candidates for fabrication of these micro features on hydrodynamic bearing. Different researchers have reported the parametric study for photochemical machining for different materials like copper, brass, german silver and use of photochemical machining for fabrication of micro channels [8], [9], [10], [11], [12], [13]. In this paper, the fabrication of micro textures on the conical hydrodynamic bearing using chemical machining is reported.

2. Material and Method:

The methodology for the work is presented in Figure 1. The material used for conical shape hydrodynamic bearing is stainless steel 410.

Machining:

The conical shaped hydrodynamic bearing is machined into required shape using turning operation for the stainless steel 410 material. The CAD drawing of the conical shaped hydrodynamic bearing is presented in Figure 2(a).

The surface roughness of the fabricated bearing is checked using Mitutoyo Surface Roughness Tester as demonstrated in Figure 2(b). The average surface roughness is observed as $0.78 \mu\text{m}$.

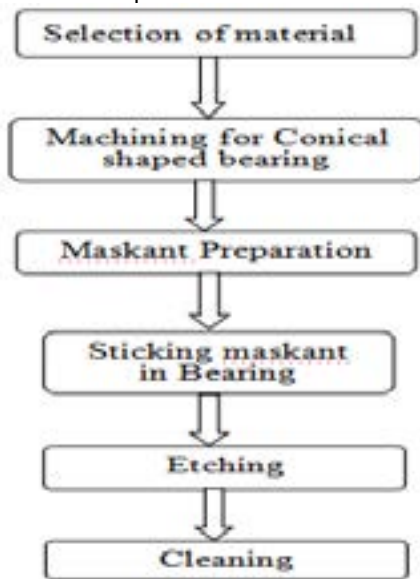
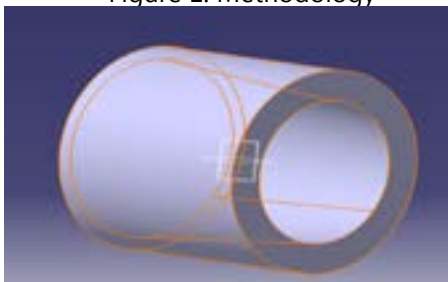


Figure 1: Methodology



(a)



(b)

Figure 2: (a) CATIA Image of conical shaped hydrodynamic bearing, (b) surface roughness measurement

Maskant Preparation and application on the bearing:

The maskant is prepared using radium paper. It is insoluble in the etchants like cupric chloride or ferric chloride. The radium maskant is prepared into required grooved texturing by using CO2 laser cutting machine. The AutoCAD drawing of grooved texturing is shown in Figure 3.

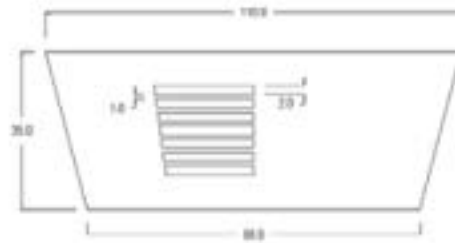


Figure 3: AutoCAD Drawing of Grooved Texturing



Figure 4: CO2 Laser Cutting machine



Figure 5: Grooved texturing on Radium Paper



Figure 6: Radium maskant applied on the inner side of the bearing

The CO2 Laser cutting machine set-up is presented in Figure 4 and the prepared Radium with grooved texturing is shown in Figure 5. The prepared radium maskant is further stuck at the required position on the inner side of the bearing as depicted in Figure 6.

Etching Process:

The ferric chloride is used as etchant. The bearing is wrapped with radium paper so that etching will be only for the selected for grooved texturing area (as shown in Figure 7). The etching set up with temperature control arrangement is demonstrated in Figure 8.



Figure 7: Bearing wrapped by radium-ready for etching



Figure 8: Etching set up

In this process material is removed from that area which is exposed to FeCl_3 solution. The etching time is kept as 15 minutes while the etching temperature is 55°C . After this etching process, the cleaning of bearing is done by using acetone solution.

3. Results and Discussion:

The fabricated grooves using chemical etching process is shown in Figure 9.



Figure 9: Bearing with grooved texturing



Figure 10: Surface roughness measurement for grooved texturing

The surface roughness is measured for the grooved texturing at all six locations using Mitutoyo Surface roughness tester (refer Figure 10). The average surface roughness is observed to be $1.11 \mu\text{m}$.

4. Conclusion

The microfeatures are fabricated on the inner surface of the conical shape journal bearing using a chemical etching process. The grooved micro texturing is first prepared on the radium maskant and further fabricated inside the hydrodynamic bearing etching process in which ferric chloride is used as etchant. The fabricated grooved micro texturing is observed to be in good agreement with the desired features as the drawing. The surface roughness is also measured and noted to be $1.11 \mu\text{m}$.

References

- [1]Hamilton D, Walowit J, Allen C. (1966) A theory of lubrication by micro-irregularities. Basic Eng.; 88:17
- [2]Nacer Tala-Ighil Michel Fillon, Patrick Maspeyrot. (2011) Effect of textured area on the performances of a hydrodynamic journal bearing. Tribology International 44 ; 211-219
- [3]Shinde, A.B. and Pawar, P.M., 2017. Multi-objective optimization of surface textured journal bearing by Taguchi based Grey relational analysis. Tribology International, 114, pp.349-357.
- [4]Shinde, A., Pawar, P., Shaikh, P., Wangikar, S., Salunkhe, S. and Dhamgaye, V., 2018. Experimental and Numerical Analysis of Conical Shape Hydrodynamic Journal Bearing With Partial Texturing. Procedia Manufacturing, 20, pp.300-310.
- [5]Shinde, A., Pawar, P., Gaikwad, S., Kapurkar, R. and Parkhe, A., 2018. Numerical Analysis of Deterministic Micro-Textures on the Performance of Hydrodynamic Journal Bearing. Materials Today: Proceedings, 5(2), pp.5999-6008.
- [6]Shinde, A.B. and Pawar, P.M., 2017. Effect of partial grooving on the performance of hydrodynamic journal bearing. Industrial Lubrication and Tribology, 69(4), pp.574-584.
- [7]Shinde, A.B., Pawar, P.M., Gaikwad, S., Shaikh, P.A. and Khedkar, Y., 2016, December. Analysis of Water Lubricated Bearing with Different Features to Improve the Performance: Green Tribology. In Techno-Societal 2016, International Conference on Advanced Technologies for Societal Applications (pp. 761-769). Springer, Cham.
- [8]Wangikar, S. S., Patowari, P. K., & Misra, R. D. (2017). Effect of process parameters and optimization for photochemical machining of brass and german silver. Materials and Manufacturing Processes, 32(15), 1747-1755.
- [9]Wangikar, S. S., Patowari, P. K., & Misra, R. D. (2018). Parametric optimization for photochemical machining of copper using overall evaluation criteria. Materials Today: Proceedings, 5(2), 4736-4742.
- [10]Wangikar, S. S., Patowari, P. K., & Misra, R. D. (2016, December). Parametric optimization for photochemical machining of copper using grey relational method.

- [10]In Techno-Societal 2016, International Conference on Advanced Technologies for Societal Applications (pp. 933-943). Springer, Cham.
- [11]Wangikar, S. S., Patowari, P. K., Misra, R. D., & Misal, N. D. (2019). Photochemical Machining: A Less Explored Non-Conventional Machining Process. In Non-Conventional Machining in Modern Manufacturing Systems (pp. 188-201). IGI Global.
- [12]Das, S. S., Tilekar, S. D., Wangikar, S. S., & Patowari, P. K. (2017). Numerical and experimental study of passive fluids mixing in micro-channels of different configurations. *Microsystem Technologies*, 23(12), 5977-5988.
- [13]Wangikar, S. S., Patowari, P. K., & Misra, R. D. (2018). Numerical and experimental investigations on the performance of a serpentine microchannel with semicircular obstacles. *Microsystem Technologies*, 24:3307, 1-14.

Fabrication of Compliant Mechanism for Micro Gripper using Photo Chemical Machining

**RUPESH BANDGAR¹, SAGAR BAGEWADI²
SACHIN KUMBHARE³**

Department of Mechanical Engineering,
SVERI's College of Engineering.

DR. NITIN D. MISAL⁵

Principal,
SVERI's College of Engineering (Polytechnic).

Abstract— Generally mechanism consists of links, joints, pairs, etc. and the force and power are transmitted by the relative motion of these parts of the mechanism. Due to the relative motion of joints, the friction occurs which leads to a deficiency in the force and power transmission. A compliant mechanism is a monolithic and joint less structure. So, it eliminates the problem of friction in the mechanism. The accurate transfer of force and power is significant while handling small size objects, sensors, assembly parts, etc. This paper is based on the development and fabrication of compliant mechanism by photo chemical machining (PCM) and their characterization. Initially, we drafted the drawing of compliant mechanism and created the photo tool of the same. Copper material was selected for the manufacturing of the mechanism. The required photo tools were generated on trace paper, and then the micro gripper was fabricated using photo chemical machining. Further, the characterization of fabricated micro grippers was performed using RAPID I Vision 5 Microscope. The error analysis of fabricated micro grippers was performed with respect to the photo tool dimensions, and the error is observed to be minimum. So, it is concluded that the micro grippers can be fabricated using PCM up to satisfactory level.

Index Terms— Compliant mechanism, Micro gripper, Photo chemical, RAPID I Vision 5 Microscope.

1. INTRODUCTION

The mechanism is a device which is used to transfer force, motion, and power. A conventional mechanism has rigid links which are connected to joint and forms a pair. This pair allows relative motion between the links. Due to the availability of joints in this mechanism, while transferring force, motion, and power, friction occurs at the joints, which result in the inaccurate transfer of inputs given to it. Moreover, the compliant mechanism is a monolithic structure and gains motion from the deflection of flexible members instead of the use of links, joints, and pairs. So, the problem of friction is eliminated with the use of this mechanism. Due to the absence of friction the compliant mechanisms give accurate and precise motion. Also, it possesses less wear and which results in less maintenance of mechanism [1]. The compliant mechanism is essential in the development and manufacturing of micro gripper. Because the micro grippers are handling the component having sizes in millimeters or microns where the characteristics of the compliant mechanism are very useful, also, the problem of handling of micro-optical and micro-electrical elements in Nano or micrometer range can be solved by using special micro gripper. Nowadays, the micro grippers are used in the wide varieties of fields like manufacturing industry, Electronics, Medical and Biological field, Material Research and in the assembly of Micro-Electro-Mechanical Systems (MEMS) [2].

The compliant mechanism is of smaller size, so for manufacturing of such mechanism, non-conventional machining processes are essential. There are various non-conventional machining methods which can be employed for manufacturing of compliant mechanism.

Also, PCM produces a burr free and stress-free flat complex metal component. The machining takes place using a controlled dissolution of work-piece material by contact with the strong chemical solution. Conventional machining tools often leave behind burrs or imperfection in the metal. These slight imperfection results in loss of uniformity that can be avoided with PCM. The heat and friction produced by conventional machining techniques can stress lighter metal alloys, resulting in deformation and affecting hardness or strength. The etchant used in PCM uniformly dissolves the metal in predefined areas. The cost of PCM is not impacted by the number of parts features or part complexity. This makes PCM most economical option for custom metal etching of thin metal parts with complex geometry. Tooling and setup cost for PCM is considerably lower than conventional methods.

Many researchers in the recent past have reported the studies related to photo chemical machining. The PCM for copper and copper alloys like brass and German silver has been performed by using ferric chloride as the etchant. The parametric optimization studies have also been reported for copper, brass and German silver. The effect of process parameters like concentration, temperature and etching time on the performances measures like material removal rate (MRR), the surface roughness (Ra), edge deviation (ED), etc. has been reported [3], [4], [5], [6]. The parametric optimization for PCM of different hard to cut materials like Inconel alloys have been carried out by researchers [7], [8], [9]. The PCM has also been employed for fabrication of micro features, micro channels [10], [11], [12] and can be used for micro features in hydrodynamic journal bearing [13].

From the above-reported literature, it can be noted that PCM can be effectively utilized for different materials like copper, brass, German silver and Inconel alloys, etc. The PCM is effectively utilized for the fabrication of micro channels and micro features. Very fewer studies have been reported for fabrication of compliant mechanism using PCM. So, there is a scope for manufacturing of compliant mechanism using PCM.

In this paper, an attempt has been for fabrication of compliant mechanism using PCM. The mechanism has fabricated on copper material. The characterization of the fabricated mechanism is performed using RAPID I Vision 5 Microscope.

2 METHODOLOGY

2.1 Material Selection

The copper material is used for this study. Copper is more elastic after gold and aluminum and which helps in compliant mechanism operations. The size of the specimen used is 25mm × 50mm × 0.5mm.

2.2 Experimental Procedure

The specimen surface is made clean to remove the burr, oxide layer, dust, etc. So, the photoresist can easily adhere to the surface.



Figure 1: Photo chemical machining Setup

The PCM setup is shown in Figure 1. The cleaning of the surface is carried out by polish paper and thinner (trichloroethylene or acetone) to remove traces of grease or oil. After cleaning the specimen was dipped out in the photoresist and dried it to get a layer of photoresist on the surface of the specimen. A photo tool is a negative film of the image which is needed to be produced, and it is generated by using the CAD drawing printed on the tracing paper. The photo tool drawing of selected compliant mechanism is demonstrated in Figure 2. The generated photo tool is put on the coated specimen and exposed to the ultraviolet source. The photoresist is sensitive to the ultraviolet radiation. After U.V. exposure the specimen is held in the developer. This will remove the unexposed area of the photoresist (Negative Film Method). After that, the specimen was washed with the water and dried it. The specimen is kept in the etchant with continuous heating that dissolves the metal chemically. The characterization of the process depends upon the parameters like temperature and dilution of the etchant.

1. Concentration (g/L) = 400

2. Temperature (°C) = 40

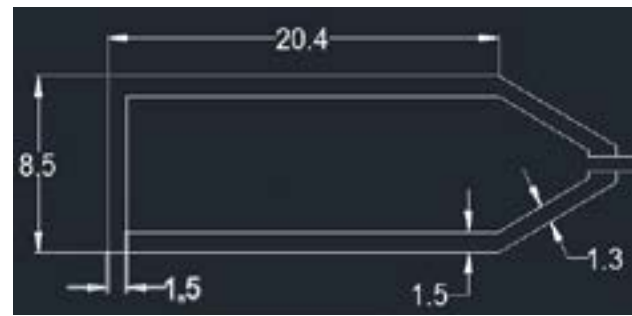


Figure 2: CAD Drawing of Photo tool

3 RESULT AND DISCUSSION

To get the exact size of the specimen by PCM process, it needs to provide some additional dimension on photo tool design of the product. So, the photo tool size is kept more than the actual size. There is some error in the desired dimension and actual dimension, and it is acceptable. So, the compliant mechanism can be manufactured by using the PCM process. The prepared photo tool is depicted in Figure 3. The characterization of photo tool is performed using RAPID I Vision 5 Microscope. The desired width of the mechanism is 1 mm. The average width for the photo tool is observed to be 1.3mm.

Using the prepared photo tool, the compliant mechanism is fabricated employing the PCM process. The fabricated compliant mechanism is shown in Figure 4. The characterization of the photo tool is performed using RAPID I Vision 5 Microscope. The average width of the fabricated compliant mechanism is 1.09 mm.

The comparative analysis for dimensions of a photo tool and fabricated compliant mechanism is carried out, and the error is calculated and presented in table 1. The average error is noted to be 0.12 mm.

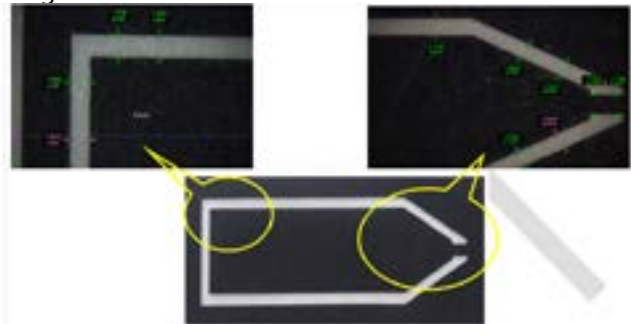


Figure 3: Characterization of the Photo tool

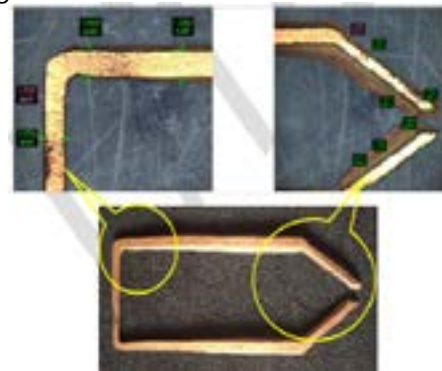


Figure 4: Characterization of fabricated Compliant Mechanism

TABLE 1
DIMENSIONAL ANALYSIS OF SPECIMEN

Sr. No.	Part Name	Desired Dimension (mm)	Photo tool Dimension (mm)	Actual Dimension (mm)	Error (mm)
1.	Gap between Jaws	1.5	1.7152	1.6667	0.1667
2.	Tapered Arm	1	1.2823	0.9833	0.0167
3.	Straight Arm	1	1.4762	1.0952	0.0952
4.	End Part	1	1.5438	1.1928	0.1928

4. CONCLUSION

Micro Electric Mechanical System or Micro systems is an emerging technology, and it has a significant potential to reshape human life patterns in the future. The micro gripper is playing an important role in handling of these micron sizes objects and to manufacture the micro gripper compliant mechanism is needed. The fabrication of compliant mechanism using PCM is carried out on copper material using ferric chloride as the etchant. The photo tool having an average width of 1.3 mm is prepared, and the compliant mechanism with an average width of 1.09 mm is fabricated using PCM. The error analysis for photo tool and the fabricated compliant mechanism is performed, and the average error is observed to be 0.12 mm.

REFERENCE

[1].L. L. Howell, Handbook of Compliant mechanisms, John Wiley & Sons, 2013.
 [2].B. Deshmukh and S. Pardeshi, "Study of various compliant micromechanism and introduction of a compliant micromotion replicating mechanism", International Journal of Mechanical Engineering & Technology, vol. 3 no. 3, pp.574-582, 2012.
 [3].S. S. Wangikar, P. P. Patowari, and R. D. Misra, "Effect of process parameters and optimization for photochemical machining of brass and German silver" Materials and Manufacturing Processes, vol. 32 no. 15, pp.1747-1755, 2017.
 [4].S. S. Wangikar, P. P. Patowari, and R. D. Misra, "Parametric optimization for photochemical machining of copper using overall evaluation criteria" Materials Today: Proceedings, vol. 5, no. 2, pp. 4736-4742, 2018.
 [5].S. S. Wangikar, P. P. Patowari, and R. D. Misra, "Parametric Optimization for Photochemical Machining of Copper Using Grey Relational Method", In Techno-Societal 2016, International Conference on Advanced Technologies for Societal Application, pp. 933-943, 2016.
 [6].S. S. Wangikar, P. P. Patowari, R. D. Misra, and N. D. Misal, "Photochemical Machining: A Less Explored Non-Conventional Machining Process", In Non-Conventional Machining in Modern Manufacturing Systems, pp. 188-201, 2018.

[4].S. S. Wangikar, P. P. Patowari, and R. D. Misra, "Parametric optimization for photochemical machining of copper using overall evaluation criteria" Materials Today: Proceedings, vol. 5, no. 2, pp. 4736-4742, 2018.
 [5].S. S. Wangikar, P. P. Patowari, and R. D. Misra, "Parametric Optimization for Photochemical Machining of Copper Using Grey Relational Method", In Techno-Societal 2016, International Conference on Advanced Technologies for Societal Application, pp. 933-943, 2016.
 [6].S. S. Wangikar, P. P. Patowari, R. D. Misra, and N. D. Misal, "Photochemical Machining: A Less Explored Non-Conventional Machining Process", In Non-Conventional Machining in Modern Manufacturing Systems, pp. 188-201, 2018.
 [7].N. D. Misal, and M. Sadaiah, "Investigation on Surface Roughness of Inconel 718 in Photo chemical Machining", Advances in Materials Science and Engineering, 2017.
 [8].N. D. Misal, A. R. Saraf, and M. Sadaiah, "Experimental investigation of surface topography in photo chemical machining of Inconel 718", Materials and Manufacturing Processes, vol. 32, no. 15, pp.1756-1763, 2017.
 [9].A. R. Saraf, N. D. Misal, and M. Sadaiah, "Mathematical modelling and optimization of photo chemical machining". In Advanced Materials Research, Vol. 548, pp. 617-622, 2012.
 [10].S. S. Ghadge, and N. Misal, "Design and analysis of micro-mixer for enhancing mixing performance", International Journal of Emerging Trends in Science and Technology, vol. 1, no. 08, pp.1342-1346, 2014.
 [11].S. S. Das, S. D. Tilekar, S. S. Wangikar, and P. K. Patowari, "Numerical and experimental study of passive fluids mixing in micro-channels of different configurations", Microsystem Technologies, Vol. 23 no. 12, pp. 5977-5988, 2018.
 [12].S. S. Wangikar, P. P. Patowari, and R. D. Misra, "Numerical and experimental investigations on the performance of a serpentine microchannel with semicircular obstacles", Microsystem Technologies, vol 24, pp. 3307-3320, 2018.
 [13].A. Shinde, P. Pawar, P. Shaikh, S. Wangikar, S. Salunkhe, and V. Dhamgaye, "Experimental and Numerical Analysis of Conical Shape Hydrodynamic Bearing With Partial Texturing" Procedia Manufacturing, vol. 20, pp. 300-310, 2018.

Mold using CO2 LASER Machining

RAAKASH BAWALE¹, SOMESH BURANDE²

RAJKUMAR BILE³, AKASH JAGTAP⁴

Department of Mechanical Engineering,
SVRI's College of Engineering.

AVINASH K. PARKHE

Assistant Professor,

Department of Mechanical Engineering

SVERI's College of Engineering (Polytechnic).

Abstract— Micro Channels are one of the most significant parts for Lab on a chip device. The fabrication of Micro Channels is a crucial task. Soft Lithography is one of the most favored methods of Micro Channel fabrication. The accuracy of the Micro Channel in the soft lithography process prominently depends on the molds. In this paper, an investigation on the use of a commercial CO₂ laser system for fabrication of micro-channel molds using Acrylic material has been reported. The depth of micro-channels is governed by the various process parameters, i.e. LASER power, scanning speed. The pilot experimentation is performed to analyze the effect of LASER power and scanning speed on the depth of the Micro Channel mold. It is observed that the channel depth is increasing linearly with increasing LASER power and noted to be decreasing with increase in speed. The straight Micro Channel configuration with Y shaped inlet having circular obstacles' (Split and Recombine approach, SAR) has been fabricated using CO₂ laser machining on Polymethylmethacrylate (PMMA) which can be used as a mold for the soft lithography process. The characterization of the fabricated Micro Channel mold has been performed using RAPID I Vision 5 microscope and Mitutoyo surface roughness tester.

Index Terms— CO2 LASER Machine, PMMA, Micro-Channel.

1. Introduction

Now a day's micro total analysis systems (μ TAS) plays significant role in many of the applications and Micro Channel is one of the prominent part of these systems. The Micro Channels are having applications in various fields like medical, diagnostics, chemical, biological, etc [1], [2], [3], [4]. The Micro Channels can be fabricated by using Acrylic material more economically and efficiently as compared to commercial materials like Silicon, Glass and Polymers, etc. Due to low cost and straight forward fabrication these Micro Channels are widely used in Medical and Engineering fields. There are various methods to fabricate the Micro Channels such as hot-embossing [5], [6] injection molding [7], micro milling [8], infrared laser ablation [9], Photo chemical machining [10], [11], [12], [13]. CO₂ laser machining is also a suitable option for fabrication of molds or direct Micro Channels. The use of CO₂ laser machining not only speeds up the fabrication process but also the high flexibility of changing the design. Thus, the CO₂ laser systems are very much useful for micromachining. In this paper, the Y shaped Micro Channel with straight and circular obstacles' configuration has been fabricated using the CO₂ laser machining with three different widths. The input parameters are also varied in order to achieve the different depths for the Micro Channel molds.

2. METHODOLOGY

The first step for manufacturing mold is preparation of 2D CAD drawings in AutoCAD software which acts as an input to the CO2 laser machining. The CO2 laser cut machining takes input as 2D CAD drawings in dxf format and it analyze the path of channel which is given in CAD drawing.

The drawings of the Y shaped Micro Channel molds with different configurations are shown in Figure 1. The material selected for the Micro Channel mold fabrications is acrylic (PMMA) because of its good surface finish property. The laser falls on the acrylic material and it cuts the acrylic material in given manner. Finally, the desired Micro Channel mold of required shape is fabricated on the acrylic material. The laser cut machining set up is as shown in Figure 2. The specifications of the Laser cut machine are given below:

- 1.Model- TIL6090
- 2.Laser Type Sealed Hermetic CO2 Laser Tube
- 3.Laser Power 60W/80W/100W
- 4.Engraving Area 600 x 900 mm
- 5.Accuracy± 0.025 mm
- 6.Power Supply220 V±10%/50HZ.
- 7.Gross Power1800 watt. aprx.
- 8.Cutting Speed 500 mm/S (Max)
- 9.Engraving Speed 500 mm/S (Max)

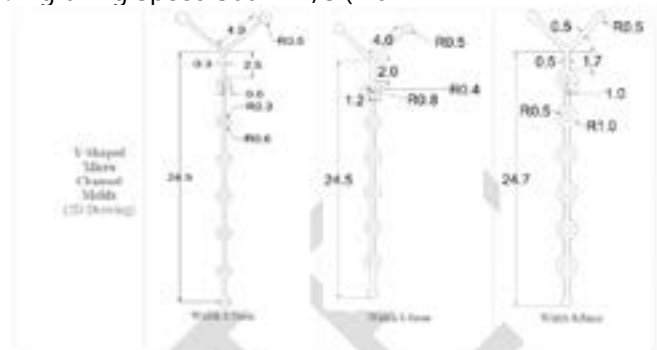


Figure 1: Y-Shaped Micro Channel geometries with different configurations

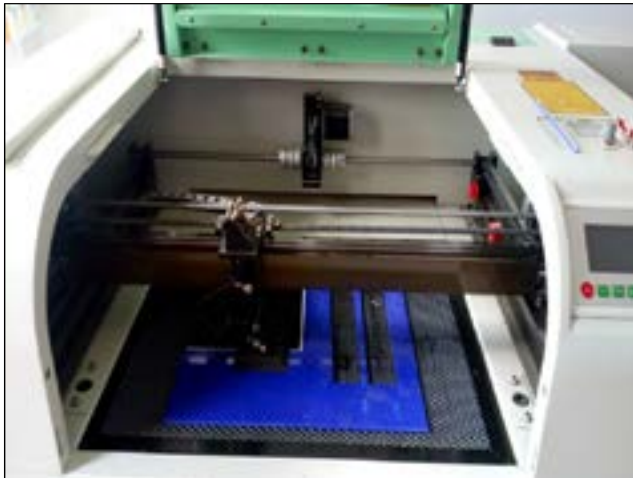


Figure 2: CO2 Laser cut machining set up

3. RESULT AND DISCUSSION

The laser machining has been carried out for the intended fabrication of Micro Channel molds on the acrylic material. The different parametric conditions have been employed for the fabrication of molds. The main parameters in laser cutting machining are laser speed and power. The width and depth of Micro Channel enhance with an increase in the laser power and the decrease of the moving velocity of the laser beam. When higher laser power and slower moving velocity have been used, the

bigger Micro Channel depth is observed to be fabricated. Observing the effect of the power on the depth and width of Micro Channels, higher aspect (depth/width) ratio could be achieved using slower moving velocity and higher laser power. The two different input parametric conditions have been used and the depths achieved have been recorded as 0.5 mm to 0.52 mm and represented in table 4.1. The fabricated Micro Channel molds on PMMA material are represented in Figure 3.

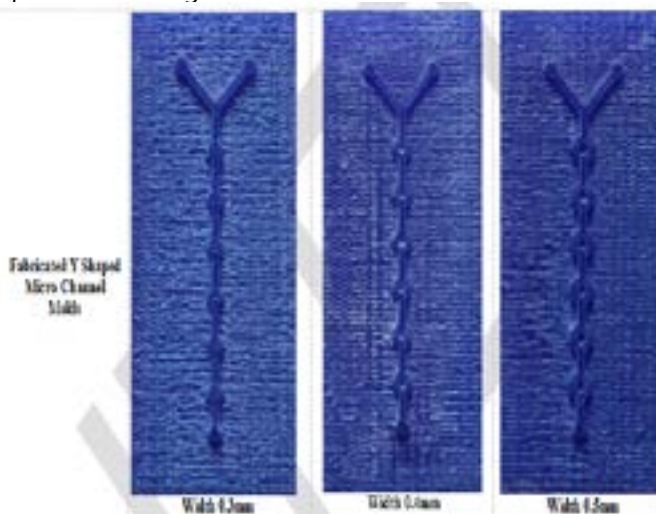


Figure 3: Y-shaped Micro Channel molds fabricated using CO2 laser machining

Table 1: Performance Parameters of LASER Machine

Width	Speed	No. of Pass	Power	Depth Achieved
0.3	100	1	60	0.505
	100	1	40	
0.4	100	1	60	0.519
	100	1	40	
0.5	100	1	60	0.516
	100	1	40	

5. CONCLUSION

The Micro Channels are major components required in Lab on a chip device. The fabrications of Y-shaped Micro Channels with different configurations like straight with circular obstacles' have been carried out using Laser cut machining. The molds are fabricated for three different widths and using two different parametric conditions. The depths recorded are as 0.5 mm and 0.52 mm. The fabricated molds can be employed for the fabrication of PDMS Micro Channels using soft lithography process. The study further can be extended for the parametric optimization of laser cut machining for fabrication of Micro Channels with different widths.

REFERENCES

- [1]. S. S. Das, S. D. Tilekar, S. S. Wangikar, and P. K. Patowari, "Numerical and experimental study of passive fluids mixing in micro-channels of different configurations", *Microsystem Technologies*, Vol. 23 no 12, pp. 5977-5988, 2018.
- [2]. S. S. Wangikar, P. P. Patowari, and R. D. Misra, "Numerical and experimental investigations on the performance of a serpentine microchannel with semicircular obstacles", *Microsystem Technologies*, vol 24, pp. 3307-3320, 2018.
- [3]. R. R. Gidde, P. M. Pawar, B. P. Ronge, N. D. Misal, R. B. Kapurkar, and A. K. Parkhe, "Evaluation of the mixing performance in a planar passive micromixer with circular and square mixing chambers", *Microsystem Technologies*, pp.1-12, 2017.
- [4]. R. R. Gidde, P. M. Pawar, B. P. Ronge, A. B. Shinde, N. D. Misal, and S. S. Wangikar, "Flow field analysis of a passive wavy micromixer with CSAR and ESAR elements", *Microsystem Technologies*, vol. 25, 2019.
- [5]. A. Gerlach, G. Knebel, A. E. Guber, M. Hecke, D. Herrmann, A. Muslija, and T. H. Sshaller, "Microfabrication of single-use plastic microfluidic devices for high-throughput screening and DNA analysis", *Microsystem Technologies*, vol. 7, no. 5-6, pp.265-268, 2002.
- [6]. L. Martynova, L.E. Locascio, M. Gaitan, G. W. Kramer, R. G. Christensen and W.A. MacCrehan, "Fabrication of plastic microfluid channels by imprinting methods" *Analytical chemistry*, vol. 69, no. 23, pp. 4783-9, 1997.
- [7]. O. Rotting, W. Ropke, H. Becker and C. Gartner, "Polymer microfabrication technologies", *Microsystem Technologies*, Vol. 8, pp.32-36, 2002.

- [8]. P. McKeown, "From micro to nano-machining-towards the nanometre era", *Sensor Review*, vol. 16, no. 2, pp. 4–10, 1996.
- [9]. H. Klank, J. P. Kutter and O. Geschke , "CO₂-Laser micromachining and back-end processing for rapid Production of PMMA-based microfluidic systems", *Lab on a Chip*, vol. 2 pp.242–6, 2002.
- [10]. S. S. Wangikar, P. P. Patowari, and R. D. Misra, "Parametric optimization for photochemical machining of copper using overall evaluation criteria" *Materials Today: Proceedings*, vol. 5, no. 2, pp. 4736–4742, 2018.
- [11]. S. S. Wangikar, P. P. Patowari, and R. D. Misra, "Parametric Optimization for Photochemical Machining of Copper Using Grey Relational Method", In *Techno-Societal 2016, International Conference on Advanced Technologies for Societal Application*, pp. 933-943, 2016.
- [12]. S. S. Wangikar, P. P. Patowari, and R. D. Misra, "Parametric optimization for photochemical machining of copper using overall evaluation criteria" *Materials Today: Proceedings*, vol. 5, no. 2, pp. 4736–4742, 2018.
- [13]. S. S. Wangikar, P. P. Patowari, R. D. Misra, and N. D. Misal, "Photochemical Machining: A Less Explored Non-Conventional Machining Process", In *Non-Conventional Machining in Modern Manufacturing Systems*, pp. 188-201, 2018

Papers published in Peer reviewed journals

A.Y. – 2018-19

Sr. No.	Title of Paper	Name of Author's	Name of Journal	ISBN/ISSN number
1.	Enhancement of Damping Force of Classical Hydraulic Damper into Semi Active Damper using MR Approach	Mane Shubham S., Abhangrao Chaitanya R., Kothawale Rajdeep R., Mete Akash R.	International Journal of New Technology and Research	ISSN 2454-4116
2.	Analysis of Weld Joint for SS 316 Material Using Taguchi Technique	Ankita A. Kashid, Pallavi M. Patil, Monika R. Olekar, Priydarshani V. Deshmane, Sonali S. Jadkar	International Journal of New Technology and Research	ISSN 2454-4116
3.	Improving Accuracy of Manual Crimping Operation through the Automation of Crimping Machine	Vishal M. Dhumal, Shivam R. Kanade, Samadhan U. Bandagar, Kiran S. Ghule	International Journal of New Technology and Research	ISSN 2454-4116
4.	Enhancement of Heat Transfer Coefficient through Forced Convection Apparatus by Using Circular and Elliptical Pipe	Ashish Shahane, Lakhan Ghodake	International Journal of New Technology and Research	ISSN 2454-4116
5.	Experimental Investigation of Natural Fiber with Epoxy Resin	Laxmikant D. Joshi, Amar A. Rajgole, Rahul Hiremath	International Journal of New Technology and Research	ISSN 2454-4116
6.	Study, Manufacturing and Analysis of Conveyor Chain Pin by using Composite Material	A.M. Khandekar, G.R. Mote, N.S. Vastre, S.A. Mosalg	International Journal of New Technology and Research	ISSN 2454-4116
7.	Computational Analysis of a Piezoelectrically Actuated Valve-less Micropump for Micro-fluidic Applications	Rohit D. Bankar, Ajay L. Godase, Ashok B. Mule, Nikhil N. Gaikwad	International Journal of New Technology and Research	ISSN 2454-4116

8.	Design and Development of a Pneumatic Car	Siddharam S. Warad, Sonal R. Swami, Akash V. Reshame, Rahul A. Hadapad, Virendra V. Mahajan	International Journal of New Technology and Research	ISSN 2454-4116
9.	Analysis of Crack on Aeroplane Wing at Different Positions using ANSYS Software	Hrushikesh N. Paricharak, Aditya A. Lotake, Sudhakar V. Mane, Darshan R. Gaikwad, Rushikesh H. Vastre	International Journal of New Technology and Research	ISSN 2454-4116
10.	Deformation Analysis of Wood Cutting Setup using ANSYS	Priyadarshani Gaikwad, Komal Gund, Kulsum Kazi, Bhairavi Fund	International Journal of New Technology and Research	ISSN 2454-4116
11.	Study of depth of etching in Photo Chemical Machining by colored Phototool	Sumit S. Khajepawar, Guruprasad V. Badave, Shubham S. Bhosale, Dnyanraj S. Telang	International Journal of New Technology and Research	ISSN 2454-4116
12.	Fabrication of Micro Channel Heat Sink by using Photo Chemical Machining	Mayuri A. Raut, Snehal S. Kale, Prajakta V. Pangavkar	International Journal of New Technology and Research	ISSN 2454-4116
13.	Fabrication of Micro Channel Mold by using CO2 Laser Machining	Mayur M. Jokare, Abhishek H. Vedpathak, Rajendra D. Pawar	International Journal of New Technology and Research	ISSN 2454-4116
14.	Comparative Stress Analysis of Connecting rod using ANSYS for Different Materials	Aditya A. Lotake, Shakir M. Mulani, Sohel M. Mulani, Rajratna D. Meshram	International Journal of New Technology and Research	ISSN 2454-4116

15.	Review on Solar Air Conditioning with Desiccant Wheel	Sunil S. Miskin, Onkar P. Dhudhane, Abhishek H. Vedpathak, Yogesh R. Barkul	International Journal of New Technology and Research	ISSN 2454-4116
16.	Experimental Analysis of Solar Dryer for Agricultural and Food Products	Kshitij Moholkar, Akshay Jadhao, Rohit Chavan, Ravindra Bhosale	International Journal of New Technology and Research	ISSN 2454-4116
17.	Design, Fabrication, and Analysis of Miniature Centrifugal Pump	Pankaj V. Patil, Digambar S. Pawar, Chetan S. Mote, Ashutosh B. Deshmukh	International Journal of New Technology and Research	ISSN 2454-4116
18.	Etching Depthvariation of Brass Material for Different Operating Conditions	Jadhav Saurabh M., Karatkar Onkar V., Bangale Kamesh N., Choudhari Deepak B.	International Journal of New Technology and Research	ISSN 2454-4116
19.	Design and Fabrication of Bench Top Injection Moulding Machine	Sachin Waghmare, Dadasaheb Maske, Pratik Waghmare, Vishal Bhosale	Global Journal of Engineering Science and Researchers	ISSN 2348-8034

Enhancement of Damping Force of Classical Hydraulic Damper into Semi Active Damper using MR Approach

Mane Shubham S., Abhangrao Chaitanya R., Kothawale Rajdeep R.,
Mete Akash R., Raut Laukik B.

Abstract— Vibration concealment can be considered as a standout amongst the most vital parameter influencing the execution of Mechanical structures and related security and solace. To diminish the framework vibration of such frameworks, a functioning vibration control system is required. the enhancement of damping force of classical hydraulic damper into semi active damper using MR approach is presented in this paper. The three unique liquids with iron particles volume division of 30%, 35 % and 40 % were set up in this investigation. It is seen that with increment in iron particles volume division and higher excitation current, damper execution improves. The damper set with thickest liquid experiences the issue of functionality at most reduced damping current. Among the 1 Degree of opportunity set utilized in this examination, the set with liquid YV2M2 with 35 % iron particles volume portion gives better execution usefulness perspective. The outcomes acquired from Damping power with MR Fluid and Magnetic Field is 40 percent more than Damping Force with customary Hydraulic Fluid.

Index Terms— Hydraulic damper, vibration, MR fluid.

I. INTRODUCTION

Magneto-Rheological dampers and the related devices have been under development for many years, but their commercial application started in late 2000A.D. in some expensive passenger vehicles. These Magneto-Rheological dampers fall under semi-active category. The Magneto-Rheological fluids, which are used in such devices, can change from liquid to semisolid when they come under the influence of magnetic field [1]. These damper have many benefits like, low cost of manufacturing, quick response, ability to change the viscosity in few milliseconds, fluids depend on the size of particles, properties of the carrier fluid used, additives and stabilizing agents used, applied magnetic field, operating construction, low operating power requirements and more effectiveness for vibration

Mane Shubham S., Mechanical Engineering Department, Student Of SVERI's College Of Engineering, Pandharpur, India
Abhangrao Chaitanya R., Mechanical Engineering Department, Student Of SVERI's College Of Engineering, Pandharpur, India
Kothawale Rajdeep R., Mechanical Engineering Department, Student Of SVERI's College Of Engineering, Pandharpur, India
Mete Akash R., Mechanical Engineering Department, Student Of SVERI's College of Engineering, Pandharpur, India
Raut Laukik B., Mechanical Engineering Department, SVERI's College Of Engineering, Pandharpur, India, (M.S.).

absorption The properties of temperature, concentration and density of particles, etc. Magnetic flux density generated in the damper due electric coil is proportional to the applied field [2]. Magnetic flux density generated in the damper due electric coil is proportional to the applied field.

The properties of the Magneto-Rheological suspension, the working mode (shear mode, flow mode or squeeze mode) and the design of the magnetic circuit consisting of Magneto-Rheological fluid, flux guide and coil considerably influence the properties of the actuator. The design of the magnetic circuit of a Magneto-Rheological fluid actuator is analyzed by finite-element-method. Yang et al. [3] presented a Magneto-Rheological damper design methodology, which was based on the magnetic circuit design according to the requirement of adaptive structure characteristics.

Cconformity of style throughout a conference proceeding. Margins, column widths, line spacing, and type styles are built-in; examples of the type styles are provided throughout this document and are identified in italic type, within parentheses, following the example. Some components, such as multi-leveled equations, graphics, and tables are not prescribed, although the various table text styles are provided. The formatter will need to create these components, incorporating the applicable criteria that follow.

II. METHOD TO PREPARE MAGNETO-RHEOLOGICAL FLUID

In this study, three different Magneto-Rheological fluids designated as YV1M1, YV2M2 and YV3M3 are prepared with 30%, 35% and 40% of volume fraction of iron particles. The ingredients required for the preparation of 200 ml of Magneto-Rheological fluid are as given in Table 1. The AP 3 grade Grease is first mixed in paraffin oil using mechanical stirred for about 20 minutes till the grease is dissolved in the oil completely. Then the oil is allowed to settle for about three hours. The iron particles are then added in the mixture of Grease and oil. This mixture is stirred for 15 to 20 minutes, until all particles get mixed in the oil completely[4].

Table 1: The details of ingredients

Details of ingredients	YV1 M1(30 %iron particles)	YV2 M2(35 %iron particles)	YV3M3 (40 %iron particles)
Low viscosity oil (Paraffin oil)	140 ml	130 ml	120 ml
Iron Particles(around 50 micron)	210.6 gm	245.7 gm	280.8 gm
AP 3 grease(12% of Oil weight)	14.1 gm	13.5 gm	12.09 gm

III. CALCULATION TO PREPARE MAGNETO-RHEOLOGICAL FLUID

The calculations of ingredients which are required to prepare 200ml of three different types of Magneto-Rheological fluids (YV1M1, YV2M2 and YV3M3) are as given below. The composition of the MR fluid preparation is referred from literature [5&6].

For YV1M1: (70% paraffin oil + 30% iron particles)

- 200ml of fluid X 70/100 of paraffin oil = 140ml of paraffin oil
140ml X specific gravity of low viscosity paraffin oil 0.84 = 117.6gm
- 117.6gm of paraffin oil X 12/100 = 14.1gm of AP3 grease
- 200ml of fluid X 30/100 of iron particles = 60 ml of iron particles
60 X 3.51 = 210.6gm of iron particles.

For YV2M2: (65% paraffin oil + 35% iron particles)

- 200ml of fluid X 65/100 of paraffin oil = 130ml of paraffin oil
130ml X specific gravity of low viscosity paraffin oil 0.84 = 109.2gm
- 109.2gm of paraffin oil X 12/100 = 13.1gm of AP3 grease
- 200ml of fluid X 35/100 of iron particles = 70 ml of iron particles
70 X 3.51 = 245.7gm of iron particles.

For YV3M3: (60% paraffin oil + 40% iron particles)

- 200ml of fluid X 60/100 of paraffin oil = 120ml of paraffin oil
120ml X specific gravity of low viscosity paraffin oil 0.84 = 100.8gm
- 100.8gm of paraffin oil X 12/100 = 12.09gm of AP3 grease
- 200ml of fluid X 40/100 of iron particles = 80 ml of iron particles
80 X 3.51 = 280.8gm of iron particles.

IV. MAGNETO-RHEOLOGICAL FLUID CHARACTERISTICS TESTING

The magnetic induction (H) and the flux density (B) of the above mentioned three types of Magneto-Rheological fluids are determined experimentally. The experimental set for the same, consists of an electromagnet, digital Gauss meter and sensor rod arrangement as shown in fig.1. The sensor probe was dipped in the cup having 30 ml Magneto-Rheological fluid and this arrangement was kept in the electromagnetic field generated by the coil.



Fig. 1: Experimental set up for Magneto-Rheological Fluid characterization

This experimental arrangement can be explained with the help of block diagram, as shown in Fig. 2. The current (I) of the coil is varied as 0.3, 0.6, 0.9, 1.2, 1.5, 1.8 and 2.1 Amperes. To vary magnetic induction (H) and flux density (B) is measured using sensor and digital gauss meter. The magnitude of magnetic induction and flux density for Magneto-Rheological fluids YV1M1, YV3M3 and YV2M2 are given in Tables 2, 3 and 4 respectively.

Table 2: Characteristics for YV1M1 (30% Fe particles)

	Current in Amp	Magnetic Flux Density (Tesla) 'B'	Magnetic induction (Amp/m) H
1.	0.3	109	9432
2.	0.6	210	18864
3.	0.9	343	28296
4.	1.2	464	37728
5.	1.5	560	47160
6.	1.8	624	56292
7.	2.1	654	66024

Table 3: Characteristics for YV3M3 (40% Fe particle)

Sr. No	Current in Amp	Magnetic Flux Density (Tesla) 'B'	Magnetic induction (Amp/m) H
1.	0.3	199	9432
2.	0.6	392	18864
3.	0.9	562	28296
4.	1.2	723	37728
5.	1.5	910	47160
6.	1.8	1065	56292
7.	2.1	1177	66024

Table 4: Characteristics for YV2M2 (35% Fe particles)

Sr. No	Current in Amp	Magnetic Flux Density (Tesla) 'B'	Magnetic induction (Amp/m)H
1.	0.3	130	9432
2.	0.6	258	18864
3.	0.9	400	28296
4.	1.2	554	37728
5.	1.5	681	47160
6.	1.8	785	56292
7.	2.1	856	66024

hydraulic damper is modified and filled with MR Fluid by varying volume fraction of oil and iron particles and it is tested in M/s Autoshox industry, Kolhapur

The experimental is carried out with damper with MR Fluid and damper with MR Fluid long with Magnet. [7]

During the experimentation, it is concluded that damping force increases when magnetic force increases and it is increased 40 percent more than that actual damper shown in Table 5.

Table 5: Actual testing and it results of YV3M3 (40% iron particle)

Damping Force With regular Hydraulic Fluid (Kg/s)	Damping Force With MR Fluid Without magnetic Field(Kg/s)	Damping Force With MR Fluid With Magnetic Field(kg/s)
26	26	40.1
27.5	25	38
27	25.5	40.3

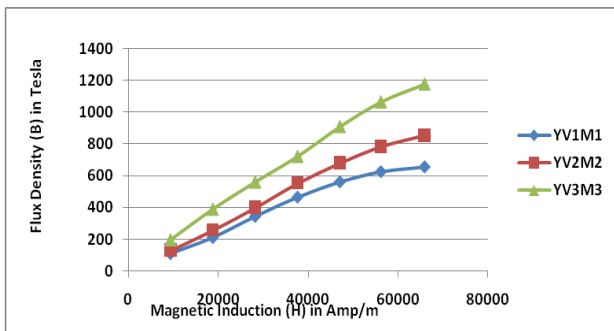


Fig. 2: B-H curve for YV1M1, YV2M2 and YV3M3

ENHANCEMENT OF DAMPING FORCE OF CLASSICAL HYDRAULIC DAMPER-



Fig. 3: Experimental Set up



Fig. 4: Experimental Set up with Magnet

The fig. 3 and 4 represents actual experimental setup for Enhancement of Damping Force of Classical Hydraulic Damper into semi active damper using MR Approach. The

V. CONCLUSION

Magneto-rheological characteristic of Magneto-rheological fluids is affected by the percentage of iron particles volume fraction in it. Hence, three different fluids with iron particles volume fraction of 30%, 35 % and 40 % were prepared in this study. From the B-H curves of these fluids, it is observed that, as the percentage of iron particles volume fraction increases in the Magneto-rheological fluid, the magnetic flux density value also increases for the same value of magnetic induction. The trend of Magneto-rheological fluid characteristics is very much similar to the results from the literature.

From this study, it is observed that with increase in iron particles volume fraction and higher excitation current, damper performance improves. However, the damper set with thickest fluid suffers from the problem of workability at lowest damping current. Among the 1 Degree of freedom set used in this study, the set with fluid YV2M2 with 35 % iron particles volume fraction gives better performance workability point of view.

To study the effect of Magneto-Rheological fluids and external permanent magnet arrangement in one degree of freedom set on force-displacement characteristics these combinations of damper set with three fluids are tested from this study it is observed that increase in iron particles volume fraction damper performance also improve. However the 1 dof set with Magneto-Rheological fluid YV3M3 suffer from the workability and in turn efficiency among the damper set used in this study set with gap and turn efficiency.

The results obtained from Damping force with MR Fluid and Magnetic Field is 40 percent more than Damping Force with regular Hydraulic Fluid.

REFERENCES

- [1] G. O. Young, "Synthetic structure of industrial plastics (Book style with paper title and editor)," in *Plastics*, 2nd ed. vol. 3, J. Peters, Ed. New York: McGraw-Hill, 1964, pp. 15–64.
- [2] W.-K. Chen, *Linear Networks and Systems* (Book style). Belmont, CA: Wadsworth, 1993, pp. 123–135.
- [3] H. Poor, *An Introduction to Signal Detection and Estimation*. New York: Springer-Verlag, 1985, ch. 4.
- [4] B. Smith, "An approach to graphs of linear forms (Unpublished work style)," unpublished.
- [5] E. H. Miller, "A note on reflector arrays (Periodical style—Accepted for publication)," *IEEE Trans. Antennas Propagat.*, to be published.
- [6] J. Wang, "Fundamentals of erbium-doped fiber amplifiers arrays (Periodical style—Submitted for publication)," *IEEE J. Quantum Electron.*, submitted for publication.
- [7] C. J. Kaufman, Rocky Mountain Research Lab., Boulder, CO, private communication, May 1995.
- [8] Y. Yorozu, M. Hirano, K. Oka, and Y. Tagawa, "Electron spectroscopy studies on magneto-optical media and plastic substrate interfaces(Translation Journals style)," *IEEE Transl. J. Magn.Jpn.*, vol. 2, Aug. 1987, pp. 740–741 [*Dig. 9th Annu. Conf. Magnetism Japan*, 1982, p. 301].
- [9] M. Young, *The Technical Writers Handbook*. Mill Valley, CA: University Science, 1989.
- [10] (Basic Book/Monograph Online Sources) J. K. Author. (year, month, day). *Title* (edition) [Type of medium]. Volume(issue). Available: [http://www.\(URL\)](http://www.(URL))
- [11] J. Jones. (1991, May 10). *Networks* (2nd ed.) [Online]. Available: <http://www.atm.com>
- [12] (Journal Online Sources style) K. Author. (year, month). *Title. Journal* [Type of medium]. Volume(issue), paging if given. Available: [http://www.\(URL\)](http://www.(URL))
- [13] R. J. Vidmar. (1992, August). On the use of atmospheric plasmas as electromagnetic reflectors. *IEEE Trans. Plasma Sci.* [Online]. 21(3). pp. 876—880. Available: <http://www.halcyon.com/pub/journals/21ps03-vidmar>

Analysis of Weld Joint for SS 316 Material Using Taguchi Technique

Ankita A. Kashid, Pallavi M. Patil, Monika R. Olekar,
Priyadarshani V. Deshmane, Sonali S. Jadkar

Abstract— The S.S 316 is a chromium-nickel-molybdenum austenitic stainless steel developed to provide improved corrosion resistance to S.S 304/304L in moderately corrosive environments. 316stainless steel is selected over other materials because of its distinct properties, cheaper cost and its availability in the market. 316stainless steel used is a boiler grade steel used in pressure vessels. Type 316 stainless steel is broadly used in application demanding corrosion resistance superior to Type 304, or good elevated temperature strength. Typical uses include exhaust manifolds, furnace parts, heat exchangers, jet engine parts, tanks, evaporators, paper and textile processing equipment.. The addition of molybdenum improves general corrosion and chloride pitting resistance. TIG welding is most popular method for welding of stainless material. SS316 is commonly used for producing milk silo in dairy industry. The objective behind this research is to optimize process parameter and to determine the influence of process parameter on the quality of weld. Welding current and Gas flow rate is process parameter selected for experimental work. In this research Taguchi method is used to optimize welding current and Gas flow rate. In this project work, X-ray radiographic test has been conducted in order to detect surface and subsurface defects of weld specimens made of SS 316 austenitic stainless steels. Effect of current, gas flow rate and metal plate thickness on quality of weld in metal inert gas arc welding of SS316 austenitic stainless steel has been studied in the present work through experimental analysis. Butt welded joints have been made by employing different levels of gas flow rate, current, and plate thickness. The quality of the weld has been assigned in terms of yield strength, ultimate tensile strength and percentage elongation of welded specimens. The observed data have been interpreted, discussed and analyzed using Taguchi methodology.

Index Terms— Weld Joint, Taguchi Technique .

I. INTRODUCTION

GTAW or TIG welding process is an arc welding process adopt a non consumable tungstenelectrod. For producing the weld, the are of weld is protected from atmosphere with a shielding gas generally Argon or Helium or sometimes mixture of Argon and Helium. A filler metal may also supply with material manually for proper welding. GTAW most commonly called TIG welding process was developed during

the Second World War.

With the development of TIGwelding process, welding is difficult to weld materials e.g. Aluminium and Magnesium becomes possible. The use of TIG today has spread variety of metals like stainless steel, mild steel and high tensile steels, Al alloy, Titanium alloy. Like other welding system, TIG welding power sources have also improved from basic transformer types to the highly electronic controlled power sourcetoday. This type of weld also allows for intricate detailing, which is an important consideration in custom iron – especially in designs that have ornate scrolls and other design elements. Other welding techniques leave slag behind, and this has to be cleaned up and removed before the design can be completed. This method, however, generally leaves no slag behind, which means fabricator can spend more time on creating design, rather than cleaning up messy welds. Taguchi involves using orthogonal arrays to order the parameters affecting the process and the levels at which they should be varied. This allows for collection of the required data to determine the factors which are mainly affect s on the product quality with minimum amount of experimentation, thus it saving time and resources. The Taguchi method is used when there are intermediate number of variables (3 to 50), few interactions between the variables, and when only a few variables contribute remarkable. A large number of experiments were to be carried out when the number of process parameters are increase. To solve this problem, the Taguchi method is uses a special design of orthogonal arrays for studying the entire parameter space with only a minimum number of experiments. Three parameters are to be considered as controlling factors, that are welding current, gas flow rate and material thickness. Each parameter having three levels viz. low, medium and high, normally denoted by 1, 2 and 3, respectively. According to the Taguchi method, if three parameters and 3 levels for experimentation, L9orthogonal array should be employed for the experimentation. In this work L9 orthogonal array is sufficient to predict the required results. It would require total 27 experiments to enhance the parameters.

A. Basic mechanism of TIG welding:

TIG welding is arc welding process which uses a non-consumable tungsten electrode to produce the weld on the component. The weld area is protected from atmosphere by providind an inert shielding gas (helium or argon), and a filler metal is usually employed. The power is supplied from source of power (rectifier), through a welding torch and is delivered to a tungsten electrode. An electric arc is further generated between the work piece and tungsten electrode

Ankita A. Kashid, Mechanical Engineering, SVERI's College of Engineering Pandharpur.

Pallavi M. Patil, Mechanical Engineering, SVERI's College of Engineering, Pandharpur

Monika R. Olekar, Mechanical Engineering, SVERI's College of Engineering Pandharpur

Sonali S. Jadkar, Mechanical Engineering, SVERI's College of Engineering

Priyadarshani V. Deshmane, Mechanical Engineering, SVERI's College of Engineering Pandharpur

using a constant-current welding power supply which produces energy and conducted across the arc through a highly ionized gas and metal vapours. The electric arc can produce temperatures up to 20,000°C and this heat can be focused to melt and join two different parts of material. The schematic diagram of TIG welding and mechanism of TIG welding is as shown in below fig. 1

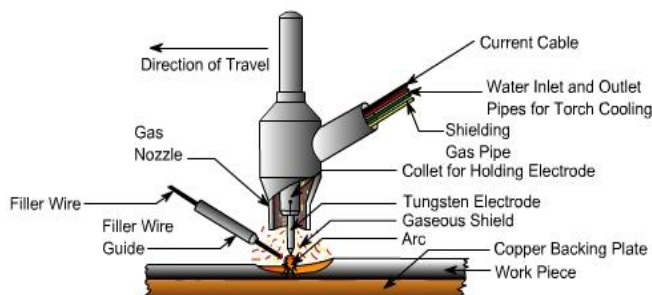


Fig 1 schematic representation of TIG welding [1].

B. General Information of SS-316

Table 1 :Technical Information of SS-316[1].

Alloy	UNS Number	SAE Number
316	S31600	30316

Types 316 and 316L are more resist to atmospheric and other mild types of corrosion as compared to the 18-8 stainless steels. Type 304 stainless steel is considered to resist the pitting and crevice corrosion in waters containing up to about 100 ppm chlorides At temperature as high as 120° F (49° C), Type 316 is more resistant to concentration of this acid up to the 5 percent. At temperature range under 100° F (38° C), this type has higher resistance to higher concentrations. Where condensation of sulphur-bearing gases occurs, these alloys are much more resistant as compared to other stainless steel types. In such applications, however, the acid concentration has marked impact on the rate of attack and should be carefully examined. The molybdenum-bearing Type 316 stainless steel also provides resistance to the wide variety of other environments.

C. Literature Review

TIG welding is widely used for different types of metal & alloy welding and still lot of research work is going for effective performance by TIG welding process. Kishore et al. [1]: In this paper they had done research on AISI1040 steel by using taguchi method. Research on the welding of material like steel is still difficult and ongoing.Exhaustive survey suggest that 5-7 control factors . The data in the present work is collected using ultrasound testing (UT), in which angle beam technique is used for the testing of weldments and results are quantified. Harish Kumar et al. [2]: In this paper they had done research on austenitic stainless steel. Nitrogen alloyed austenitic stainless steels are designated as 316LN which contain the low carbon due to which the risk of sensitization can be deminish. This paper addresses the laser

welding aspects, which may be of considerable interest because it offers several advantages over other welding processes. Magudeeswaran et al.[3]: The activated TIG (ATIG) welding process primarily focuses on increasing the penetration depth and the reduction in the weld bead width has not been paid much attention. The enhance process parameters are reported as 1 mm electrode gap, 140 A current, 130 mm/min travel speed, and 12 V voltage. Bharatha et al. [4]: The objective of this research is used to determine the influence of various welding parameters on the weld bead of AISI 316 welded joint. In this research work the ANOVA technique is used to identify the influence of the welding speed, current, electrode, root gap on the strength of the material. The result shows that speed is most influencing factor to have highest bend strength and current that is to be used while welding is the most influencing factor to get higher tensile strength. Buddu et al. [5]: The development of advanced fusion reactors like DEMO will have various challenges in materials and fabrication. The double walled design for vacuum vessel with thicker stainless steel material (40–60 mm) has been schemed in the advanced fusion reactors like ITER. The present paper describes characterization of welding joints of SS316L plates with higher thicknesses like 40 mm and 60 mm, prepared using multi-pass Tungsten Inert Gas (TIG) welding process. The weld quality has been evaluated with non-destructive tests by X-ray radiography and ultrasonic methods. Balaji et al. [6]: The joining of similar grades of stainless steel by TIG welding with the various parameters like current, gas flow rate, and bevel angle is reported and the SS 316L is selected over the other grades due to its less carbon content.

D. Scope

Only one material SS-316 grade stainless steel has been considered in this project. The materials other than this or different material may be considered in future. More than one material will be consider for future work. In this experiment only weld defects and Tensile strengths are considered. In future, the other than weld defects and weld strength, other test may be considered for analysis such as bending test, microstructure test, hardness test etc. Forthis work only current, gas flow rate, thickness is considered. In future, other than current, gas flow rate, thickness, another parameter may be considered such as voltage, speed, root gap, nozzle to workpiece distance etc. In this experiment consider only 3 levels and 3 parameters i.e. L9 orthogonal array is selected for experimentation. In future more than 3 levels and 3 parameters may be considered. For more levels and parameters get high accuracy in result and get more reliable parameters for TIG welding.

II. MATERIALS AND METHODOLOGY OF SS-316

The Chemical Composition of SS-316 is given in below Table 2

Table 2: chemical composition of SS-316 [1]

Alloy	C	Mn	P	S	Si	Cr	Ni	Mo	Cu	N
316	.01	2.0	.01	.01	1.0	16.00-18.0	10.00-14.0	2.00-3.0	0.7	-
6	8%	0%	4%	3%	0%	0%	0%	0%	5%	-

A. Design of Orthogonal array by using Taguchi method

The following is the experimental procedure which is done in this project such as follows:-

1. Commercial SS-316 plate of thickness 3, 5, 8 mm will be selected as work piece material for the present experiment.
2. SS-316 plate will be cut with dimension of 100 mm x 50 mm with the help of band-saw and grinding done at the edge to smooth the surface to be joined. The dimensions will have taken by references of research papers.
3. After cutting material into dimensions go for Taguchi method, for this decided 3 levels i.e. low medium and high and 3 parameters i.e. welding current, gas flow rate, material thickness. These three parameters were taken as variable for present study and their three levels were chosen for which responses were measured, for which L9 orthogonal array was selected as experimental design method. These parameters with their levels were shown in table 3.
4. After that surfaces will polished with emery paper to remove any kind of external material. Before welding all sheets were cleaned chemically by acetone in order to remove any source of contaminants like rust, dust oil etc.
5. After sample preparation, SS-316 plates are fixed in the working table with flexible clamp side by side and welding done so that a butt join can be formed.
6. Then TIG welding on plates will done by using Taguchi array design.
7. After that for Non Destructive Testing i.e. Radiography Testing.
8. After getting result of Radiography testing means for Destructive testing i.e. tensile testing.

Table 3 : Process parameters and levels

Parameter	Unit	Level 1	Level 2	Level 3
Welding current	A	125	137	151
Gas Flow Rate	l/min	18	21	24
Metal Plate Thickness	mm	3	5	8

Once the orthogonal array is selected, the experiments are carried out as per the level combinations. It is important that all experiments are to be conducted. The performance parameters (output) are noted for each experimental run for analysis. In below

Table 4 the experimental design using orthogonal array is shown:

Table 4 : Experimental design using orthogonal array

Experiment Number	Levels		
	Welding Current	Gas Flow Rate	Thickness
1	125A	18 l/min	3 mm
2	125A	21 l/min	5 mm
3	125A	24 l/min	8 mm
4	137A	18 l/min	3 mm
5	137A	21 l/min	5 mm
6	137A	24 l/min	8 mm
7	151A	18 l/min	3 mm

8	151A	21 l/min	5 mm
9	151A	24 l/min	8 mm

III. RESULT AND DISCUSSION

In this total 9 experiments were taken as L9 orthogonal array is selected. In this paper only 4 experiments were added as per optimized result.

A. Experiment no.1

First take Radiography test on weld coupon by using ASME SEC-V & SEC IX. The Tensile test is conducted on the SS316 Tig weldment on a Universal Testing Machine as per ASTM A370-2017 standards to determine the ultimate tensile stress of the weldment. For first experiment following parameters are considered. Table 5 and Table 6 shows the radiography result and tensile test result respectively.

Table 5 Radiography Result of 1st test coupon.

Film Size (in inches)	Identification No.	Observation
3x5	SVERI/TIG/TC4 AB	Min PO

Table 6 Tensile test result of 1st weld coupon

Sr.No	Parameter/Description	Actual Value
1	Thickness	8.02
2	Width	20.00
3	Area	160.80
4	Ultimate Tensile Strength	615.00
5	Ultimate Tensile Load	99.00
6	Specimen Shape	FLAT
7	Fracture	WELD

In this experiment welding current 125A, gas flow rate 24 l/min, thickness 3mm. Minimum porosity is obtained in radiography test and get tensile strength about 615 N/mm². Here weld joint is acceptable.

B. Experiment no.2

For second experiment following parameters are considered and The below Table 7 and Table 8 shows the tensile test result and radiography test result respectively.

Table 7 Result of Tensile test of 2nd weld coupon

Sr.No	Parameter/Description	Actual Value
1	THICKNESS	3
2	WIDTH	20
3	AREA	60
4	ULTIMATE TENSILE STRENGTH	600
5	ULTIMATE TENSILE LOAD	36
6	SPECIMEN SHAPE	FLAT
7	FRACTURE	WELD

Table 8 Radiography result of 2nd weld coupon.

Film size	Identification No.	Observation
-----------	--------------------	-------------

(in inches)		
3x5	SVERI/TIG/TC4 AB	NSD

In this experiment welding current 125A, gas flow rate 18 l/min, thickness 8mm. No any defect is obtained in radiography test and get tensile strength about 600 N/mm². Here weld joint is acceptable.

C. Experiment no.3

For third experiment following parameters are considered. The below Table 9 and Table 10 shows the result of tensile test and radiography test respectively

Table 9 Result of Tensile test of 3rd weld coupon

Sr.No	Parameter/Description	Actual Value
1	THICKNESS	3
2	WIDTH	20
3	AREA	60
4	ULTIMATE TENSILE STRENGTH	583.00
5	ULTIMATE TENSILE LOAD	34.98
6	FRACTURE	WELD
7	SPECIMEN SHAPE	FLAT

Table 10 Radiography result of 3rd weld coupon.

Film size (in inches)	Identification No.	Observation
3x5	SVERI/TIG/TC4 AB	NSD

In this experiment welding current 137A, gas flow rate 18 l/min, thickness 3mm. No any defect is obtained in radiography test and get tensile strength about 583 N/mm². Here weld joint is not acceptable.

D. Experiment no.4

For fourth experiment following parameters are considered.

The below Table 11 and Table 12 shows the result of tensile test and radiography test respectively.

Table 11 Result of Tensile test of 4th weld coupon

Sr.No	Parameter/Description	Actual Value
1	THICKNESS	5
2	WIDTH	20
3	AREA	100
4	ULTIMATE TENSILE STRENGTH	621.00
5	SPECIMEN SHAPE	FLAT
6	ULTIMATE TENSILE LOAD	62.10
7	FRACTURE	WELD

Table 12 Result of Radiography Test of 4th weld coupon

Film size (in inches)	Identification No.	Observation
3x5	SVERI/TIG/TC4 AB	NSD

In this experiment welding current 137A, gas flow rate 21 l/min, thickness 5mm. No any defect is obtained in radiography test and get tensile strength about 621 N/mm². Here weld joint is acceptable.

IV. CONCLUSION

All the experimental steps were carried out under precautionary measures in order to keep the error factor low and to increase the reliability of the results. The following conclusions were arrived from the non destructive testing i.e. Radiography testing investigation. As current decreases minor defects are formed such as under fill. Also as current increases heat affected zone increases as well porosity increases. For medium current good quality weld obtained. The radiography results showed the defect of minimum porosity, thus the result concludes that the defect does not create a major impact.

According to Destructive testing following conclusion is arrived. The tensile test has showed that the Current of 137A, Gas flow rate 21 l/min and a Thickness 5 mm offers the maximum tensile strength of 621 MPa. The tensile test has also showed that the Current of 137A, Gas flow rate 18 l/min and a Thickness 3mm offers the minimum tensile strength of 583.00 MPa.

REFERENCES

- [1] Mr.L.Suresh Kumar, Dr.S.M.Verma, P.Radhakrishna Prasad, P.Kirankumar Dr.T.SivaShanker "Experimental Investigation for Welding Aspects of AISI 304 & 316 by Taguchi Technique for the Process of TIG & MIG Welding", International Journal of Engineering Trends and Technology, Volume 2, Issue 2- 2011, ISSN: 2231-5381, 28-33.
- [2] R.K.Rajkumar, FatinHamimi, NachimaniCharde "Investigating the Dissimilar Weld Joints of AISI 302 Austenitic Stainless Steel and Low Carbon Steel", International Journal of Scientific and Research Publications, Volume 2, Issue 11, November 2012, ISSN 2250-3153
- [3] M.T.Z. Butt, M.S. Ahmad and M. Azhar, "characterization for GATW AISI 316 to AISI 316 & SA 516 grade 70 steels with welded & prewelded annealing conditions", Journal of Quality and Technology Management, Volume VIII, Issue II, December 2012.
- [4] Harish Kumar D., A. Somireddy, K. Gururaj, "A review on critical aspects of 316ln austenitic stainless steel weldability", International Journal of Materials Science and Applications 2012; 1(1), December 30, 2012, 1-7.
- [5] C.Balaji, S. V. Abinash Kumar, S. Ashwin Kumar, R. Sathish, "Evaluation of mechanical properties of SS 316 L weldments using tungsten inert gas welding", International Journal of Engineering Science and Technology (IJEST), Vol. 4 No.05 May 2012, ISSN : 0975-5462, 2053- 2057.
- [6] Akash.B.Patel, Prof.Satyam.P.Patel. "The Effect of Activating Flux in Tig Welding", International Journal of Computational Engineering Research, Vol. 04, Issue, 1, January 2014, ISSN 2250-3005, 65-70
- [7] B. Ramesh Kumar, "weld quality analysis of TIG, laser and electron beam welded SS 304 and 316 materials with NDT techniques", Proceedings of the National Seminar & Exhibition on Non-Destructive Evaluation NDE 2011, December 8-10, 2011, 346-349.
- [8] Balaji Chandrakanth, S. V. Abinash Kumar, S. Ashwin Kumar, R. Sathish, "Optimization and Non-destructive Test Analysis of SS316L Weldments Using GTAW", Materials Research, Received: February 18, 2013; Revised: October 12, 2013.
- [9] E. Ahmadi, A.R. Ebrahimi, "The effect of activating fluxes on 316L stainless steel weld joint characteristic in TIG welding using the Taguchi method", Journal of Advanced Materials and Processing, Vol.1, No.1, 2012, 55-62.
- [10] Pradeep Deshmukh, M. B. Sorte, "Optimization of Welding Parameters Using Taguchi Method for Submerged Arc Welding On Spiral Pipes".

Improving Accuracy of Manual Crimping Operation through the Automation of Crimping Machine

Vishal M. Dhumal, Shivam R. Kanade, Samadhan U. Bandagar, Kiran S. Ghule,
Kiran V. Chandan, Manoj R. Shewale

Abstract—Crimping machine is used in wire harnessing operation for creating a joint between wire and crimping pin with pressing of conductor crimp and insulation crimp. The holding of wire is done by manually without any guiding to the worker. So accuracy of crimping machine is mainly depending upon the skill of worker to hold the wire at accurate position. So for accurate joint, worker plays an important role. Guiding to worker is important so that accuracy will not depend upon worker efficiency and skill. So to achieve the right position to launch pressing die to go for pressing sensor should be at right position. For sensing the accurate position the sensor model which constitute Arduino, color recognition sensor, etc, which help to sense the change in color on insulation of wire. This color change is done by using the marker and sensed in the form of frequency change as marking of different color is done on the wire. This helps Arduino to work as mentioned in program to identify change in color frequency. Then through the LED attached on Arduino signal come to worker as the wire is at accurate position. Then pedal is activated by Arduino to do pressing operation. This will reduce the work done by worker and provide guidance to worker for working in any condition or situation.

Index Terms: Arduino, Crimping machine, sensor, wire harness.

I. INTRODUCTION

Now days, the companies are facing the problems regarding the worker efficiency, skills, accuracy of certain operation, etc. in manufacturing. These companies are looking for automation as a solution of this problem. So achieving the automation in company Core-Tech Aurangabad Pvt. Ltd. has facing the problem of lack in accuracy due to many problems in crimping machine [1]. Normally they do 1200 to 1500 crimping operation in a day. In that 40 to 50 fails due to the improper attachment of crimping with wire. This problem occur due to the many reasons some of them are not holding

wire at accurate position between crimping pin and punch [2], proper load applied on the crimping pin joint, etc. Crimping pin with conductor crimp and insulation crimp is shown in fig.

Vishal M. Dhumal, UG Student, Mechanical Department, SVETI's College of Engineering, Pandharpur, Maharashtra, India.

Shivam R. Kanade, UG Student, Mechanical Department, SVETI's College of Engineering, Pandharpur, Maharashtra, India.

Samadhan U. Bandagar UG Student, Mechanical Department, SVETI's College of Engineering, Pandharpur, Maharashtra, India.

Kiran S. Ghule, UG Student, Mechanical Department, SVETI's College of Engineering, Pandharpur, Maharashtra, India.

Kiran V. Chandan, Assistant Professor, Mechanical Department, SVETI's College of Engineering, Pandharpur, Maharashtra, India.

Manoj R. Shewale, Director, Coretech Aurangabad Pvt. Ltd. Waluj MIDC, Aurangabad, Maharashtra, India.

1. The crimping machine before experimentation is shown in fig.2. The normal joint formed between crimping pin and wire is given in fig.3.



Fig.1 Crimping pin

Project objectives are as follows

- 1) To guide the worker about the accurate position between the crimping pins and punch
- 2) To increase the productivity by reducing the losses due to worker inefficiency

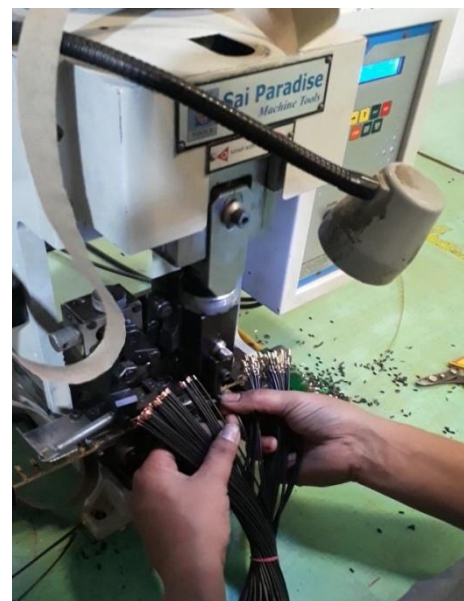


Fig.2 Crimping Machine



Fig.3 Crimping Operation.

II. LITERATURE REVIEW

Klaus states about the stroke of crimping machine and the necessity of managing the stroke length for accurate

crimping joint between electric conductor and electric connector.[1]

Gerst explains about the automatic crimping tool and crimping is done on the basis of carrier steep mechanism. [2] Basic information of Arduino and its pin is useful for doing experimentation on it. The utilization of Arduino software in giving the program to Arduino is done by Arduino IDE. [3]

The sorting of object is a very difficult to maintain his proper place. Because in industry the continuous process of operations is done. Sensor Color Reorganization- tcs3200 will help to maintain the sorting of the products. [4]

Wiring harness is a predetermined structural set of wire, terminal and connector thought vehicle body for providing electrical supply. It is used for connecting the electrical devices for automotive vehicle .The wire harness thus connected to electric devices by engaging each set of harness end terminals with each electric device connector attached to the vehicle frame. [5]

III. COMPONENTS OF SENSOR MODEL

A. Arduino Uno

The Arduino Uno is used for programming purpose especially for color recognition sensor. The Arduino has two microcontrollers, one reset button, one USB connection port, adapter port, 13 input output pins, etc. The first microcontroller is used for making interface between the second microcontrollers to load program, change program, etc [1]. The second microcontroller is used for actual performance as the program is loaded on that. The reset button is used for clearing second microcontroller program loaded on it. The 13 pin is specially provided with LED for indication of result. The many pins ground pin, input/output pins having voltage are present.

B. Color Recognition Sensor TCS 3200

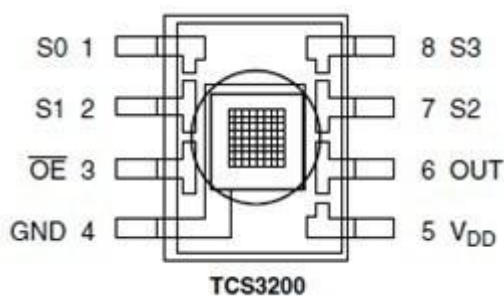


Fig. 4 Color Reorganization Sensor [4].

This sensor has 8 pins which controls the input and output of a sensor. On that S0 and S1 are recognized as output frequency control ports and S2 and S3 are used color light to detect. There are also ports like GND, VCC, OUT and OE. These ports have special meaning like having the ground the voltage as shown in fig. 4.

C. Cables

As different types of jumper cables are used like male to male, female to female, male to male jumper cables which is are used to make the connection between the Arduino and sensor. USB cable is also used for making interface between the Arduino and computer.

D. Relay

Relay is an electromagnetic switch used for turn on and off circuit. The main parts of relay are electromagnet, movable arm, switch point contacts. The relay has mainly two circuits control circuit and load circuit.

IV. ASSEMBLY OF COMPONENT

The assembly is done in Arduino and sensor by following ways in Fig.5.

The S0 pin is attached with the 4 number port and S1 port is attached with 5 number ports on 13 input output pins on Arduino board [1]. The S2 and S3 normally known as a current to frequency converter ports which are used for output port are attached to 6 and 7 number of ports. Ground port is attached to GND port of Arduino to ground the supply. OUT port is attached with the 8 number of port on the Arduino board [4]. This all connection is done through the male to female jumper cables. Then Arduino is joined with the USB cable to the pc. Then reset button is pressed on Arduino for clearing the past program from Arduino board. Then through the ArduinoIDE new program can be loaded. [1]

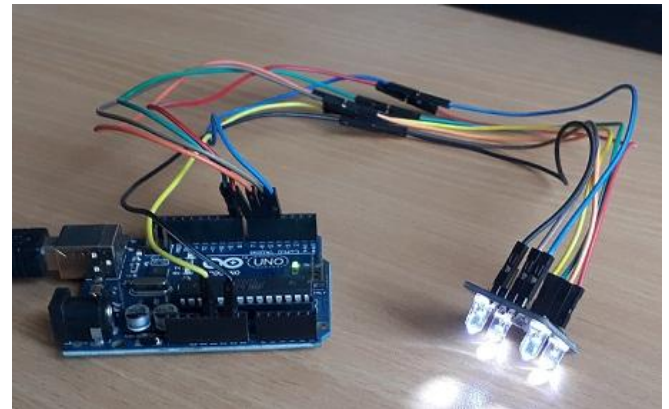


Fig.5 Assembly of Components

V. WORKING OF COMPONENTS

The checking of components is done by analyzing the various parameters like sensor output result and input result. The various constraints are applied for the sensor through the program. In program if S0 and S1 are provided with low and high value then the change in this values gives frequency scaling as per needed. As low and low to S0 and S1 gives the result as power down. This is shown as in Table 1.

Table 1: Output Response for S0 and S1

S0	S1	Output Response
LOW	LOW	No Response
LOW	HIGH	High scaling
HIGH	LOW	Medium scaling
HIGH	HIGH	Low scaling

As the sensing the small color change the high scaling of output is used. For that purpose S0 is provided with low and S1 is provided with high. This helps to achieve response in RGB color frequencies on pc. For the S2 and S3 port for

focusing on the specific color the one from RGB color is chosen for that Table 2 is provided.

Table 2: Output color frequency for S2 and S3

S2	S3	Color Frequency
Low	Low	Red
Low	High	Blue
High	Low	No color
High	High	Green

As specifically the wire has much color in that red is chosen for the experiment purpose. So that S2 is provided with low and S3 is also provided with low. By looking at the pc we can find different values of red color coming from the diodes. This color frequency readings coming from Arduino are used for sensing the change in color of the wire.

VI. EXPERIMENTATION

A. Program for Arduino

The program for Arduino is done on the Arduino IDE software in normal coding technique. The normal program for color recognition is used for the sensor and some changes in the program are done like using if statement for specific frequency selection, using of only red color than green, blue so that specific color frequency will appear. Use of if statement as if normal color of wire is blue then the frequency on monitor will come about 1100 to 1110 but if the color changed then frequency will reduce or increase as per the marking color used. Normally black color is used so that increase in the frequency is used. IF (frequency>1115) then show the LED light and activate the relay circuit. Then the relay is activated as the correct position is achieved. The pressing operation is done by punch. For black color of wire white color is used which decrease the frequency so that '<' symbol is used.

B. Performance.

To hold the sensor at the accurate position the holding stand is used. This will help to block the sunlight coming from outside to the sensor and also provide support to it. The material used for the stand is nylon and square shape nylon three plates of side 4cm are taken and then one plate is cut with center dimensions of sensor as shown in Fig.6. Then the sensor is hold closed to crimping line at a distance of 2cm [3]. Then consider the different wires of length and marking is done on 4cm length. The marking length is of 2mm to 4mm are made.

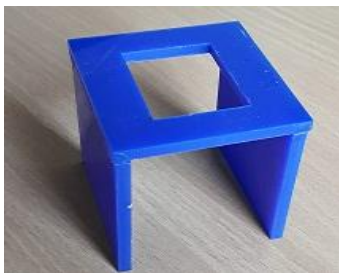


Fig.6 Holding Stand for sensor

These dimensions are specified due to obtain change in color frequency. The Arduino takes reading in mille seconds for each time. So the time required for reading and checking is less than one second. If the wire is at accurate position then

the LED get activated and the control circuit of relay is get completed and this will complete the circuit of between the pressure pedal and relay so that punch will activated for pressing operation as shown in fig.7.



Fig.7 Actual Performance of Model

VII. RESULT

The sensor module work properly giving following results-

1. Guides worker for good crimping operation.
2. Give good efficient crimping joint between wire and crimping pin.
3. Accuracy and precision of crimping operation is maintained.
4. Productivity of operation is maintained as operation takes less time.
5. The rejection rate of crimping operation is less as between 2 to 10 for a day.

VIII. CONCLUSION

Experimentation performed in the paper is satisfying the company as worker efficiency and skills are not playing any vital role in achieving the accuracy of crimping operation. The time required for the operation is 1 to 2 sec. The productivity is increased as the accuracy is increased and time required is less. The marking on the wire should be accurate to achieve best results.

ACKNOWLEDGMENT

The author wish to thanks the director Mr. Manoj Shewale Coretech Pvt. Ltd. Aurangabad, Dr. B. P. Ronge, Principal of College of Engineering Pandharpur & Guide Mr. K.V. Chandan.

REFERENCES

- [1]. Enneper, K., Monsieur, D. and Schwager, E., Kabelwerke Reinshagen GmbH, 1992. *Crimping machine*. U.S. Patent 5,168,736.
- [2]. Gerst, M., Sasse, T. and Zajicek, J., Whitaker Corp, 1998. *Automatic crimping tool*. U.S. Patent 5,752,405
- [3]. Arduino, S.A., 2015. Arduino. *Arduino LLC*.
- [4]. Soetedjo, A., Ashari, M.I. and Ardiles, C., 2017. Development of Industrial Control Training Module using Distance and Color Sensors

for Detecting Objects. *International Journal of Engineering and Management*, 1(1), pp.1-8.

- [5]. Adachi, M., Sumitomo Wiring Systems Ltd, 2003. *Structure for wiring a wire harness between an automobile body and a mobile article, and a method of protecting an electric wire group of a wire harness*. U.S. Patent 6,635,825.

Enhancement of Heat Transfer Coefficient through Forced Convection Apparatus by Using Circular and Elliptical Pipe

Ashish Shahane, Lakhan Ghodake, Digambar.T. Kashid, D. S. Ghodake

Abstract— It is very essential to develop a forced convection system to carry out the analytical and experimental investigation of the heat transfer coefficient with the use of the elliptical and circular pipe. Convection is nothing but the transfer of heat through a fluid which is in bulk fluid motion. Depending on the motion of the fluid, it is classified as natural and forced convection. Buoyancy effect is the natural cause which occurs due to fluid motion in natural convection. On the other hand, in forced convection, the motion of the fluid is caused by external means like a pump or fan. In this system three, 130 Volt heaters are wound over 800 mm test section of Circular pipe having a 25mm diameter and Elliptical pipe having 22 mm minor and 28 mm major diameter. Variable dimmer stat is used to control input to heater and control valve to control mass flow rate, to determine the average coefficient of heat transfer in turbulent flows inside smooth and straight Circular and Elliptical pipes. The research consists of a regression analysis performed between the Reynolds number and the Prandtl number finally to calculate the heat transfer coefficient of Circular and Elliptical pipes by experimental investigation. After calculating all the results of both the pipes finally we got that efficiency of Elliptical pipe is more than circular pipe also heat transfer coefficient is maximum in the elliptical pipe than the circular pipe and it also led to increasing the heat transfer rates. The deviation of the heat transfer coefficient is maximum as compared to Elliptical pipe.

Index Terms—Elliptical pipe, Circular pipe, heat transfer, Forced Convection, Thermocouple, Augmentation.

I. INTRODUCTION

Nowadays, heat exchange equipment is in demand due to material availability and the high cost of energy. The use of heat exchangers is extensively seen in radiators for space vehicles, air conditioning gadgets, thermal power plants, automobiles etc. Techniques to improve heat transfer are the major topics for the researchers today. As per the survey made the energy use is increased by 1.6 times in the world, from 4.03×10^{20} J in 1999 to 6.4×10^{20} J in 2020.

Ashish Shahane, Mechanical Engineering Department, SVERI's College of Engineering, Pandharpur, Maharashtra, India,
Lakhan Ghodake, Mechanical Engineering Department, SVERI's College of Engineering, Pandharpur, Maharashtra, India
Digambar.T. Kashid, Mechanical Engineering Department, SVERI's College of Engineering, Pandharpur, Maharashtra, India
D. S. Ghodake, Mechanical Engineering Department, Sinhgad Institute of Technology, Lonavala, Pune, Maharashtra, India

Hence, if the effectiveness of the energy uses could increase by 10%, by means of various heat transfer enhancement techniques, this will result in 6.4×10^{19} J of benefit in term of energy consumption to the society.

The economic operation and design of the process plant are ruled by the effective use of heat. With the continuous increase in volume and power in production, the dimensions and mass of heat exchangers also increase which in turn involves multi-million dollars investment for capital and operation cost. Hence it is a vital requirement to reduce overall dimension characteristics of heat exchangers.

Due to the needs like optimization and conservation, the development of heat exchangers is taking place. Different techniques are used to improve the heat transfer rates, which are normally referred to as heat transfer enhancement or heat transfer augmentation techniques. With the help of these techniques, the following experimentation is carried out.

II. LITERATURE REVIEW

Adegun [1] presented the numerical simulation of enhanced forced convective heat transfer in inclined elliptic ducts with multiple internal longitudinal fins. Hajmohammadi [2] presented the optimal design of tree-shaped inverted fins penetrated into heat generating bodies to enhance the heat transfer rate. Hajmohammadi [3] presented the optimal geometric structure of a micro-scale channel heat sink, by assuming slip boundary condition and investigated the 3D fluid flow and heat transfer phenomena inside the microchannel heat sink. Mapa and Mazhar [4] discussed the heat transfer using nanofluid in a mini heat exchanger utilizing commercially available equipment. Faizal and Ahmed [5] investigated the channel height between the plates to determine the configuration that gives the optimum heat transfer. Jozef Cernecky [6], the paper deals with visualization of temperature fields in the vicinity of profiled heat transfer surfaces and subsequent analysis of local values of Nusselt numbers by forced air convection in an experimental channel. Priyank [7] studied the effect of Reynolds number and relative roughness pitch on the heat transfer coefficient and friction factor has been studied. It is reported that the highest Nusselt number at a higher value of Reynolds number was provided by the roughened duct having circular and square rib with highest relative roughness height. Square sectioned rib provides a higher value of enhancement as compared to circular rib at a higher value of Reynolds number. Sagar [8] performed a numerical analysis of heat transfer for three different angles of w-shaped turbulator placed at the bottom side wall of the square duct and reported that Nusselt number and friction factor in a duct with W-rib insert increases

Enhancement of Heat Transfer Coefficient through Forced Convection Apparatus by Using Circular and Elliptical Pipe

as compare to smooth duct without an insert. Pankaj [9] carried out an experimental analysis to study turbulent flow heat transfer in a rectangular duct with and without internal ribs and observed that the local Nusselt number distribution is strongly depended on position, orientation, and geometry of the ribs. Also, the discrete V-shaped ribs produce overall less heat transfer enhancement than continuous V-shaped ribs. Few researchers have carried out the study on micro pipes like micro channels and reported the performance of the microchannels [10-12].

III. EXPERIMENTAL SETUP

The schematic diagram of the open loop experimental setup is shown in Fig. 1 the loop consists of a blower unit fitted with a pipe in a horizontal orientation. The blower fan runs at constant speed. The outlet of a blower is connected to an MS pipe having inside diameter 25.4mm through a reducer. The U-pipe manometer is connected across the orifice meter to measure the flow rate of air flowing through the pipe.

Nichrome bend heater of 200W encloses the thermally developing section to a length of 300mm and the test section to a length of 500mm to cause electric heating. Supply to the heater is given from dimmer stat. Power input to the test pipe heater is varied using a dimmer stat, which is used to vary the voltage of the AC current passing through the heater and by keeping the current less than 2A. Two thermocouples are placed one at the entrance i.e. before the thermally developing section and the other at the exit i.e. after the test section to measure air inlet and outlet temperature (T_1 and T_{10}) respectively. Three thermocouples i.e. T_2 , T_3 , and T_4 are placed on the thermally developing section and other five thermocouples i.e. T_5 , T_6 , T_7 , T_8 , and T_9 are placed on the test section to measure the temperature at various points along the pipe surface. The outer surface of the test section is well insulated to minimize convective heat loss to the surrounding. The control valve at the exit section controls the

airflow rate into the test section. Necessary precautions have been taken to prevent leakages from the system. The actual photograph and schematic of the experimental setup are as shown in the below Fig. 1 and Fig. 2 respectively.

Nomenclature

SYMBOLS	DESCRIPTION
A	Cross section area of pipe, (m ²)
A _s	Surface area of Test Section, (m ²)
T	Temperature (°C)
T ₁ , T ₁₀	Air temperature at inlet and outlet, (°C)
T ₂ , T ₃ , T ₄ , T ₅ , T ₆ , T ₇ , T ₈ , and T ₉	Test section temperatures, (°C)
T _s	The average surface temperature of the working fluid, (°C)
T _a	Bulk temperature, (°C)
U	Air velocity through test section, (m/s)
K	Thermal conductivity, W/mK
H	Convective heat transfer coefficient, W/ m ² K
D	The inner diameter of the test section, (m)
C _p	Specific heat of air, J/kgK
L	Length of the test section, (mm)
M	The mass flow rate of air, (kg/sec)
N _u	Nusselt number
Pr	Prandtl number
Q _t	Total heat transferred to air, (W)
Q _D	Discharge through an orifice, (m ³ /sec)
Re	Reynolds number
μ	Dynamic viscosity, (kg m/sec)
B	The ratio of Orifice Diameter to Pipe Diameter
P	Density, (kg/m ³)

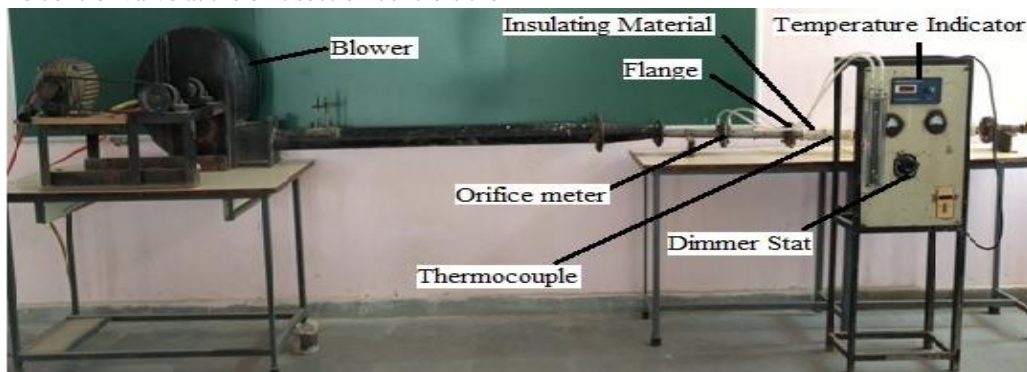


Fig. 1. Experimental Setup

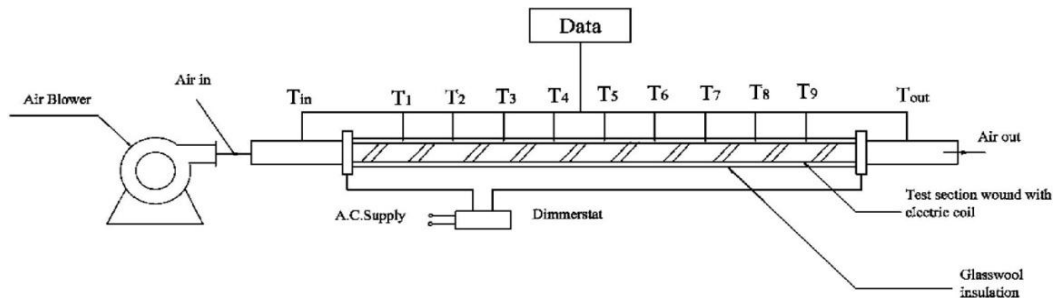


Fig. 2. Schematic Diagram of Experimental Setup

IV. OBSERVATIONS

A. Observations for Circular Pipe

- i. Test Section Length, $L=0.8\text{m}$
- ii. I.D of Test Section, $D=0.0250\text{m}$
- iii. Cross-Sectional Area of Pipe, $A=4.90625 \times 10^{-4} \text{ m}^2$
- iv. The surface area of the test section, $A_s=0.0628 \text{ m}^2$

B. Observations for Elliptical Pipe

- i. Test section length, $L=0.8\text{m}$
- ii. Hyd.D of the test section, $D=0.0250\text{m}$
- iii. The cross-sectional area of a pipe, $A= 4.90625 \times 10^{-4} \text{ m}^2$
- iv. The surface area of the test section, $A_s=0.0628 \text{ m}^2$

TABLE I. OBSERVATION TABLE FOR CIRCULAR PIPE

SR.No	U(m/s)	T1	T2	T3	T4	T5	T6	T7	T8	T9	T10
1	7.3	37	82	84	84	86	89	82	90	89	53
2	5.6	33	84	88	87	90	93	86	95	94	51
3	4.3	34	92	92	96	98	102	106	110	103	55

TABLE II. OBSERVATION TABLE FOR ELLIPTICAL PIPE

SR.No	U(m/s)	T1	T2	T3	T4	T5	T6	T7	T8	T9	T10
1	7.3	34	63	69	68	61	74	66	78	85	50
2	5.6	36	65	72	71	65	79	69	83	90	53
3	4.3	35	68	75	74	68	84	71	85	92	54

V. CALCULATIONS

A. Sample Calculations for Circular Pipe

Calculation procedure for circular pipe of 25mm diameter at 130V voltage, 2A current and $U=4.3 \text{ m/s}$.

Estimation of Reynolds Number and Prandtl Number

Mean bulk temperature,

$$T_a = (T_1 + T_{10})/2 = 44.5 \text{ } (^{\circ}\text{C}) \dots (1)$$

Mean surface temperature,

$$T_s = (T_1 + T_2 + T_3 + T_4 + T_5 + T_6 + T_7 + T_8 + T_9)/5 = 99.875 \text{ } (^{\circ}\text{C}) \dots (2)$$

Properties of air at 1atm at mean bulk temperature i.e. at T_a ,

$$\text{Density}_{\text{air}} = 1.1115 \text{ (kg/m}^3\text{)}$$

$$C_p = 1007 \text{ (J/kg.k)}$$

$$K = 0.027403 \text{ (W/m.k)}$$

$$\mu = 0.000019356 \text{ (kg/m.s)}$$

$$P_r = 0.71136$$

Volume flow rate,

$$Q_D = A \times U \text{ (3)}$$

$$Q_D = 0.00211 \text{ (m}^3\text{/s)}$$

Mass flow rate,

$$\dot{m} = \text{Density}_{\text{air}} \times Q_D = 0.002346 \text{ (kg/s)} \dots (4)$$

Heat transferred to air,

$$Q_t = \dot{m} \times C_p \times (T_{10} - T_1) = 49.60566 \text{ (W)} \dots (5)$$

Experimental convective heat transfer coefficient,

$$h_{\text{expt}} = Q_t / (A_s \times (T_s - T_a)) \dots (6)$$

$$h_{\text{expt}} = 14.25773 \text{ (W/m}^2\text{k)}$$

Experimental Nusselt number,

$$\text{Nu}_{(\text{expt})} = (h_{\text{expt}} \times L_c) / K = 13.00746 \dots (7)$$

Reynolds number,

$$\text{Re}_e = (\text{Density}_{\text{air}} \times U \times D) / \mu = 6173.086 \dots (8)$$

Theoretical Nusselt number by Dittus-Boelter equation,

$$\text{Nu}_{(\text{theo})} = 0.023 \times (\text{Re}_e)^{0.8} \times (P_r)^{0.3} = 22.37466 \dots (9)$$

Theoretical convective heat transfer coefficient,

$$h_{\text{expt}} = (\text{Nu}_{(\text{theo})} \times K) / L_c = 14.25773 \text{ (W/m}^2\text{k)} \dots (10)$$

B. Sample Calculations for Elliptical Pipe

Calculation procedure for Elliptical pipe of 25mm Hydraulic diameter at 130V voltage, 2A current and $U=4.3 \text{ m/s}$.

Estimation of Reynolds Number and Prandtl Number

Mean bulk temperature,

$$T_a = (T_1 + T_{10})/2 = 44.5 \text{ } (^{\circ}\text{C}) \dots (11)$$

Mean surface temperature,

$$T_s = (T_1 + T_2 + T_3 + T_4 + T_5 + T_6 + T_7 + T_8 + T_9)/5 = 77.125 \text{ } (^{\circ}\text{C}). (12)$$

Properties of air at 1atm at mean bulk temperature i.e. at T_a ,

$$\text{Density}_{\text{air}} = 1.1115 \text{ (kg/m}^3\text{)}$$

$$C_p = 1007 \text{ (J/kg.k)}$$

$$K = 0.0274 \text{ (W/m.k)}$$

$$\mu = 0.000019356 \text{ (kg/m.s)}$$

$$P_r = 0.7113$$

Volume flow rate,

$$Q_D = A \times U \dots (13)$$

$$Q_D = 0.00211 \text{ (m}^3\text{/s)}$$

Mass flow rate,

$$\dot{m} = \text{Density}_{\text{air}} \times Q_D = 0.00235 \text{ (kg/s)} \dots (14)$$

Heat transferred to air,

$$Q_t = \dot{m} \times C_p \times (T_{10} - T_1) = 44.8813 \text{ (W)} \dots (15)$$

Experimental convective heat transfer coefficient,

$$h_{\text{expt}} = Q_t / (A_s \times (T_s - T_a)) \dots (16)$$

$$h_{\text{expt}} = 21.8952 \text{ (W/m}^2\text{k)}$$

Experimental Nusselt number,

$$\text{Nu}_{(\text{expt})} = (h_{\text{expt}} \times L_c) / K = 19.9751 \dots (17)$$

Reynolds number,

$$\text{Re}_e = (\text{Density}_{\text{air}} \times U \times D) / \mu = 6173.09 \dots (18)$$

Theoretical Nusselt number by Dittus -Boelter equation,

$$\text{Nu}_{(\text{theo})} = 0.023 \times (\text{Re}_e)^{0.8} \times (P_r)^{0.3} = 22.3741 \dots (19)$$

Theoretical convective heat transfer coefficient,
 $h_{\text{expt}} = (Nu_{\text{(theo)}} \times K) / L_c = 21.8952 \text{ (W/m}^2\text{k)} \dots(20)$

VI. RESULTS AND DISCUSSION

As the Reynolds number increased, the difference of temperature between inlet and outlet (T_1, T_{10}) was observed to be decreasing with increase in Reynolds number. This is due to a more mass flow rate of air supplied to the test at higher Reynolds number. $T_2, T_3, T_4, T_5, T_6, T_7, T_8$ and T_9 denote

the wall temperature of the horizontal pipe at different locations. They are observed to decrease with the increase of Reynolds numbers. The result will be compared with Circular pipe to estimate the enhancement of heat transfer rate in the presence of Elliptical pipe.

It is observed from table III and IV that, experimentally obtained Nusselt number values are lesser than those obtained from using Dittus-Boelter correlation values for both pipes.

III. RESULT TABLE FOR CIRCULAR PIPE

Sr.No	U(m/s)	Ts	Ta	Re	Nu(expt)	Nu(theo)	h(expt)	h(theo)	Qt
1	4.3	99.875	44.5	6173.086	13.00746	22.37466	14.25773	24.52532	49.60566
2	5.6	89.625	42	8152.599	17.13111	27.95522	18.65373	30.43988	55.81715
3	7.3	85.75	45	10451.44	19.67436	34.09424	21.59457	37.42184	55.28907

IV. RESULT TABLE FOR ELLIPTICAL PIPE

Sr.No	U(m/s)	Ts	Ta	Re	Nu(expt)	Nu(theo)	h(expt)	h(theo)	Qt
1	4.3	77.125	44.5	6173.086	19.97514	22.3741	21.89515	24.5247	44.88131
2	5.6	74.25	44.5	7748.344	25.52515	26.83557	27.97863	29.415	52.29744
3	7.3	70.5	42	10538.76	33.17096	34.32872	36.11919	37.37986	64.67701

Fig. 3 shows the variation of heat transfer coefficient with Reynolds number for a circular pipe. The values obtained from experimentation of heat transfer coefficient are lesser than those obtained from using Dittus-Boelter correlation values i.e. theoretically calculated values.

Fig. 4 shows the variation of Nusselt No. with Reynolds number for a circular pipe. The experimentally obtained values of Nusselt No. are lesser than those obtained from using Dittus-Boelter correlation values i.e. theoretically calculated values.

Fig. 5 shows the variation of heat transfer coefficient with Reynolds number for Elliptical pipe. The experimental heat transfer coefficient values are lesser than those obtained from using Dittus-Boelter correlation values i.e. theoretically calculated values.

Fig. 6 shows the variation of Nusselt No. with Reynolds number for a circular pipe. The experimentally obtained values of Nusselt No. are lesser than those obtained from using Dittus-Boelter correlation values i.e. theoretically calculated values.

Fig. 7 presents the variation of heat transfer coefficient with Reynolds number for both Elliptical pipe and Circular pipe. The experimental heat transfer coefficient values for Elliptical pipe are more than Circular pipe.

Fig. 8 shows the variation of Nusselt No. with Reynolds No. for both Elliptical pipe and Circular pipe. The experimentally obtained values of Nusselt No. for Elliptical pipe are more than Circular pipe.

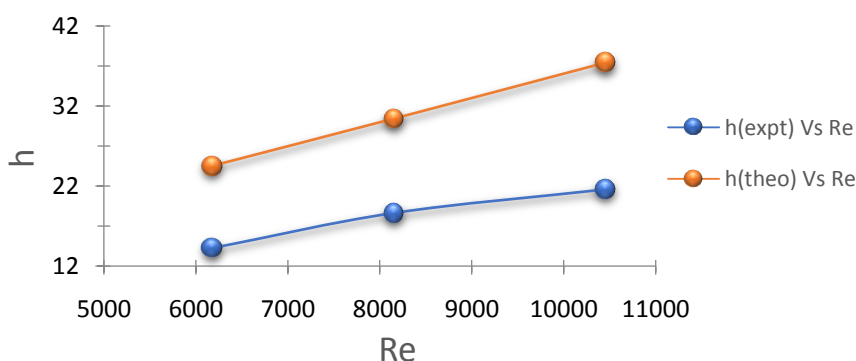


Fig. 3. Variation of Heat Transfer Coefficient with Reynolds No. for Circular Pipe

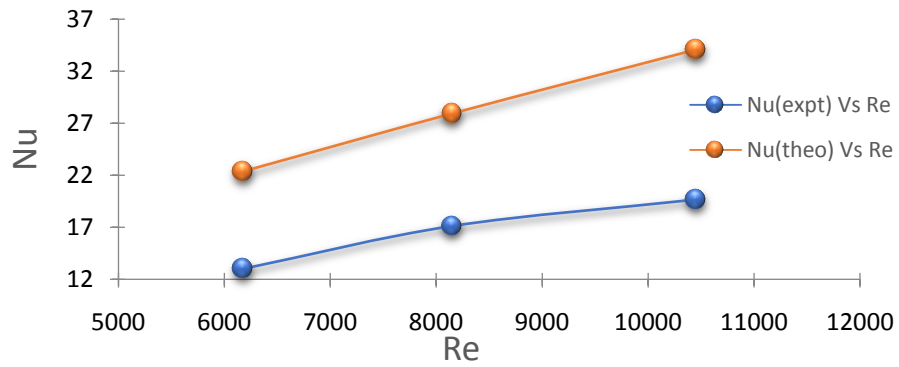


Fig. 4. Variation of Nusselt No. with Reynolds No. for Circular Pipe

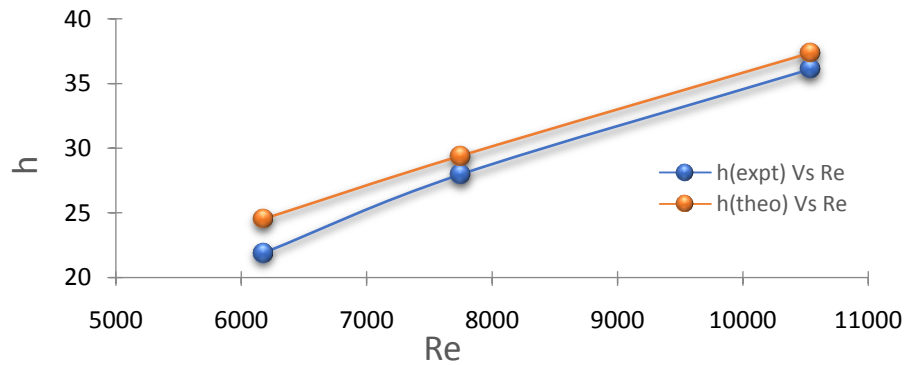


Fig. 5. Variation of Heat Transfer Coefficient with Reynolds No. for Elliptical Pipe

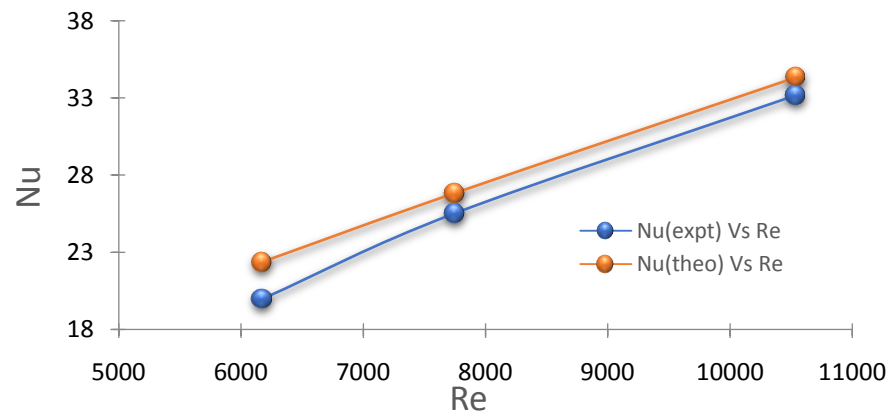


Fig. 6. Variation of Nusselt No. with Reynolds No. for Elliptical Pipe

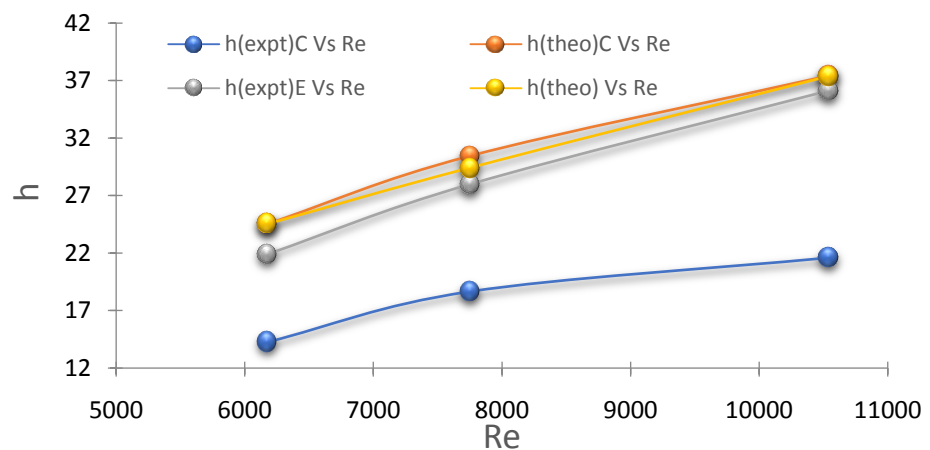


Fig. 6. Variation of Nusselt No. with Reynolds No. for Elliptical Pipe

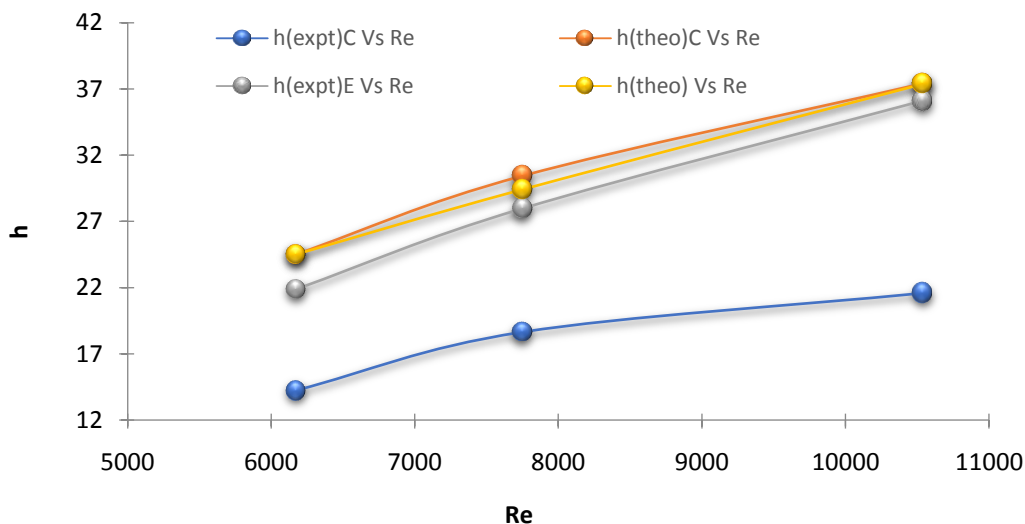


Fig. 7. Variation of Heat Transfer Coefficient with Reynolds No. for both Pipes

VII. CONCLUSION

Experimental investigations were performed to investigate the heat transfer characteristics in an externally heated horizontal circular pipe and elliptical pipe. It is found that the heat transfer coefficient is maximum in an elliptical pipe than a circular pipe and led to increase heat transfer rates. Also, from the above charts and result table III and IV, it is clear that the theoretical values of heat transfer coefficient for a different reading of elliptical pipe are nearly the same to the experimental values. To conclude, an elliptical pipe is more efficient over a circular pipe in forced convection apparatus.

REFERENCES

- [1] I.K. Adegun, T.S. Jolayemi, O.A. Olayemi, A.M. Adebisi, Numerical simulation of forced convective heat transfer in inclined elliptic ducts with multiple internal longitudinal fins", Alex. Eng. J. (2017).
- [2] M.R. Hajmohammadi, Optimal design of tree-shaped inverted fins, Int. J. Heat Mass Transfer 116 (2018) 1352–1360.
- [3] M.R. Hajmohammadi, P. Alipour, H. Parsa, Microfluidic effects on the heat transfer enhancement and optimal design of microchannels heat sinks, Int. J. Heat Mass Transf. 126 (2018) 808–815.
- [4] L.B. Mapa, Sana Mazhar, Enhancement of heat transfer in a shell and pipe heat exchanger using MgO nanofluid, J. Res. Appl. Sci. Eng. Technol. 3 (9) (2015).
- [5] M. Faizal, M.R. Ahmed, Experimental studies on a corrugated plate heat exchanger for small temperature difference applications, Experimental Thermal and Fluid Science 36 (2012) 242–248.
- [6] Jozef Cernecky, Jan Koniar and Zuzana Brodnianska "The Effect of Heat Transfer Area Roughness on Heat Transfer Enhancement by Forced Convection" Journal of Heat Transfer fellow ASME APRIL 2014, Vol. 136 /041901-1 to 8.
- [7] Priyank Lohiya, Shree Krishna Choudhary. "Numerical study on heat transfer of turbulent duct flow through ribbed duct", International Journal of Engineering Sciences and Research Technology, Volume 4, Issue 7, Pages: 178-182, July 2015.
- [8] Sagar S. Desai, Rupesh J. Yadav, and Omkar R. Chavan. "Numerical Heat Transfer Study of Turbulent Square Duct Flow through W-Type Turbulators", Volume 4, No.4, Pages: 320-3024, Dec 2014
- [9] Pankaj N., Rahul M. Sherekar, Sachin V. Bhalerao. "Experimental analysis of turbulent flow heat transfer in a rectangular duct with and without continuous and discrete v-shaped internal ribs", International Journal of Research in Advent Technology, Volume 2, Issue 1, Pages: 59-66, January 2014.
- [10] Das, S.S., Tilekar, S.D., Wangikar, S.S. and Patowari, P.K., "Numerical and experimental study of passive fluids mixing in micro-channels of different configurations", *Microsystem Technologies*, Vol. 23, no. 12, pp.5977-5988, 2017.
- [11] Wangikar, S.S., Patowari, P.K. and Misra, R.D., "Numerical and experimental investigations on the performance of a serpentine microchannel with semicircular obstacles" *Microsystem Technologies*, pp.1-14, 2018.
- [12] Gidde, R.R., Pawar, P.M., Ronge, B.P., Shinde, A.B., Misal, N.D. and Wangikar, S.S., "Flow field analysis of a passive wavy micromixer with CSAR and ESAR elements", *Microsystem Technologies*, vol 25, no. 3, pp.1017-1030, 2019.

Achievement/Award

A. Y. – 2018-19

Sr. No.	Name of Students	Name of Paper/Article	Name of Award
1.	Hrushikesh N. Paricharak, Aditya A. Lotake, Sudhakar V. Mane, Darshan R. Gaikwad, Rushikesh H. Vastre	Analysis of Crack on Aeroplane Wing at Different Positions using ANSYS Software	Best Article Award

International Journal of New Technology and Research
Best Article Award
Presented to

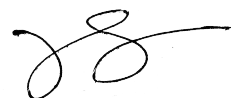
Hrushikesh N. Paricharak, Aditya A. Lotake, Sudhakar V. Mane, Darshan R. Gaikwad, Rushikesh H. Vastre, Digambar T. Kashid

For Their Papers

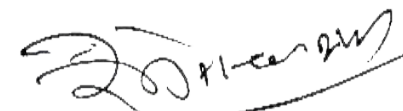
Analysis of Crack on Aeroplane Wing at Different Positions using ANSYS Software

Paper ID- IJNTR05040027

In Volume V Issue IV



Managing Editor



Managing Director

Number of students participated in National Conferences

A.Y. – 2019-20

Sr. No.	Title of Paper	Name of Authors	Name of Conference	National / International
1.	CO2 Laser Machining of Wood	Gauri R. Gore, Shivani S. Kothawale, Anjali P. Gavali, Pranoti R. Bhosale,	National Conference on Mechanical, Materials & Renewable Energy Technology (NCMMRET-2020), 10-11 January 2020, Bhubaneswar, Odisha, India. [Proceedings of the TEQIP-III BPUT (ATU), Odisha sponsored]	National
2.	Fabrication of Logos on Brass Material Employing Photochemical Machining	Athrav M. Kulkarni, Madan K. Patil, Aniket A. Bansode, Aman A. Mulani,	National Conference on Mechanical, Materials & Renewable Energy Technology (NCMMRET-2020), 10-11 January 2020, Bhubaneswar, Odisha, India. [Proceedings of the TEQIP-III BPUT (ATU), Odisha sponsored]	National
3.	Development of Pick and Place Robot	Arati Gajanan Lale, Dhanashree Bharat Sonawane, Namrata Raju Parvat, vaishnavi Mahesh Lakheri,	National Conference on Mechanical, Materials & Renewable Energy Technology (NCMMRET-2020), 10-11 January 2020, Bhubaneswar, Odisha, India. [Proceedings of the TEQIP-III BPUT (ATU), Odisha sponsored]	National
4.	New Design Approach of Helical Coil Spring by Using FEA	Amit R. Khyade, Rohan S. Kale, Mudasar M. Bagwan, Vedant D. Mangrulle,	National Conference on Mechanical, Materials & Renewable Energy Technology (NCMMRET-2020), 10-11 January 2020, Bhubaneswar, Odisha, India. [Proceedings of the TEQIP-III BPUT (ATU), Odisha sponsored]	National
5.	Design And Development of Sugar Cane Lifter	Vishal Ghongade, Akshay Karande, Mujamil Shaikh, Shridhar Kotyal,	National Conference on Research and Developments in Material Processing, Modelling and Characterization 2020	National

6.	Development of Pick And Place Robot	Dhanashree Sonawane, Arati Lale, Namrata Parvat, Vaishnavi Lakheri,	National Conference on Research and Developments in Material Processing, Modelling and Characterization 2020	National
7.	Application of Genetic Algorithm (GA)	Pranoti R Bhosale	National Conference on Research and Developments in Material Processing, Modelling and Characterization 2020	National



In association with
VTU & AKU



**TEQIP-III, BPUT ODISHA (ATU)
&
EINSTEIN ACADEMY OF TECHNOLOGY & MANAGEMENT**
(NAAC B++ Grade Engineering Institution)

Present this

Certificate of Participation

To

Prof. / Dr. / Mr. / Ms. Amit R. Khyade & Rohan S. Kale
of SVERI's College of Engineering, Pandharpur, Maharashtra
for participating and presenting a research paper in the TEQIP-III, BPUT Odisha (ATU) sponsored Two-day National Conference on "Mechanical, Materials and Renewable Energy Technology" held on 10th & 11th January 2020 in the Department of Mechanical Engineering, Einstein Academy of Technology & Management, Bhubaneswar, Odisha, India.

Given this on the 11th day of January Two Thousand Twenty at Bhubaneswar, Odisha, India.

Prof. (Dr.) Ranjan Kumar Jena
Coordinator, TEQIP-III, BPUT Odisha (ATU)

Dr. Bhabani Prasanna Pattanaik
Convener, NCMMRET-2020

Prof. (Dr.) Suwendu Prasad Sahu
Principal, EATM, Bhubaneswar



In association with
VTU & AKU



TEQIP-III, BPUT ODISHA (ATU)
&
EINSTEIN ACADEMY OF TECHNOLOGY & MANAGEMENT
(NAAC B++ Grade Engineering Institution)

Present this

Certificate of Participation

To

Prof. / Dr. / Mr. / Ms. Mudasar M. Bagwan & Vedant D. Mangrulkar
of SVERI's College of Engineering, Pandharpur, Maharashtra
for participating and presenting a research paper in the TEQIP-III, BPUT Odisha (ATU) sponsored Two-day National Conference on "Mechanical, Materials and Renewable Energy Technology" held on 10th & 11th January 2020 in the Department of Mechanical Engineering, Einstein Academy of Technology & Management, Bhubaneswar, Odisha, India.

Given this on the 11th day of January Two Thousand Twenty at Bhubaneswar, Odisha, India.

Prof. (Dr.) Ranjan Kumar Jena
Coordinator, TEQIP-III, BPUT Odisha (ATU)

Dr. Bhabani Prasanna Pattanaik
Convener, NCMMRET-2020

Prof. (Dr.) Suwendu Prasad Sahu
Principal, EATM, Bhubaneswar



In association with
VTU & AKU



TEQIP-III, BPUT ODISHA (ATU)
&
EINSTEIN ACADEMY OF TECHNOLOGY & MANAGEMENT
(NAAC B++ Grade Engineering Institution)

Present this

Certificate of Participation

To

Prof. / Dr. / Mr. / Ms. Anati Gajanan Lale & Dhanashree Bhanat Sonawane
of SVERI's College of Engineering, Pandharpur, Maharashtra

for participating and presenting a research paper in the TEQIP-III, BPUT Odisha (ATU) sponsored Two-day National Conference on "Mechanical, Materials and Renewable Energy Technology" held on 10th & 11th January 2020 in the Department of Mechanical Engineering, Einstein Academy of Technology & Management, Bhubaneswar, Odisha, India.

Given this on the 11th day of January Two Thousand Twenty at Bhubaneswar, Odisha, India.

Prof. (Dr.) Ranjan Kumar Jena
Coordinator, TEQIP-III, BPUT Odisha (ATU)

Dr. Bhabani Prasanna Pattanaik
Convener, NCMMRET-2020

Prof. (Dr.) Savendu Prasad Sahu
Principal, EATM, Bhubaneswar



In association with
VTU & AKU



TEQIP-III, BPUT ODISHA (ATU)
&
EINSTEIN ACADEMY OF TECHNOLOGY & MANAGEMENT
(NAAC B++ Grade Engineering Institution)

Present this

Certificate of Participation

To

Prof. / Dr. / Mr. / Ms. Namrata Raju Panvat & Vaishnavi Mahesh Lakheri
of SVERI's College of Engineering, Pandhanpur, Mahanastira

for participating and presenting a research paper in the TEQIP-III, BPUT Odisha (ATU) sponsored Two-day National Conference on "Mechanical, Materials and Renewable Energy Technology" held on 10th & 11th January 2020 in the Department of Mechanical Engineering, Einstein Academy of Technology & Management, Bhubaneswar, Odisha, India.

Given this on the 11th day of January Two Thousand Twenty at Bhubaneswar, Odisha, India.

Prof. (Dr.) Ranjan Kumar Jena
Coordinator, TEQIP-III, BPUT Odisha (ATU)

Dr. Bhabani Prasanna Pattanaik
Convener, NCMMRET-2020

Prof. (Dr.) Suvendu Prasad Sahu
Principal, EATM, Bhubaneswar



In association with
VTU & AKU



TEQIP-III, BPUT ODISHA (ATU)
&
EINSTEIN ACADEMY OF TECHNOLOGY & MANAGEMENT
(NAAC B++ Grade Engineering Institution)

Present this

Certificate of Participation

To

Prof. / Dr. / Mr. / Ms. Gauri R. Gore & Shivani S. Kothawale
of SVERI's College of Engineering, Pandharpur, Maharashtra
for participating and presenting a research paper in the TEQIP-III, BPUT Odisha (ATU) sponsored Two-day National Conference on "Mechanical, Materials and Renewable Energy Technology" held on 10th & 11th January 2020 in the Department of Mechanical Engineering, Einstein Academy of Technology & Management, Bhubaneswar, Odisha, India.

Given this on the 11th day of January Two Thousand Twenty at Bhubaneswar, Odisha, India.

Prof. (Dr.) Ranjan Kumar Jena
Coordinator, TEQIP-III, BPUT Odisha (ATU)

Dr. Bhabani Prasanna Pattanaik
Convener, NCMMRET-2020

Prof. (Dr.) Suwendu Prasad Sahu
Principal, EATM, Bhubaneswar



In association with
VTU & AKU



TEQIP-III, BPUT ODISHA (ATU)
&
EINSTEIN ACADEMY OF TECHNOLOGY & MANAGEMENT
(NAAC B++ Grade Engineering Institution)

Present this

Certificate of Participation

To

Prof. / Dr. / Mr. / Ms. Anjali P. Gavali & Pranoti R. Bhosale
of SVERI's College of Engineering, Pandharpur, Maharashtra
for participating and presenting a research paper in the TEQIP-III, BPUT Odisha (ATU) sponsored Two-day National Conference on "Mechanical, Materials and Renewable Energy Technology" held on 10th & 11th January 2020 in the Department of Mechanical Engineering, Einstein Academy of Technology & Management, Bhubaneswar, Odisha, India.

Given this on the 11th day of January Two Thousand Twenty at Bhubaneswar, Odisha, India.

Prof. (Dr.) Ranjan Kumar Jena
Coordinator, TEQIP-III, BPUT Odisha (ATU)

Dr. Bhabani Prasanna Pattanaik
Convener, NCMMRET-2020

Prof. (Dr.) Suwendu Prasad Sahu
Principal, EATM, Bhubaneswar



In association with
VTU & AKU



TEQIP-III, BPUT ODISHA (ATU)
&
EINSTEIN ACADEMY OF TECHNOLOGY & MANAGEMENT
(NAAC B++ Grade Engineering Institution)

Present this

Certificate of Participation

To

Prof. / Dr. / Mr. / Ms. Athnav M. Kulkarni & Madan K. Patil
of SVERI's College of Engineering, Pandharpur, Maharashtra
for participating and presenting a research paper in the TEQIP-III, BPUT Odisha (ATU) sponsored Two-day National Conference on "Mechanical, Materials and Renewable Energy Technology" held on 10th & 11th January 2020 in the Department of Mechanical Engineering, Einstein Academy of Technology & Management, Bhubaneswar, Odisha, India.

Given this on the 11th day of January Two Thousand Twenty at Bhubaneswar, Odisha, India.

Prof. (Dr.) Ranjan Kumar Jena
Coordinator, TEQIP-III, BPUT Odisha (ATU)

Dr. Bhabani Prasanna Pattanaik
Convener, NCMMRET-2020

Prof. (Dr.) Surendra Prasad Sahu
Principal, EATM, Bhubaneswar



In association with
VTU & AKU



TEQIP-III, BPUT ODISHA (ATU)
&
EINSTEIN ACADEMY OF TECHNOLOGY & MANAGEMENT
(NAAC B++ Grade Engineering Institution)

Present this

Certificate of Participation

To

Prof. / Dr. / Mr. / Ms. Aniket A. Bansode & Bandu A. Kamble
of SVERI's College of Engineering, Pandharpur, Maharashtra
for participating and presenting a research paper in the TEQIP-III, BPUT Odisha (ATU) sponsored Two-day National Conference on "Mechanical, Materials and Renewable Energy Technology" held on 10th & 11th January 2020 in the Department of Mechanical Engineering, Einstein Academy of Technology & Management, Bhubaneswar, Odisha, India.

Given this on the 11th day of January Two Thousand Twenty at Bhubaneswar, Odisha, India.

Prof. (Dr.) Ranjan Kumar Jena
Coordinator, TEQIP-III, BPUT Odisha (ATU)

Dr. Bhabani Prasanna Pattanaik
Convener, NCMMRET-2020

Prof. (Dr.) Surendu Prasad Sahu
Principal, EATM, Bhubaneswar

Number of students participated in International Conferences

A.Y. – 2019-20

Sr. No.	Title of Paper	Name of Authors	Name of Conference	National / International
1.	Parametric Study on CO2 LASER Machining of Wood	Anjali P. Gavali, Gauri R. Gore Pranoti R. Bhosale, Shivani S. Kothawale	International Virtual Conference on Recent Advances in Science, Engineering, Agriculture and Technology	International

PARAMETRIC STUDY ON CO₂ LASER MACHINING OF WOOD

Sandeep S. Wangikar¹, Anjali P. Gavali², Gauri R. Gore³, Pranoti R. Bhosale⁴, Shivani S. Kothawale⁵

Associate Professor¹ and UG Student^{2,3,4,5}, Department of Mechanical Engineering, SVERI's College of Engineering, Pandharpur, Maharashtra

ABSTRACT

Laser has been used to produce intricate parts very effectively and successfully. Wood components are becoming popular day by day. Therefore, it's needs of the era to work on different machining and engraving methods or processes employed for it. Co2 laser machining is one of the non-conventional machining processes which can be used effectively for engraving on different types of wood materials. The parametric study of wood materials by using co2 laser machining is discussed in this paper. The pilot experimentation is performed by varying the laser power and scanning speed. The artwork or logos are effectively produced on the wood using the laser machining up to required depth. In this work, cutting quality was evaluated by measuring the upper kerf width, the lower kerf width, the cut section roughness and the operating cost. The effect of each factor on the quality measures was determined. The optimal cutting combinations were presented in favors of high-quality process output and in favors of low material cost.

Keywords: CO2 laser machining, laser power, scanning speed, wood.

INTRODUCTION

Unconventional technologies have gradually found its place in wood machining. The justification for their deployment increases with the increasing demands for quality, machining accuracy and efficiency. CO₂ laser machining can be effectively used for engraving the different shapes on wood material. There are other techniques also available like CNC engraving, milling etc. The conventional methodology like hand graving using knife or some other tools is time consuming method and also less accurate for producing intricate parts or shapes on different types of wood.

CO₂ laser as a suitable tool is often used in industry for a cutting metal and non-metallic Material. It's application in the wood industry is primarily in the Cutting using a power laser beam and wood engraving. The principle of using the laser machining of the materials lies in focusing the laser beam on the surface of the material. The advantages that the laser cutting tool does not destroy and that laser beam can be focused to the diameter of several micrometers [1-6]. Various researchers have reported the similar type of study using different non-conventional machining processes like photochemical machining for the fabrication of different components [7-16].

The parameters considered in CO₂ laser machining were laser power, scanning speed etc. The analysis for effect of input parameters on the performance parameters like material removal rate, undercut, surface roughness has been suggested by means of researchers for the wood material. CO₂ laser machining is efficient not only in speed but also in accuracy. So, CO₂ laser machining is useful for fabrication micro channel. In this paper the square shaped microchannel is manufactured with the help of CO₂ laser machining with twelve different depths.

II. MATERIALS AND METHODS

A) The material selected for engraving is wood. It is cut in the required size and shape and kept ready for CO₂ laser machining or engraving.

At first, the design of the required configuration is prepared with the help of two-dimensional drawing in AutoCAD software. The designed diagram is acting as an input for a CO₂ laser machining. The CO₂ laser cut machining takes input as 2D CAD drawing in dxf format and it analyses the path of channel which is given in CAD drawing. The CO₂ laser machining setup is as depicted in fig. 1 and the component shape (area) which is required to be machined by CO₂ laser machining is presented in Figure 2.



Figure 1: CO2 Laser Machining Set-up

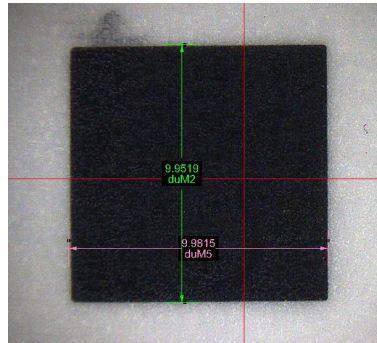


Figure 2: component shape (area) to be machined

B) SPECIFICATION

The specifications of CO2 Laser machine is as given below:

- Model- TIL6090
- Laser Type Sealed Hermetic CO2 Laser Tube
- Laser Power 60W/80W/100W
- Engraving Area 600 x 900 mm
- Accuracy ± 0.025 mm
- Power Supply 220 V $\pm 10\%$ / 50HZ.
- Gross Power 1800 watt. Approximate
- Cutting Speed 500 mm/S (Max)
- Engraving Speed 500 mm/S (Max)

III. RESULT & DISCUSSION

Using CO2 laser machining process, the pilot experimentation is carried out on wood material. The furthestmost vital parameters in CO2 laser cutting machine are chosen as laser scanning speed and power. The recorded depths for different scanning speeds at different power are recorded and presented in Table 1.

Table 1: Recorded Depth (in microns)

Power/Speed	100	125	150	175
30	1243	1035	898	725
40	1108	744	529	451
60	1538	1120	943	839
70	1565	1230	998	909

The depth of the engraved letters is observed to be increasing with increase in laser power as shown in Figure 3, while the finish of the engraved letters is noted as superior for increased laser scanning speed. The sample specimens of wood engraved using CO2 laser machining are demonstrated in Figure

4. Further, optimization of parameters is required to be studied for achieving the best combination of depth and surface finish of engraved parts.

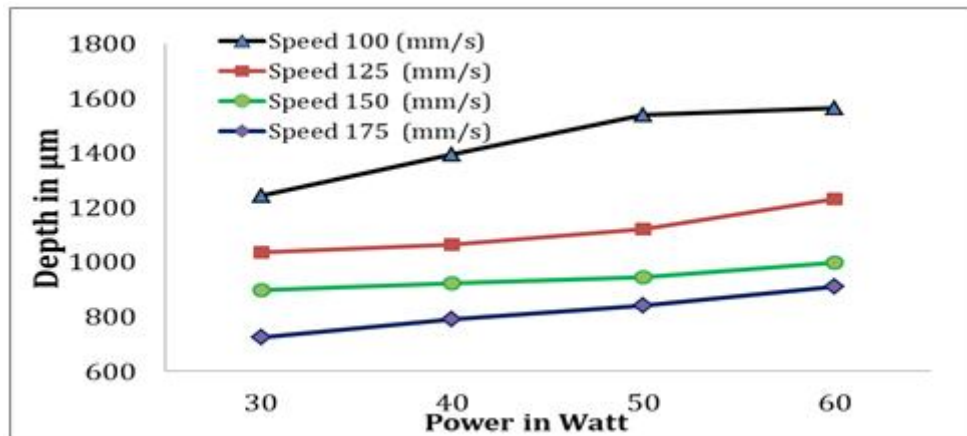


Figure 3: Effect of Power and Speed on depth

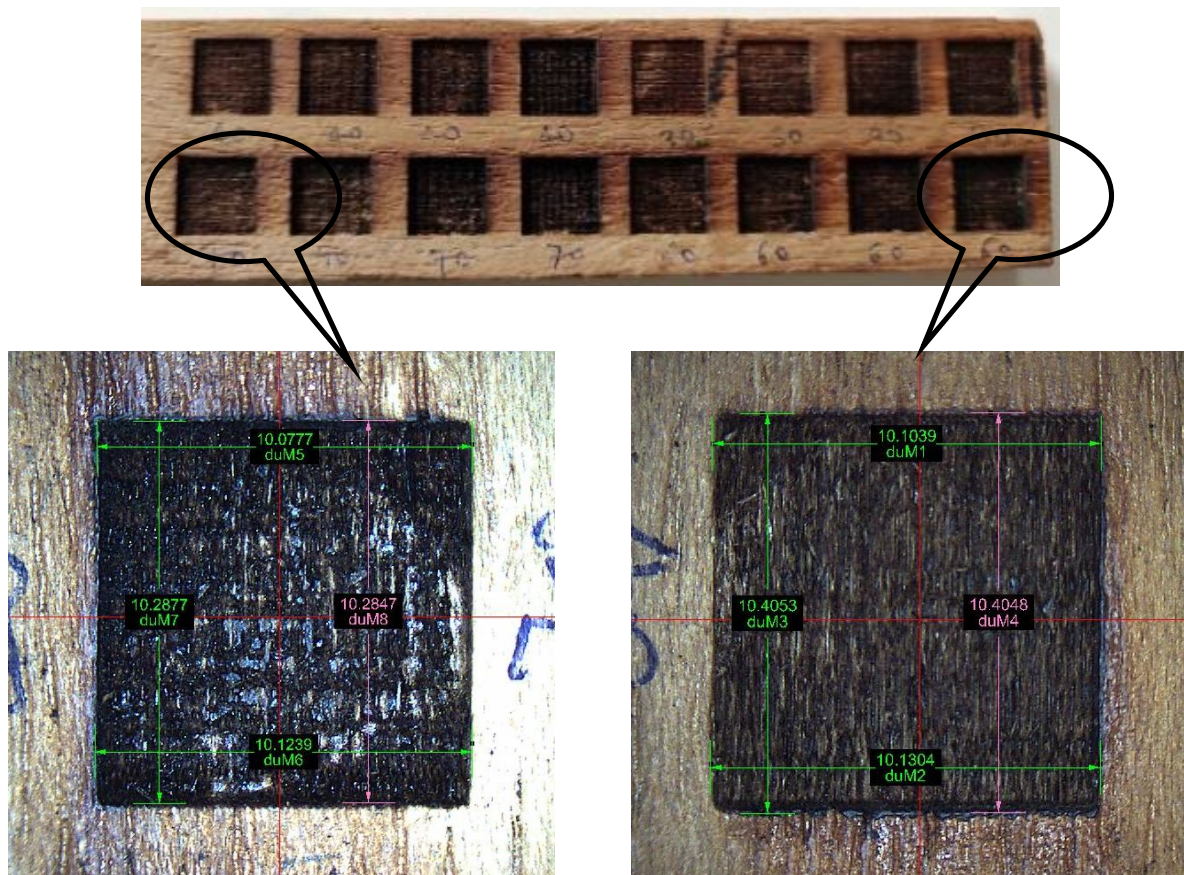


Figure 4: Sample engraved wood specimens

IV. CONCLUSION

The CO₂ laser machining is performed on wood material for engraving purpose. The machining is performed at different scanning speeds and power. The depth of the engraving is recorded. Based on the experimentation, following conclusions are drawn.

- The depth of engraving increases with increase in laser power.
- With increase in the scanning speed, the depth of the engraving is observed to be decreasing.
- The surface finish of the engraved wood component is noted to be increasing with increase in the scanning speed.

Thus, it can be concluded that CO₂ laser machining is effectively engraving on wood material. Further, there is scope for the optimization of process parameters which will produce higher depth with better surface finish.

REFERENCES

1. N.V.Chavan , R.M.Bhagwat, S.S. Gaikwad, S. S. Shete , D.T. Kashid and S.S.Wangikar, “ Fabrication & Characterization of Microfeatures onPMMA Using CO₂ Laser Machining,” International Journal for Trends in Engineering and Technology, vol. 36(1), pp.39-32,(2019).
2. H. Klank, J. P. Kutter and O. Geschke , “CO₂-Laser micromachining and back-end processing for rapid Production of PMMA-based microfluidic systems”, Lab on a Chip, vol. 2 pp.242–6, (2002).
3. A. Ā. Choudhury and S. Shirley,”Optics & Laser Technology Laser cutting of polymeric materials: An experimental investigation,”Optics and Laser Technology, vol. 42, no. 3, pp. 503–508, (2010).
4. A Gerlach, G. Knebel, A. E. Guber, M Hecke, D.Herrmann., A. Muslija, and T.H. Sshaller,”Microfabrication of single-use plastic microfluidic devices for high-throughput screening and DNA analysis,” Microsystem Technologies, vol. no.5-6, pp.265-268, (2002).
5. O. Rotting, W. Ropke, H. Becker and C. Gartner,”Polymer microfabrication technologies,” Microsystem Technologies, Vol.8, pp.32–36, (2002).
6. H. Qi, T. Chen, L. Yao and T. Zuo, “Micromachining of microchannel on the polycarbonate substrate with CO₂ laser direct-writing ablation,”vol. 47, pp. 594–598, (2009).
7. S.S.Wangikar,P.K. Pattowari and R.D. Mishra, “ Effect of process parameters and optimization for photochemical machining of brass and germen silver,” Materials and Manufacturing Processes, vol.32(15), pp.1747-1755,(2017).
8. S.S.Wangikar, P.K.Patowari, and R.D.Misra, “Parametric Optimization for Photochemical Machining of Copper Using Grey Relational Method,”In Techno-Societal 2016,International Conference on Advanced Technologies for Societal Applications , pp.933-943, Springer(December 2016).
9. S.S.Wangikar,P.K. Patowari, and R.D.Misra,” Parametric Optimization for Photochemical Machining of Copper using Overall Evaluation Criteria,” Materials Today Proceedings, vol 5(2), pp.4736-4742, (2016).
10. R. R. Gidde, P. M. Pawar, B. P. Ronge, A. B. Shinde, N. D.Misal and S. S. Wangikar, “Flow field analysis of a passive wavy micromixer with CSAR and ESAR elements,”Microsystem Technologies, vol. 25, (2019).
11. S. S. Wangikar, P. P. Patowari, R. D. Misra, and N. D.Misal,“Photochemical Machining: A Less Explored Non-Conventional Machining Process,” In Non-Conventional Machining in Modern Manufacturing Systems, pp. 188-201,(2018).
12. S. S. Das, S. D. Tilekar, S. S. Wangikar, and P. K. Patowari,“Numerical and experimental study of passive fluids mixing in micro-channels of different configurations,”Microsystem Technologies, Vol. 23(12), pp. 5977-5988, (2018).
13. S. S. Wangikar, P. K. Patowari and R. D. Misra, “Numerical and experimental investigations on the performance of a serpentine microchannel with semicircular obstacles”, Microsystem Technologies, Vol. 24(8), pp.3307-3320, (2018).
14. S. V. Jadhav, P. M. Pawar, A. B. Shinde and S. S. Wangikar, “Performance Analysis of Elliptical Pin Fins in the Microchannels”In Techno-Societal 2018, pp. 295-304, Springer, Cham.
15. H. D. Kulkarni, A. B. Rasal, O. H. Bidkar, V. H. Mali, S. A. Atkale, S. S. Wangikar and A. B. Shinde, “Fabrication of Micro-Textures on Conical Shape Hydrodynamic Journal Bearing”, International Journal for Trends in Engineering and Technology, Vol. 36(1), pp.37-41, (2019).
16. M. A. Raut, S. S. Kale, P. V. Pangavkar, S. J. Shinde, S. S. Wangikar, S. V. Jadhav and D. T. Kashid, “Fabrication of Micro Channel Heat Sink by using Photo Chemical Machining” International Journal of New Technology and Research, Vol. 5(4), pp.72-75, (2019).

Papers published in Peer reviewed journals

A.Y. – 2019-20

Sr. No.	Title of Paper	Name of Authors	Name of Journal	ISSN/ISBN No.
1.	Fabrication of Microchannels having Different Obstacles Using Photo Chemical Machining process	Mansi M. Kame, Manali V. Sarvagod, Pooja A. Namde, Supriya C. Makar,	NOVYI MIR Research Journal	ISSN : 0130-7673
2.	Vibration Analysis and Fault Diagnosis of Injection Molding Machine	Pruthvijit V. Gaikwad, Suhas S. Phalake, Sagar N. Gaikwad, BhushanP. Sawant,	NOVYI MIR Research Journal	ISSN : 0130-7673
3.	Static & Dynamic Research of Composite Blade using Condition Monitoring Method	Akshay A. Hake, Nagesh S. Ronge, Vijay A. Bhingare,	International Journal of Recent Technology and Engineering	ISSN: 2277-3878
4.	Material on a Diet: Study and Investigation of Aluminum – Fly Ash Metal Matrix Composite	Prathamesh Mhamanea, Shubham Kadam, Viraj Phanse,	Science Direct Materials Today: Proceedings 24 (2020)	ISSN: 2214-7853
5.	Comparative CFD Analysis of Mini Impeller using different Materials	Ashutosh B. Deshmukh, Aditya Lotake, Hrushikesh Paricharak,	Science Direct Materials Today: Proceedings 24 (2020)	ISSN: 2214-7853
6.	Design of Mini Abrasive Vertical Belt Grinding Machine	Rahul Khadtare, Pravin Chavan, Govind Wagh, Shubham Atkale	AEGAEUM Journal	ISSN: 0776-3808
7.	Performance Evaluation Of VCRC By Using R134a And R600a Refrigerants: A Study	Mahesh Ghodake, Avinash Devmare, Chaitanya Kawale, Sachin Gosavi	AEGAEUM Journal	ISSN: 0776-3808
8.	Superiority of Graphene over Activated Carbon in terms of Adsorption Capacity, Proposed Mechanism and Interaction with Metal Ions and Biological Particulates	Debojeet Bhattacharjee,	AEGAEUM Journal	ISSN: 0776-3808
9.	Design of an Earth Air Heat Exchanger System for Space Cooling in Hot and Dry Climate of Pandharpur, India	Vishal Kadam, Suraj Shende, Pankaj Kate, Vishal Waghmare, Onkar Patil	AEGAEUM Journal	ISSN: 0776-3808

10.	A Review on Heat Transfer Enhancement of Wavy Fin and Tube Heat Exchanger by Using Vortex Generator's	Sagar B. Khade, Vikram D. Vhanmane, Sunil M. Torane, Adarsh V. Chavan,	AEGAEUM Journal	ISSN: 0776-3808
11.	A Literature review of MR Damper - Design and Analysis	Rohan Haridas Pore, Arohan Anandrao Jadhav, Sakharam Ekanath Dhat, Amit Bandu Pardeshi,	AEGAEUM Journal	ISSN: 0776-3808
12.	Development of Pick And Place Robot	Samadhan J. Shinde Dhanashree Sonawane, Arati Lale, Namrata Parvat, Vaishnavi Lakheri.	AEGAEUM Journal	ISSN: 0776-3808
13.	Study of Etchant Concentration Effect on the Edge Deviation for Photochemical Machining of Copper	Rushikesh M. Bhagwat, Suraj S.Gaikwad, Shivam S.Shete, Nikhil V.Chavan	NOVYI MIR Research Journal	ISSN No: 0130-7673
14.	Fabrication of Split and Recombing Microchannel Mold Using Photochemical Machining	Mansi Ghogale, Mansi Bhumka, Sonali Chavan, Muskan Attar	AEGAEUM JOURNAL	ISSN NO: 0776-3808

Fabrication of Microchannels having Different Obstacles Using Photo Chemical Machining process

Mansi M. Kame¹, Manali V. Sarvagod², Pooja A. Namde³, Supriya C. Makar⁴,
Subhash V. Jadhav⁵, Sandeep S. Wangikar⁶

^{1,2,3,4,5, 6}Department of Mechanical Engineering, SVERI's College of Engineering, Pandharpur,

Maharashtra, India-413304

¹mansimakme@coep.sveri.ac.in, ²manalivsarvagod@coep.sveri.ac.in, ³poojaanamde@coep.sveri.ac.in,

⁴supriyacmakar@coep.sveri.ac.in, ⁵svjadhav@coe.sveri.ac.in, ⁶sswangikar@coe.sveri.ac.in.

Abstract: Microchannels are widely used in many applications like micro fluidic, medical, biological and industrial applications. Microchannels are those channels having dimensions, less than one mm and greater than one micron. There are many methods to fabricate the microchannels, and it depends on the material on which microchannels are to be fabricated and the fabrication process used. There are many traditional and nontraditional methods for the fabrication of different microchannels. There are many materials which are used to manufacture the microchannels like glass, silicon, polymer, copper, aluminum, brass, etc. In this study, the copper microchannels are fabricated, having different shapes of obstacles by the photochemical machining process. Configuration of the obstacles, affect the microchannels performance. Based on this study, we conclude that the photochemical machining is one of the simplest and low-cost fabrication processes for the fabrication of microchannels.

Keywords – Micro Channel, Photochemical Machining.

1. INTRODUCTION

1.1. Microchannel

Usually a photochemical is defined as a channel whose dimension is less than one millimetre and greater than one micron. Microchannels have characteristic sizes in the range of submicron scale [1]. Above one millimetre the fluid flow exhibits behaviour that is the same as a macroscopic but flow at the microscopic level may differ from that of a macroscopic scale. Microchannels can be fabricated using different materials. Glass, polymers, silicon, metals, etc. can be used for the same. [2] The fabrication can be done using various processes. Surface and bulk micromachining, molding, embossing, and conventional machining with micro cutters are some of them. Microchannels have many advantages due to their high surface-to-volume ratio and their small volumes [3]. The large surface-to-volume ratio leads to a high rate of heat and mass transfer. It is observed that both the type of fabrication method used and the dimensions affect their performance.

1.2. Fabrication methods

Both conventional and nonconventional methods can fabricate microchannels. But as we know that the parameters like shape, surface finish, diameter, length, height etc. adversely affects the performance of the microchannels. The non-conventional method is generally proffered to avoid or minimise these effects on microchannels. One of the easiest ways of fabrication is the Photo Chemical Machining process. The fabrication aspect of microchannels and suitable processes have been reported by different researchers [4-8]. Various fabrication methods like Micro Cutting, (Wet and Dry) Etching, Lithography, embossing and molding are used for the fabrication of microchannels.

*Subhash V. Jadhav, *Sandeep S. Wangikar

1.3. Photo Chemical Machining Process

One of the widely used nonconventional machining processes is the Photochemical machining (PCM). This process is also called as photo etching or photochemical milling or photo fabrication. PCM employs a chemical milling for fabricating the components. This process is done on sheet metals using a photoresist and etchants (solvents) to machine away selected areas corrosively [2]. Until now, many researchers have studied and published papers related to the work, efficiency properties and performance of the microchannels [1-2]. The PCM procedure depends on the amalgamation of photoresist imaging and substance carving [1]. Figure.1 shows the machine which can be used to pass the ultraviolet rays through the material. In this process, the different features are manufactured by dissolving away metal. Absence of burrs, residual stresses, changes in magnetic and mechanical properties is the characteristics of these processes. No change in hardness or ductility happens due to this process. PCM method is mainly used to produce thin, complex, 2-D parts due to its ease of creating a complex product with low cost and less delivery time apart from other advantages.



Figure.1: Experimental Setup

1.4. Photochemical Procedure

Photochemical Process is as per given below [9-13]:

- The procedure begins with the printing of the required shape on the photo film, which is called Photo Tool. The required shape should be accurate in dimension. So that Printing and further process will be correct.
- Material is selected as per the availability, requirement, customer need and application of the microchannel. Copper, aluminium, Brass, Glass are some of the materials that can be used materials for the microchannels.
- The photoresist is then applied to the material or specimen. Photoresists are mostly used in making of the microcircuits. The photoresist is those substances which loses its resistance when it comes in contact with an etchant or solvent. There are two types of photoresist used for the process. It can be Positive photoresist or Negative photoresist. Photoresist absorbs the ultraviolet rays passing through the photo tool.
- The developer is applied to the specimen to expose the required area for the etching process.
- By corrosion phenomenon, material removal takes place in etching using Ferric chloride or cupric chloride as an etchant.
- After taking specimen out from the machine, we cleaned by water and here we got the components by using Photochemical machining.

2.1. Material selection:

- In this paper, we have used the copper as a material for the fabrication of microchannel. As we all know that copper has a wide range of use, easy availability and high accuracy. The optimum set of parameters for PCM of copper has been given, which will be helpful for further research in this area [9].

2. Fabrication of Microchannels

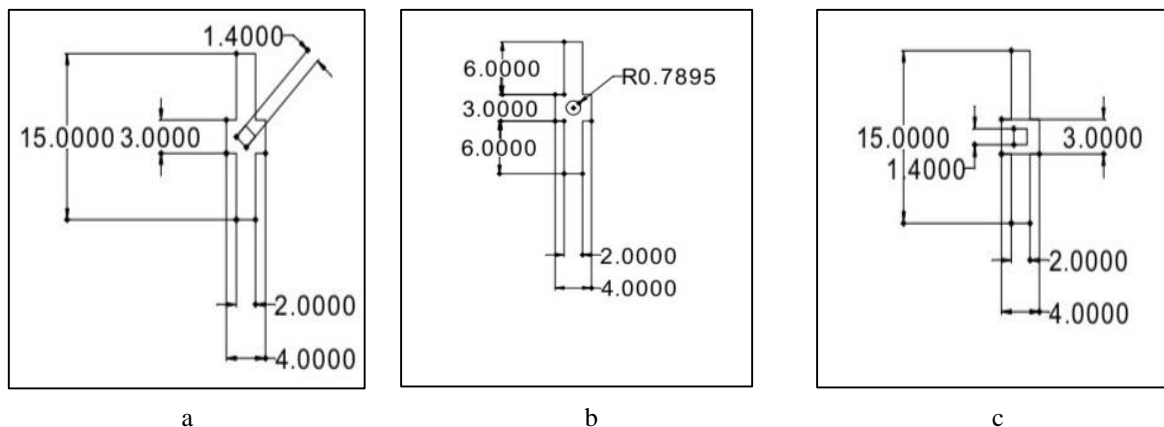
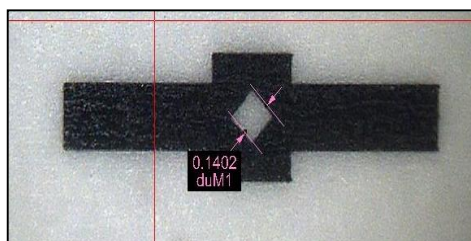
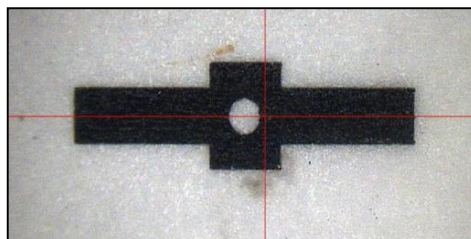


Figure 2: Dimensions Of Different Components

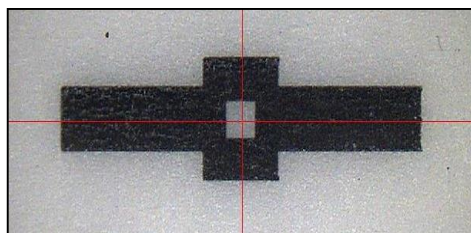
- a) Microchannel with a diamond shape obstacle. b) Microchannel with circle shape obstacle. c) Microchannel with a square shape obstacle.



a



b



c

Figure.3: Photo Tools

- a) For Diamond Obstacle. b) For circle obstacle. c) For a square obstacle.

2.2. Experimental Setup:

The experimental set up used for the photochemical machining is presented in Figure1. Ferric chloride is used as an etchant for this. The temperature kept constant 41°C for all specimens and time as 15 minutes for the same. Photo tool of the CAD drawing is made by taking print on transparent paper. The etching is done on the specimens. A CAD drawing of the specimens are shown in figure.2 as following with different obstacles in a microchannel:

Figure 2.a shows the microchannel with diamond shape obstacle with the same length of a side, i.e. 1.4 mm. In this microchannel, a square obstacle is tilted by 45° to the horizontal plane. Figure 2.b shows the microchannel having circular obstacle which radius is 0.7895 mm. Figure 2.c shows the microchannel with square shape obstacle having a length, i.e. 1.4 mm. Photo tool for the above components is shown in Figure.3. This Photo tool is printed on the tress paper, which is very sensitive [2].

3. Result and Discussion

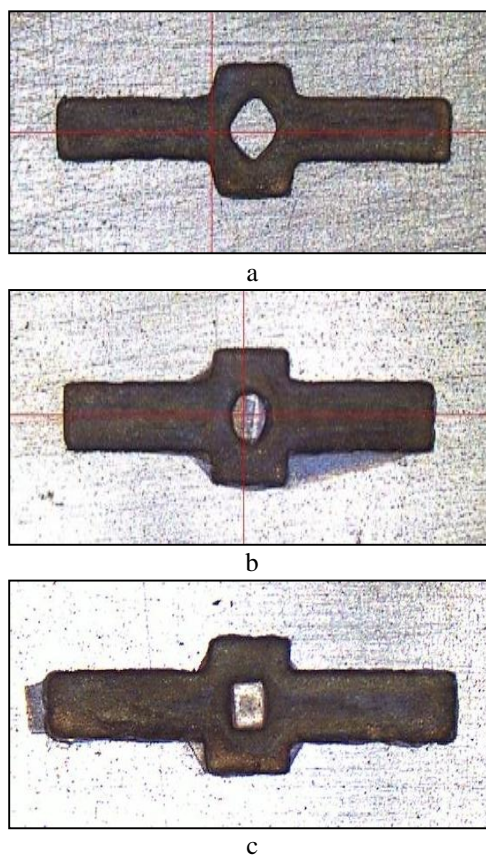


Figure.4: Fabricated Microchannels

a) Microchannel with Diamond shape obstacle. b) Microchannel with a circular obstacle. c) Microchannel with a square obstacle.

To get the precise size and shape of the fabricated part, by PCM process, it needs to keep control of the time and temperature of etchant. Temperature and time affect the variation in depth variation. There is the difference between ideal measurements and actual measurement, i.e. error.

Thus the specimens can be made by using the PCM process. The practical result after the procedure is shown in Figure.4. Fabrication of micro channel by using photochemical machining:

4. Conclusion

PCM is a high quality, fast processing, economical and simple machining process. In this paper, microchannels are fabricated by using a photochemical machining process. After characterisation of the fabricated specimens, it is observed that to ensure proper control and finish of the component being etched; it is essential that the parameters like time and temperature are appropriately controlled. Different etchant concentration requires different timing and temperature. Therefore, there is scope for further optimisation of these parameters for understanding the relationship between the time. Temperature and concentration in the photochemical machining process¹.

5. References

- [1]. M. A. Raut, S. S.Kale, P. V.Pangavkar, S. J. Shinde, S. S.Wangikar, S. V. Jadhav and D. T. Kashid, "Fabrication Of Microchannel Heat Sink By Using Photochemical Machining", *Journal of New Technology and Research.*, vol.3, no.12, (2017), pp.1-4.
- [2]. C. V. Vhare, V. R. Chavan, A. A. Shinde, R. D.Solage and S. S.Jadhav, "Edge Deviation Analysis For Photochemical Machining Of Copper", *Journal of New Technology and Research.*, vol.3, no.12, (2017), pp.1-3.
- [3]. A. A. Khan and K. Y. Kim, "Evaluation of various channel shapes of a microchannel heat sink", *Journal of Air-Conditioning and Refrigeration.*, vol.24, no.3,(2016), pp.2-9.
- [4]. S. S. Wangikar, P. K. Patowari and R. D. Misra, "Effect of process parameters and optimisation for photochemical machining of brass and German silver Materials and Manufacturing Processes", *Vol .32, no.15, (2017). Pp.1747-1755.*
- [5]. S. S. Wangikar, P. K. Patowari and R. D. Misra, " Parametric Optimization for Photochemical Machining of Copper Using Grey Relational Method", *Journal In Techno-Societal 2016, International Conference on Advanced Technologies for Societal Applications, (2016), December. pp. 933-943.*
- [6]. S. S. Wangikar, P. K. Patowari and R. D. Misra, " Parametric Optimization for Photochemical Machining of Copper using Overall Evaluation Criteria", *Journal in Materials Today Proceedings. Vol.5, no.2, (2018), pp.4736-4742.*
- [7]. S. S. Wangikar, P. K. Patowari, R. D. Misra. And N. D. Misal, " Photochemical Machining: A Less Explored Non-Conventional Machining Process. In Non-Conventional Machining in Modern Manufacturing Systems," *Journal in IGI Global, (2019), pp.188-201.*
- [8]. Misal, N. D., & Sadaiah, M. (2017). Investigation on Surface Roughness of Inconel 718 in Photochemical Machining. *Advances in Materials Science and Engineering, 2017.*
- [9]. Misal, N. D., Saraf, A. R., & Sadaiah, M. (2017). Experimental investigation of surface topography in photochemical machining of Inconel 718. *Materials and Manufacturing Processes, 32(15), 1756-1763.*
- [10]. Wangikar, S. S., Patowari, P. K., & Misra, R. D. (2018). Numerical and experimental investigations on the performance of a serpentine microchannel with semicircular obstacles. *Microsystem Technologies. 24(8), 3307-3320.*
- [11]. Das, S. S., Tilekar, S. D., Wangikar, S. S., & Patowari, P. K. (2017). Numerical and experimental study of passive fluids mixing in micro-channels of different configurations. *Microsystem Technologies, 23(12), 5977-5988.*

- [12]. Chavan, N. V., Bhagwat, R. M., Gaikwad, S. S., Shete, S. S., Kashid, D. T., & Wangikar, S. S. (2019). *Fabrication & Characterization of Microfeatures on PMMA Using CO2 Laser Machining*. *International Journal for Trends in Engineering and Technology*. 36(1), 39-32.
- [13]. Kulkarni, H. D., Rasal, A. B., Bidkar, O. H., Mali, V. H., Atkale, S. A., Wangikar, S. S., & Shinde, A. B. (2019). *Fabrication of Micro-Textures on Conical Shape Hydrodynamic Journal Bearing*. *International Journal for Trends in Engineering and Technology*. 36(1), 37-41.

Vibration Analysis and Fault Diagnosis of Injection Molding Machine

¹Pruthvijit V. Gaikwad, ²Suhas S. Phalake, ³Sagar N. Gaikwad,
⁴Bhushan P. Sawant, ⁵Sandipraj Y. Salunkhe, ⁶Digambar T. Kashid

^{1,2,3,4,5,6}SVERI's College of Engineering, Pandharpur, Maharashtra, India-413304
pruthvijitgaikwad@gmail.com, suhasp0303@gmail.com, gaikwadsagar9655@gmail.com,
bpsawant@outlook.com, sysalunkhe@coe.sveri.ac.in, dtkashid@coe.sveri.ac.in

Abstract: Plastic molded components find widespread domestic and industrial application as it is an essential factor in the weight reduction of the machine components are the one which are exposed the most towards getting damaged and failure. In industrial applications, these components are considered as a critical mechanical component and a defect in such a components, unless detected in time, causes malfunction and may even lead to catastrophic failure of machinery which results in significant time and economic loss. These types of failures might take place during the manufacturing process. Therefore it is important to review the problem and monitor the condition of the injection molding machine so that the details of failure would occur before any harsh consequences take place. Therefore early detection and indication are necessary for the safety and reliability of the device. This paper describes various vibration monitoring techniques suitable to analyze the defect in the injection molding machine. By performing this test, these techniques would reveal information about the progressing faults. From the different maintenance techniques, conditioning monitoring which is one of the techniques, and is highlighted. It uses the vibration having high frequencies which are generated from faulty components, is therefore investigated and compared. From the different conditioning monitoring techniques, the vibration analysis method is being elaborated and consequently utilized as a medium to fulfil the aim. An experimental set up is used to testify and investigate right parts and faulty parts by using different measurement tools pulse software, visteck analyzer to measure amplitude, sensors to obtain faulty signals. Also, the vibration signatures caused due to damages at moving parts are examined. The result indicates that defective parts have a substantial effect on the vibration spectrum. This paper, therefore, reveals frequencies domain signals from vibration analysis. Overall this paper has demonstrated that different techniques are useful in detecting the problems in injection molded machine components.

Keywords: Catastrophic Failure, Manufacturing Defect, Early Detection, High Frequency, Vibration Analysis, Visteck Analyzer.

1. INTRODUCTION

This deals with vibration analysis and fault diagnosis of a plastic injection molding machine. This is carried out to measure vibration frequencies occurring at different points and detecting the faults in the plastic injection molding machine. Plastic injection molding machines are typically subjected to very high levels of cyclic stresses, shocks and vibrations due to the nature of the injection molding process. As the injection molding process continues to develop and evolve, future injection molding machines will likely utilize faster injection times, thinner wall components, new materials with poorly understood failure characteristics, and higher injection pressures. This cyclic loading, shock, and vibration of the parts of the injection molding machine at high stress levels cause fatigue over time which, if undetected, can result in cracking, fracture, bending, or other damage within the injection molding machine. In some cases, catastrophic system failure of the injection molding machine can occur.

Vibration analysis is the most potent tool for fault diagnosis of the plastic injection molding machine. Acoustic analyzer captures the sound waves and analyze; this analysis helps to find faults and vibration generating in the parts like motor, ram, drive unit (gearbox), barrel and moving platen. There are different types of tools, with the help of which vibration analysis of these faults can be calculated and also

specific data can be obtained. Devices like vistec (amplitude meter), pulse software, different sensors, acoustic analyzer and more are used to measure the different parameter produce from the plastic injection molding machine. The vibration analysis technique gives the precise and early information about the failure with the help of this preventive information maintenance of the device can be done.

Following are the points, of which the vibration is measured,

- Motor: - This is the primary source of the generation of the vibration on the machine. This is used for the power supply of all the parts which are operating on a hydraulic unit like ram, moving platern, gearbox, mold clamping cylinder, injection cylinder, etc.
- Ram: - Injection molding machines use a ram or screw-type plunger to force molten plastic material into a mould cavity which creates vibrations. In screw type plunger these vibrations are slightly more. We measured the vibrations at the ram bearing.
- Drive unit: - This is the second major source of the vibration this contains various gear assembly in it, drive unit gives power to the injection cylinder, mold clamping cylinder and the hydraulic unit.
- Barrel: - The screw rotates inside the barrel and contains the molten plastic in it.
- Moving platern (Mold): - This Moving platern (mold) moves forward and backward for opening and closing of the mold cavity.

2. LITERATURE REVIEW

Beebe (2004) indeed stated that providing the required capacity for production at a lower cost is one of the vital purposes of maintenance in any industry. Therefore it should not be considered as a repair function, but it must be regarded as a reliability function [1]. For any organization which exists, production is one of the major reasons. Other organizations like hospitals, military transports, and buildings need their measures of ongoing success or output, but for batch production plants or any manufacturing industry, production is an evident process. If the reliability is high, the cost in making the machine is high and also its maintenance of service. Maintenance often includes machine replacement or upgrades. Maintenance management contributes significantly to the latter sector of manufacturing technology (Rao, 1996) [2]. Ross (2008, pp.5) described that there are some planned and unplanned types of maintenance [3]. Some of the techniques probably used in maintenance management are:

- Time based maintenance
- Conditioning based maintenance
- Preventive maintenance
- Breakdown maintenance
- Corrective maintenance

Garg and Krishna (1990) stated that the maintenance technique helps to select the measurable parameters associated with the machine, which either affect the condition of the device or manufacturing quality [4]. Hutton (1996) stated that more than twenty years ago, it was predicted that uses of these techniques would be quite common in the industry optimizing the way those large machines and processes will be maintained and managed [5]. In significant assets, conditioning monitoring tests can be scheduled prior schedule overhaul by setting computer-based, manual or maintenance management.

2.1 Condition Monitoring

Since last two decades, industries have spent a significant amount on conditioning monitoring to produce efficient instrumentation to minimize the various problem [5]. According to Hutton (1996), conditioning monitoring mostly focuses on the vibration data, including a sample of lubricant, temperature readings and measurement of shocks from rolling element bearing defects. Beebe (2004) defined conditioning monitoring as “conditioning monitoring on or off-line is a type of maintenance

inspection where an operational asset is monitored and the data obtained analyzed to detect signs of degradation, diagnose the cause of faults, and predict for how long it can be safely or economically run". There are several benefits of conditioning monitoring which potentially affects the improved productivity, maintenance cost and increased plant availability (Mathew and Alfredson, 1984) [6]. To analyze the conditioning monitoring, two different factors need to be considered; those factors are technical issues like measurement and analysis and organizational and environmental issues (Rao, 1996) [2].

3. EXPERIMENTAL SETUP

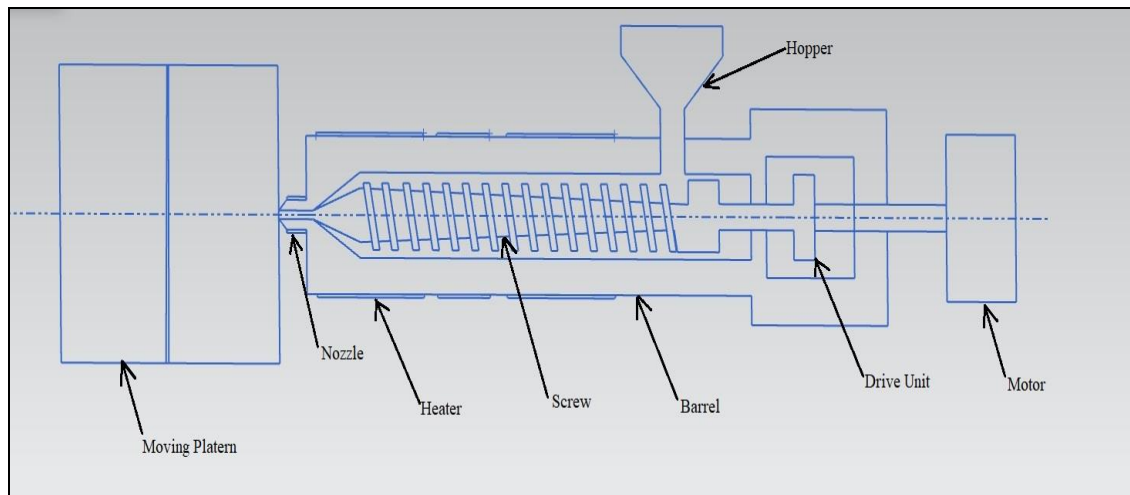


Figure 1: Schematic diagram of an injection-moulding machine

Experimentation is conducted on the actual machine, and vibration spectrums at various points of device are taken as follows, which is as shown in Fig. 1.

- Main Bearing of Motor: - Vibration level of motor and the connected shaft is measured at this location.
- Drive Unit/Gear Box: - Vibrations generated in the gearbox due to meshing of gears, vibrations are measured at this location.
- Ram: - Vibrations generated due to ram/screw plunger are measured at ram bearing.
- Barrel: - Vibrations generated in the barrel are measured on the barrel surface.
- Moving Platen (mold): - Vibrations generated in moving platen (mold) are measured on the top surface of its body.

3.1 FFT Analyzer

A FFT analyzer set up, used for the experimentation is as shown in Fig. 2. It is used to measure the magnitude of an input signal versus frequency within the full frequency range of the instrument. The primary use is to measure the power of the spectrum of known and unknown signals. The input signals that most common spectrum analyzers measure is electrical; however, spectral compositions of other signals, such as acoustic pressure waves and optical light waves, can be considered through the use of an appropriate transducer. Spectrum analyzers for different types of signals also exist, such as optical FFT analyzers which use direct optical techniques such as a monochromatic to make measurements. By analyzing the spectra of electrical signals, dominant frequency, power, distortion, harmonics, bandwidth, and other spectral components of a signal can be observed that are not easily detectable in time domain

waveforms. These parameters are useful in the characterization of electronic devices, such as wireless transmitters.

The display of a spectrum analyzer has frequency on the horizontal axis and the amplitude displayed on the vertical axis. To the casual observer, a spectrum analyzer looks like an oscilloscope and some lab instruments can function either as an oscilloscope or a FFT analyzer [7].

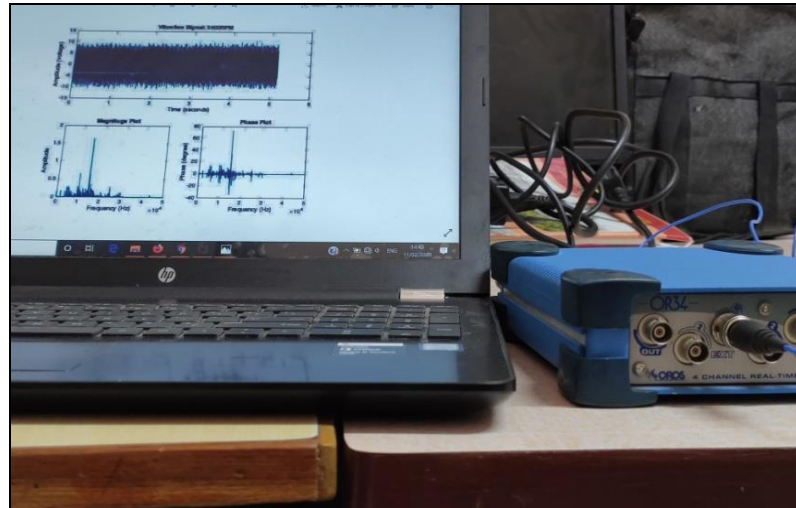


Figure 1: FFT Analyzer

4. RESULT AND ANALYSIS

The present study deals with the analysis of the effect of vibration on the performance and life of Plastic Injection Molding Machine. The investigation is carried out for bearing of a drive motor, screw/ram, gearbox, barrel, and moving platen.

4.1 Motor bearing: - Frequency FFT for the bearing is shown in Fig.3 using vibration analysis, any fault which may rise or has arisen on the bearing can be monitored continuously, and detailed analysis can be made regarding the health of motor bearing. Bearing distress changes in vibration pattern or it clear itself in vibration [8]. Therefore vibration analysis is one of the troubleshooting and most powerful diagnostic tools in major processing of bearing. When a motor is accelerated, more vibrations are generated, then the amplitude of vibration reaches its peak point as 0.36m/s^2 [9].

4.2 Drive Unit (Gear Box):- Frequency spectrum for drive unit (gearbox) is shown in Fig.4 this assembly is used for transferring required power to the hydraulic unit when the input from motor fluctuates or load on output fluctuates then it generates vibrations [10]. The amplitude reaches a peak value (0.685 m/s^2) when this kind of fluctuations occur.

4.3 Barrel: - Frequency spectrum for barrel is shown in Fig.5 unless you are running abrasive fillers screw wear is generally the result of metal-to-metal contact between the barrel liner and the screw flights. Wear can be quite slow or very rapid, depending on the contact force between the screw flight and the barrel liner and the lubricating effect of the polymer. Feed screw and barrel wear is an essential factor for maintenance and engineering departments in both extrusion and injection molding, and rightfully so. Excessive wear in a plasticating unit poses a litany of serious performance issues, naturally affecting cost and overall quality. It shows the amplitude of vibration as 1.15m/s^2 at the frequency of 161.9 Hz .

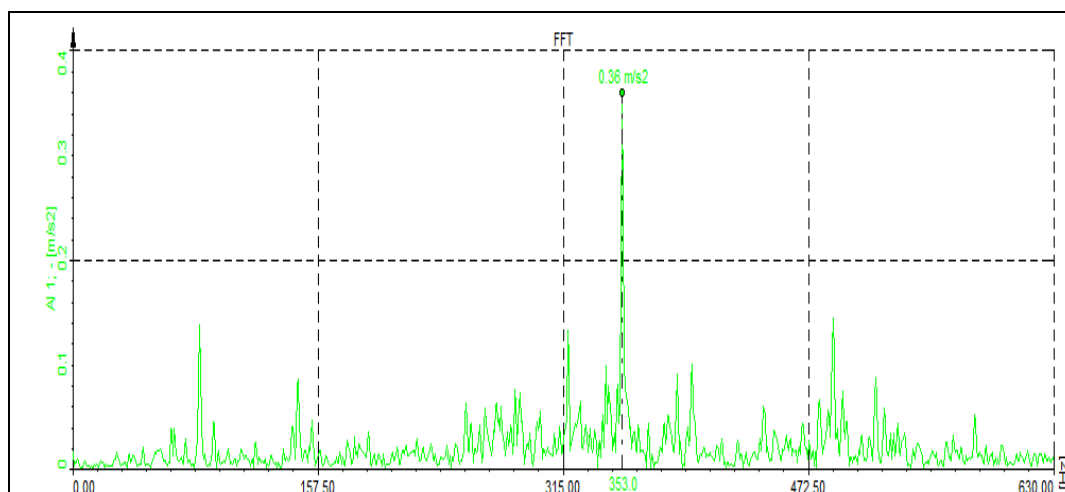


Figure 2: Frequency spectrum for bearing

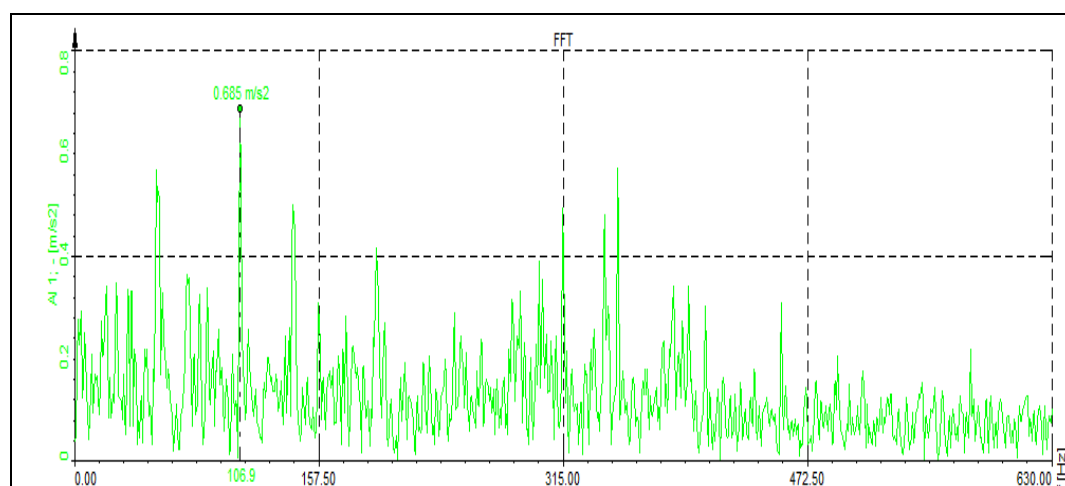


Figure 3: Frequency spectrum for drive unit (gearbox)

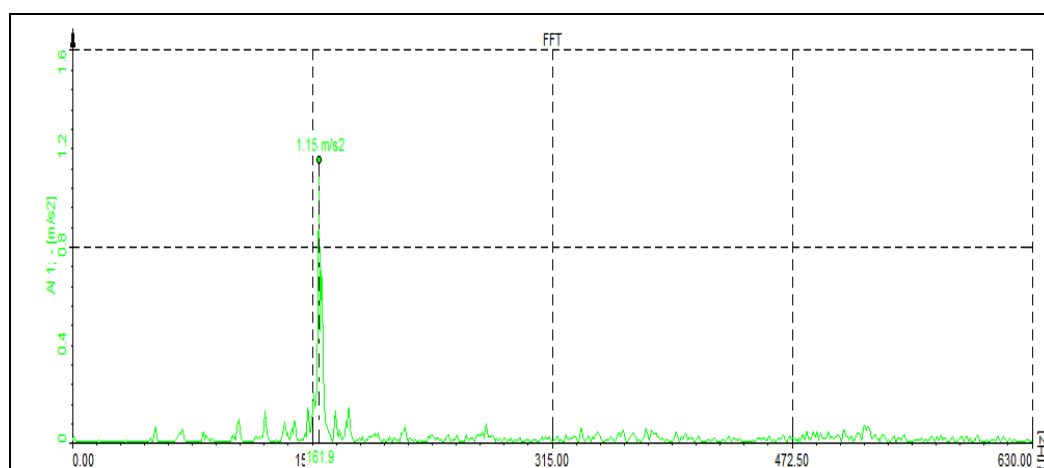


Figure 4: Frequency spectrum for barrel

4.4 Screw/Ram: - Frequency spectrum for screw/ram is shown in Fig.6 screws are generally made in four materials. viz Nitralloy nitride, D2, CPM 11V and Carbide. These materials handle just about any resins that can be used in the plastics industry. Nitralloy Nitride is the most common because it is used

on all general-purpose application and comes typically standard on all OEM machines. Nitalloy is very good on any mild material application without fillers or corrosives. It shows the amplitude of vibration as 1.91 m/s^2 with the frequency of 316.4 Hz.

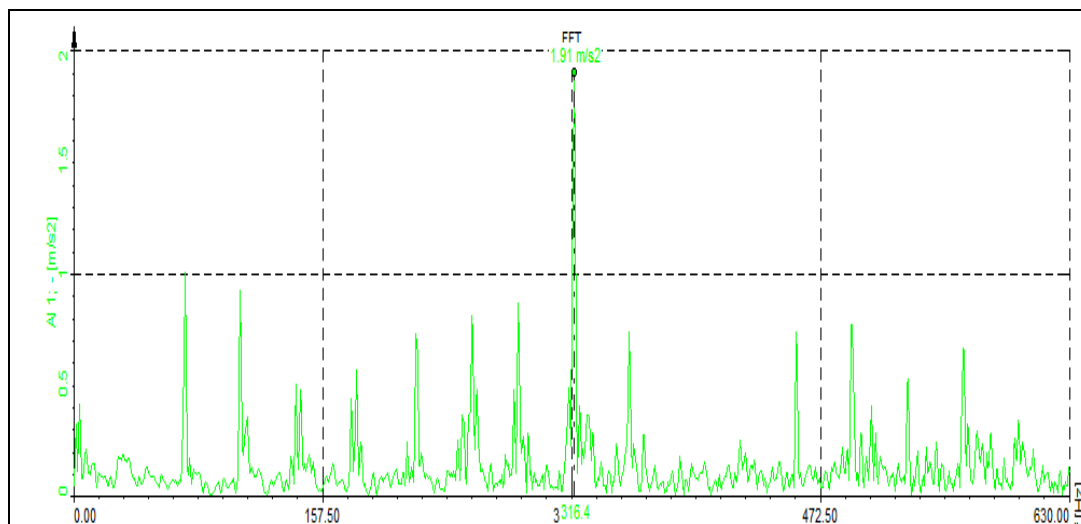


Figure 5: Frequency spectrum for screw/ram

4.5 Moving Platern: -Frequency spectrum for moving platrens screw thread is shown in Fig.7 because of the forward and backward motion of moving mold it generates vibrations which result in screw thread failures. It shows the value of the amplitude of vibration on FFT analyzer as 0.622 m/s^2 with the frequency of 70.31 Hz.

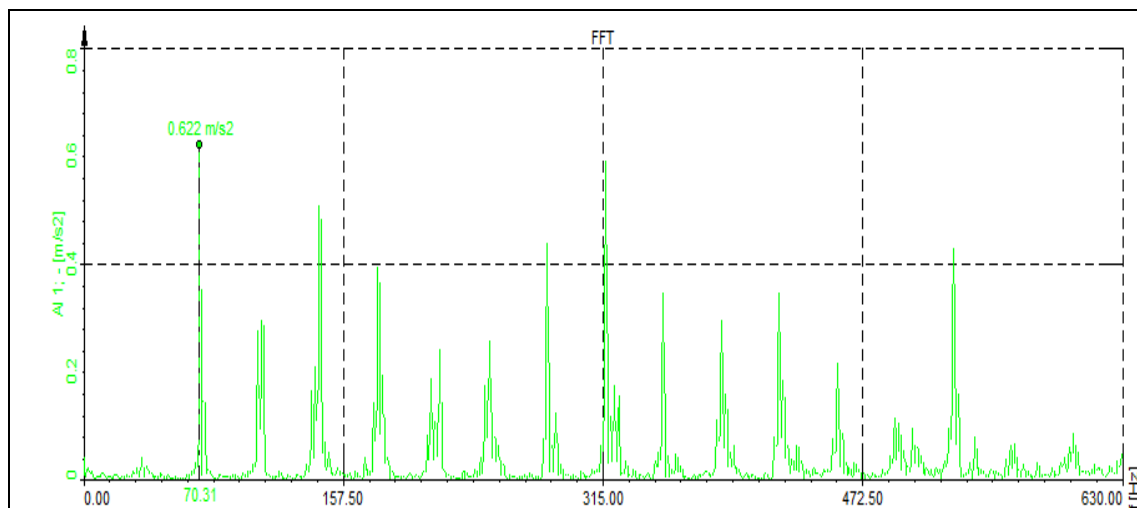


Figure 6: Frequency spectrum for moving platerns screw thread

3. CONCLUSION

From the analysis discussed above, it can be concluded that

- 1) Each graph shows the separate characteristics of vibration and indicates a fault. Spectrum analysis is a better tool for the identification of defects in machinery.
- 2) Early detection of faults is possible in vibration analysis.
- 3) This early detection of faults will lead in avoiding breakdown results in saving of time and money.
- 4) It helps in increases the life of the machine along with growth in productivity.

REFERENCES:

- [1] R. Beebe, "Predictive maintenance of the pump using condition monitoring," Elsevier Ltd, (2004), pp.1-13.
- [2] B. Rao, "Handbook of Condition Monitoring", Elsevier Advanced Technology, (1996), pp.1-34.
- [3] D. Ross, "Handbook: Total Productive Maintenance," Section 5, pp.1-5.
- [4] H. Garg and G. Krishna, "Industrial Maintenance and Maintenance of spare parts management"(1990), pp.32.
- [5] R. Hutton, "The Impact of Information Technology on Condition Monitoring", Profitable Condition Monitoring (1996), pp.23-27.
- [6] J. Mathew and R. Alfredson, "The condition monitoring of rolling element bearing using vibration analysis," Journal of Vibration, Acoustic and Stress Reliability Design," (1984) vol. 10(6), pp. 47-53.
- [7] S. Qian, " Introduction to Time,-Frequency and Wavelet Transforms", Prentice Hall, New Jersey, (2002).
- [8] P. Botsaris and D. Koulouriotis, "A Preliminary Estimation of Analysis Methods of Vibration Signals Fault Diagnosis in Ball Bearings," 4th International Conference on NDT, (2007).
- [9] B. Li, G. Goddu, and M. Chow, "Detection of common motor bearing faults using frequency-domain vibration signals and a neural network based approach, "In Proceeding of the American Control Conference, (1998), vol. 4.
- [10] R. McClintic, C. Byington, M. Lebold and K. Maynard, "Review of vibration analysis method for gearbox diagnostic and prognostic," In Proceedings of the 54th Meeting of the Society for Machinery Failure Prevention Technology, (2000), pp.623-634.

Static & Dynamic Research of Composite Blade using Condition Monitoring Method

Akshay A. Hake, Nagesh S. Ronge, Vijay A. Bhingare, Avinash K. Parkhe, Pradnya K. Bhuse, Sanjay N.

Abstract: *The use of composite materials has been increased in different industries like civil, mechanical, aerospace engineering due to their better properties. The rotating blade plays an important role in engineering structures such as turbine blades, airplane propellers, and helicopter blades. This deals with static analysis of composite blade to estimate the material uncertainty by measuring the deflection. The composite blade is fixed like a cantilever beam. To measure this deflection the Hall Effect Sensor is developed which is non contact device works on magnetic field. If magnet is come in front of sensor it creates magnetic field between them and that change in voltage or field is calibrated in terms of deflection of blade. The same process is carried for all the blades to check their uncertainty present in it. Also, it is deals with the dynamic analysis of blade to check their behavior in the axis under rotating condition for different RPM. The acceleration is considered as performance parameter to check the behavior of blade. Also, the setup is developed for accelerations measurement GY-521 Accelerometer. The accelerometer has kept at free end of blade and accelerations are taken in three directions for each rpm and it is represented in a graphical form. The analysis is carryout for both damaged and undamaged blade. The both studies are carried out using condition monitoring approach to observe their behavior of blade in static & dynamic condition before used in any application.*

Keywords: *Uncertainty, Hall Effect, Static, Dynamic, GY-521, Arduino, Accelerations.*

I. INTRODUCTION

This deals with static analysis of composite blade to estimate the material uncertainty. The deflection is measured to check the uncertainties present in material. The composite blade is fixed like a cantilever beam. To this deflection the Hall Effect Sensor is developed which is non contact device works on magnetic field. If magnet is come in front of sensor it create magnetic field between them and that change in voltage or field is calibrated in terms of deflection of blade. The same process is carried for all the blades to check their uncertainty present in it. Also, it is deals with the dynamic analysis of blade to check their behavior in the axis under rotating condition for different RPM. The acceleration is considered as performance parameter to check the behavior

Revised Version Manuscript Received on 10 September, 2019.

Akshay A. Hake, SVERI's, College of Engineering, Pandharpur, Maharashtra, India.

Nagesh S. Ronge, SVERI's, College of Engineering, Pandharpur, Maharashtra, India.

Vijay A. Bhingare, SVERI's, College of Engineering, Pandharpur, Maharashtra, India.

Avinash K. Parkhe, SVERI's, College of Engineering, Pandharpur, Maharashtra, India.

Pradnya K. Bhuse, SVERI's, College of Engineering, Pandharpur, Maharashtra, India.

Sanjay N, SVERI's, College of Engineering, Pandharpur, Maharashtra, India.

of blade. Also, for accelerations measurement, the setup is developed using GY-521 Accelerometer and Arduino. The accelerometer has kept at free end of blade and rotates it for different rpm. During rotating condition accelerations are taken in three directions for each and results are represented in a graphical. This study is carried out for both damaged and undamaged using the same parameter. [1, 2, 3]

The researches have been conducted on composite blades. Ronge et al. presented experimental setup for damage identification of rotating blade for both damaged and undamaged using health monitoring approach. Kachareet. al represented the measurement of acceleration using dynamic setup. Kachareet. al presented theory of health monitoring of blade and parameters related to same. The proposed approach is further extended to study large deflection behavior of an initially curved cantilever beam subjected to distributed and combined load. These results are successfully validated with existing results for straight beams and some new results are furnished for initially curved cantilever beams. Mohammad Dado et al. studied the very large deflection behavior of prismatic and non-prismatic cantilever beams subjected to various types of loadings. The formulation is based on representing the angle of rotation of the beam by a polynomial on the position variable along the deflected beam axis. Beléndez, T. et al. presented the classical problem of deflection of a cantilever beam of linear elastic material, under the action of a uniformly distributed load along its length (its own weight) and an external vertical concentrated load at the free end, is experimentally and numerically analyzed. We present the differential equation governing the behavior of this system and show that this equation, although straightforward in appearance, is in fact rather difficult to solve due to the presence of a nonlinear term.

The both static and dynamic studies are carried out using condition monitoring approach to observe the behavior of blade before their use in any application.

II. INTRODUCTION COMPOSITE BLADE

The composite blade of uniform cross-section having dimension 800x60x22 mm. This is an eight layer sandwich composite blade.





Figure 1 Composite blade

Material Properties:

Table 1 Material Properties of Composite blade

Young's Modulus	Poisson's Ratio	Mod. of Rigidity	Density
135 Gpa (Ex Dir.)			
10 Gpa (Ey Dir.)	0.26	5 Gpa	1600 kg/ms
10 Gpa (Ez Dir.)			

III. STATIC ANALYSIS OF COMPOSITE BLADE

3.1 Hall Effect Sensor & Arduion (Uno):

The Hall Effect is an ideal sensing technology. The Hall element is constructed from a thin sheet of conductive material with output connections perpendicular to the direction of current flow. When subjected to a magnetic field, it responds with an output voltage proportional to the magnetic field strength. The voltage output is very small (μV) and requires additional electronics to achieve useful voltage levels. When the Hall element is combined with the associated electronics, it forms a Hall Effect sensor. The reasons for using a particular technology or sensor vary according to the application. Cost, performance and availability are always considerations.

Arduion is an open-source platform used for building electronics projects. Arduino consists of both a physical programmable circuit board (referred to as microcontroller) and a piece of software that runs on your computer, used to write and upload computer code to the physical board. We use the Arduino Uno for our study which is one of the more popular boards in the Arduino family and the configuration of it as shown in figure below.

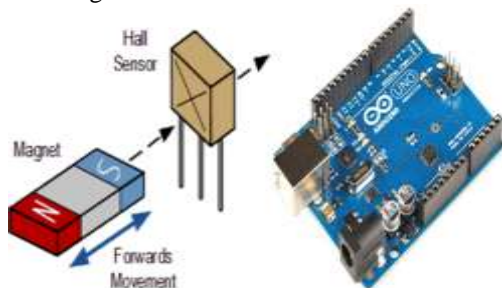


Figure 2 Hall Effect Sensor. Figure 3 Arduino Uno

3.2. Experimental Analysis:

The experimentation has carried on composite blade for by varying load at free end to find the deflection using Hall Effect sensor. The designed Hall Effect sensor will generate maximum voltage up to 220 volt, if distance between sensor and magnet is up to 6 mm. Initially, we put 1 to 2 mm

distance between sensor and magnet then it shows some voltage will assumed as zero. When 10 N load is applied at free end of the blade the voltage difference is generated between initial and final reading. The change in voltage difference is calibrated in terms of deflection of blade. The same process is carried out for other loads (20N to 80N) and its voltage differences are calculated using in graphical form which are generated during experimentation.

The experimental setup for the above proposed work and blade in loading and unloading condition is shown by following figures.

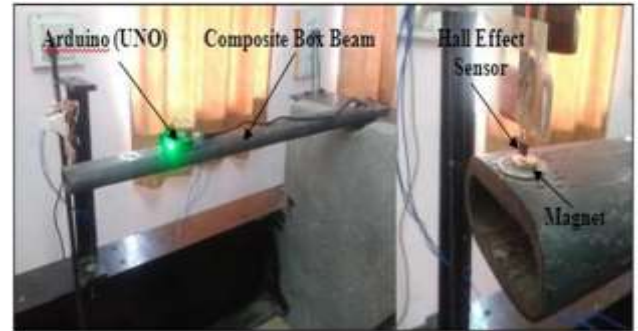


Figure 4 Experimental setups using Hall Effect Sensor



Figure 5 Composite blade in unloading and loading condition

During experimentation it has analyzed that for 10 N load 16 v voltage generated and by using this voltage we calculate the deflection of blade for this particular load. The same process has carried on four blade. The sample calculations of first blade for 10 N and 20 N loads are given below.

1) Sample calculation for 10 N:

$$\frac{6 \text{ mm}}{220 \text{ V}} = \frac{\delta}{16 \text{ V}}$$

Therefore, $\delta = 0.43 \text{ mm}$

2) Sample calculation for 20 N:

$$\frac{6 \text{ mm}}{220 \text{ V}} = \frac{\delta}{25 \text{ V}}$$

Therefore, $\delta = 0.68 \text{ mm}$

The voltage difference in initial and final reading for different loads is shown by following graphs. The following graphs are generated during the experimentation of first blade. The same voltage differences are calculated for remaining three blades by generating the same graphs to find its deflection for different loads.

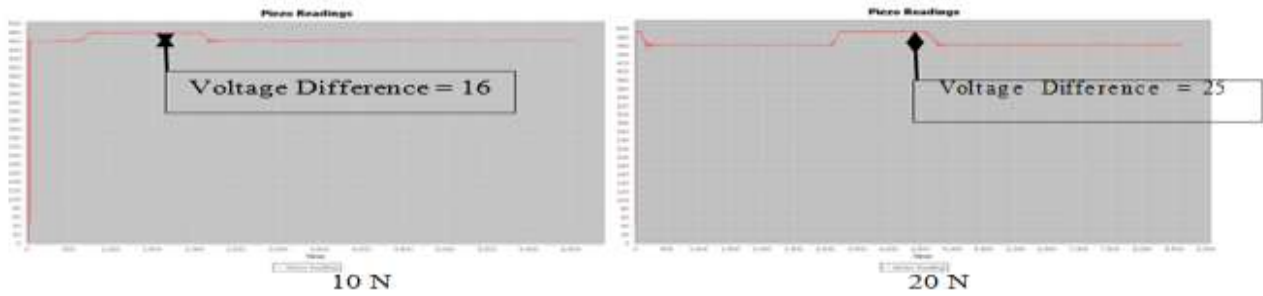


Figure 6 Voltage difference in initial and final reading

Table 2 Deflection of composite blade

Sr. No.	Load (N)	Experimental Deflection (mm)			
		Blade 1	Blade 2	Blade 3	Blade 4
1.	10	0.43	0.40	0.43	0.38
2.	20	0.68	0.68	0.62	0.73
3.	30	0.95	1.00	0.95	0.98
4.	40	1.36	1.30	1.39	1.36
5.	50	1.63	1.66	1.69	1.58
6.	60	1.77	1.77	1.71	1.69
7.	70	2.18	2.20	2.15	2.23
8.	80	2.72	2.78	2.78	2.67

Above table represents voltage difference of four composite blade along with its free end deflection for different loads. The experimental results for deflection of four blades for different loads are also shown by following graph.

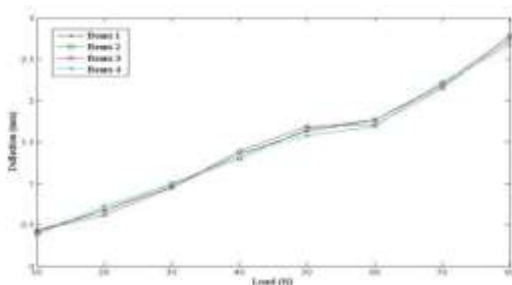


Figure 7 Load Vs Deflection

IV. DYNAMIC ANALYSIS OF COMPOSITE BLADE & RESULTS

4.1 EXPERIMENTAL SETUP FOR ACCELERATION MEASUREMENT:

The experimental setup for acceleration measurement has shown below. The accelerometer is mounted at free end of

blade with arduino connection shown in figure below.



Figure 8 Experimental setup using GY-521 Accelerometer

The blade is mounted on rotating disk and rotating it for different rpm and using that proposed setup. Here we required to find the accelerations of the rotating beam in terms of g value because the direct reading of sensor is not considered as accelerations, we want to make some conversions or calculations to obtain necessary results only. The values obtained from the GY-521 accelerometer or raw values are used to find the a_x , a_y , a_z in terms of g value.. The scaling factor depends on the acceleration limit. Table 1 shows the scaling factors for acceleration limit as per standards available.

Table 3 Accelerometer Scaling factors

Acceleration Limit	Sensitivity or Scaling factor
2g	16384
3g	8192
4g	4096
5g	2048

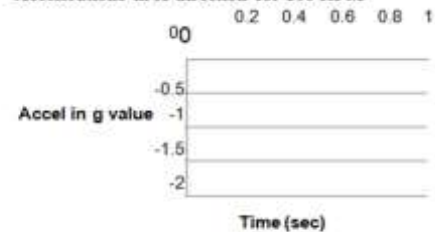
Converting the raw data:

$$\text{Required value } V(a_x, a_y, a_z) = \frac{\text{raw value}}{\text{Sensitivity} \times \text{Scaling factor}} (\text{g value})$$

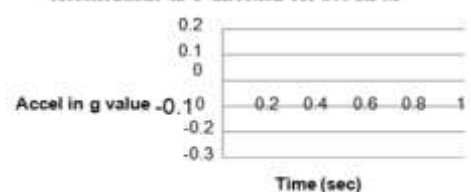
4.2 ACCELERATIONS IN UNDAMAGED ROTATING COMPOSITE BLADE FOR DIFFERENT RPM:

In the first phase the study is carried out for undamaged blade by measuring the acceleration in the direction using the proposed setup. During the rotating condition the movement of blade is taking place in three directions and their results are represented in graphical form which is shown by following

Accelerations in X-direction for 100 RPM



Accelerations in Y-direction for 100 RPM



figures.

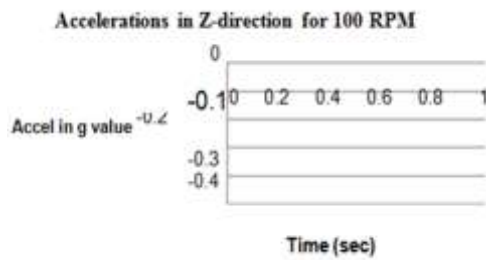


Figure 9 Accelerations in undamaged blade (100 rpm)

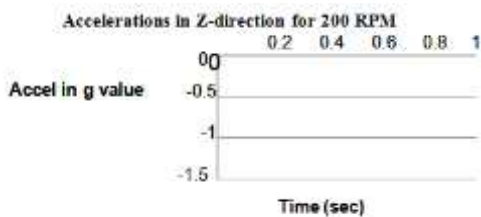
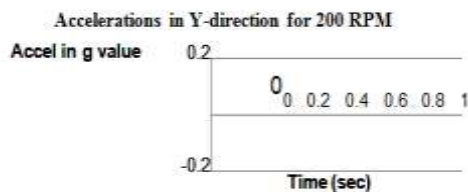
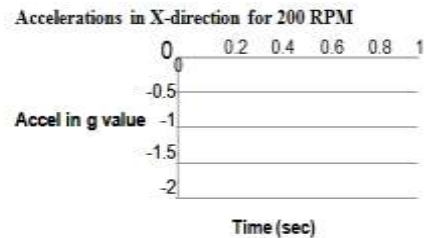


Figure 10 Accelerations in undamaged blade(200 rpm)

Figure 9 and 10 shows the accelerations (in g value) in a rotating composite box blade for different rpm. The X-direction represents axial direction, Y direction represents the horizontal rotating direction of blade and Z represents the vertical movement of the blade in rotating condition.

4.3 ACCELERATIONS IN DAMAGED ROTATING COMPOSITE BLADE FOR DIFFERENT RPM:

In the 2nd phase similar study is carried out for damaged blade using same process and setup and their results are again represented in following graphical form for different rpm.

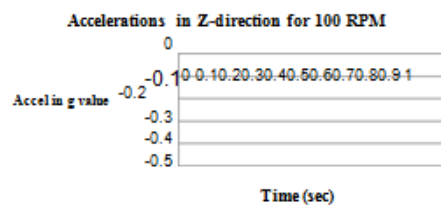
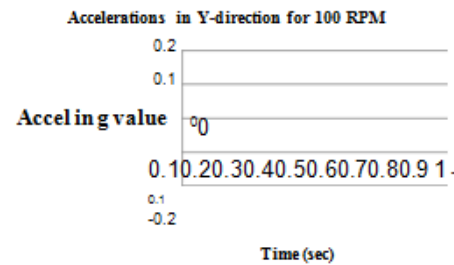
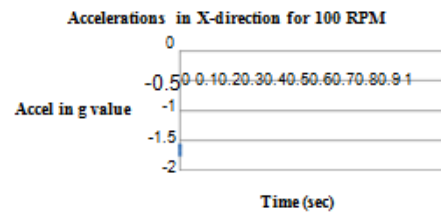


Figure 11 Accelerations in damaged blade (100 rpm)

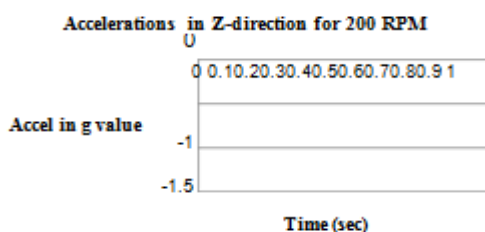
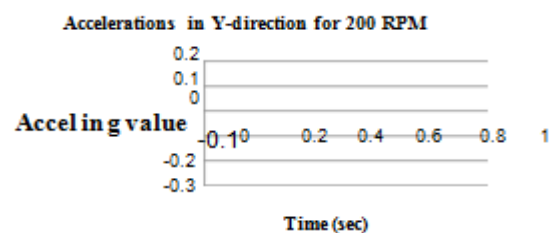
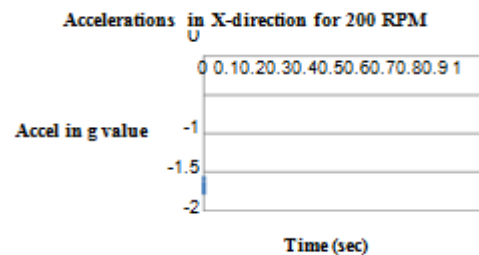


Figure 12 Accelerations in damaged blade (200 rpm)

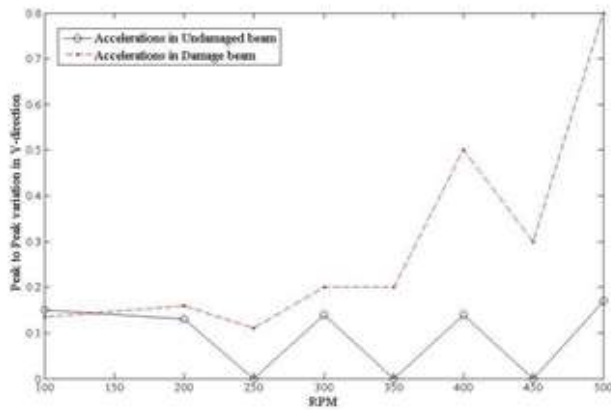


Figure 13 RPM vs accelerations in Y-direction of blade

V. CONCLUSION

During the manufacturing of composite material or blades the uncertainties has formed due to some defects or errors manufacturing process and it has studied by the different parameters like deflection, stress, strain, natural frequency etc. The experimentation has carried on composite blade for deflection measurement and this is of for all four blades by the same process and it is carried out to analyze the uncertainty present in material or blade. Also Static and Dynamic analysis was carried out on blade for acceleration measurement. From the above study on composite blade following conclusions are drawn:

The use of dial gauge indicator for deflection measurement will create problems during measurement due its contact with composite blade.

To avoid this situation non contact device is designed and developed for deflection measurement named as Hall Effect Sensor.

As deflection results of all four blades are compared with each other then there is no more difference between them. All the results are near to each other to their respective load is also shown in graphical form.

The acceleration results for damaged and undamaged blade are compared to check the behavior in rotating condition. Using the above graphical results it is observed that the accelerations are increased for damaged blade as their stiffness are get loosed and due to structure of blade get damaged. From the above results and graph the maximum deformation is taking place in Y direction for the rotating blade.

REFERENCES

1. RongeBabruvahan, PrashantPawar, and AvinashParkhe, "Experimental analysis of composite rotor blade models for damage identification." In *Advances in Science and Engineering Technology International Conferences (ASET)*, 2018, pp. 1-6.
2. P. S. Kachare, Avinash K. Parkhe, A. A. Utpat, "Free Vibration Analysis of Rotating Composite Box Beam using GY-521 Accelerometer", *International Journal of Scientific and Research Publications*, Volume 9, Issue 2, February 2019, ISSN 2250-3153.
3. P. S. Kachare, A. K. Parkhe, A. A. Utpat, S. Y. Salunkhe, "Health Monitoring of Static Composite Beam for Material Uncertainty and its Numerical Validation", *International Journal of New Technology and Research (IJNTR)* ISSN:2454-4116, Volume-5, Issue-3, March

2019 Pages 79-83.

4. SushantaGhuku, KashiNathSaha.: A theoretical and experimental study on geometric nonlinearity of initially curved cantilever beams. In: *Engineering Science and Technology, an International Journal*, (2015)
5. Mohammad Dado.: A new technique for large deflection analysis of non-prismatic cantilever beams. In: *Mechanics Research Communications* 32, 692–703, (2005)
6. TarsicioBelendez, CristianNeipp.: Large and small deflections of a cantilever beam. In: *European Journal of Physics*, Volume 23, (2002)
7. M. Sitar.: Large deflections of nonlinearly elastic functionallygraded composite beams. *Archives of Civil and Mechanical Engineering* 14, 700-709, (2014)
8. Belendez, T.: Numerical and Experimental Analysis of a Cantilever Beam: A Laboratory Project to Introduce Geometric Nonlinearity in Mechanics of Materials. In: *International Journal of Engineering Education*, Volume 19, Issue 6, 885-892, (2003).

ICMN-2K19

Materials on a Diet: Study and Investigation of Aluminium – Fly Ash Metal Matrix Composite

Prathamesh Mhamane^{a,*}, Shubham Kadam^b, Viraj Phanse^c, S. B. Bhosale^d

^{a,b,c}UG Student of Mechanical Engineering Department, SVERI's College of Engineering Pandharpur, Pandharpur, 413304, India

^dAssistant Professor at Department of Mechanical Engineering, SVERI's College of Engineering Pandharpur, Pandharpur, 413304, India

Abstract

Metal Matrix Composite (MMC) have wide applications in industry as they have lightweight and various properties. Composite materials are widely used in industry as they have less weight with high strength. In this study, we have used the Aluminium which is the most common material used in engineering applications. One of the cheapest industrial waste materials is Fly Ash, which can be successfully turned as industrial wealth by adding in the Aluminium to form Al-Fly Ash as Metal Matrix Composite with lesser weight and higher strength. Aluminium with varying percentage of fly ash (5%, 10% and 15%) were successfully added by using the Stir Casting method to form Metal Matrix Composite. In this investigation, we have studied the different properties of the Aluminium - Fly Ash as Metal Matrix Composite. From our study, we found that this Metal Matrix Composite which contains Fly Ash can be used in Automobile, Aerospace and other applications in Engineering where lesser weight with higher strength is expected.

© 2019 Elsevier Ltd. All rights reserved.

Selection and peer-review under responsibility of International Conference on Advances in Material Science & Nanotechnology, ICMN-2K19.

Keywords: Aluminium; Fly Ash; Industrial waste as wealth; Stir Casting;

1. Introduction

Metal Matrix Composite (MMC) is grabbing engineers' attention as it is having various properties like durability and high strength to weight ratio. In MMCs the metal matrix is used with the reinforcement to achieve the desired property with the lesser weight and cost. Aluminium is one of the common metals which are used in various

* Prathamesh Mhamane. Tel.: +91- 7385536025.

E-mail address: prathameshgmhamane@outlook.com

engineering applications. As Aluminium is having less weight, it comes with lesser strength. Fly Ash is the industrial waste with low density produced by the thermal power plants as well as many industries. In India 1100 lacks ton Fly Ash per year is produced by the burning of 2500 lacks tons of coal per year for power generation. [1] It is one of the cheapest reinforcements we can use. Also, this can convert industrial waste into industrial wealth. Aluminium and Fly Ash Metal Matrix Composite is a composite material with higher strength as soft and ductile Aluminium is mixed with brittle and hard particles of Fly Ash. Use of Fly Ash in various materials can reduce pollution as well as increase strength and reduce the weight of the material. To form the Al-Fly Ash as MMC, the Stir Casting method is used. For investigation of the performance of MMCs we have added Fly Ash in different proportion (5%, 10%, 15%). This composite has many applications in Automotive and Aerospace sector.

2. Previous Studies

As Metal Matrix Composite (MMC) is having a high scope for research and innovations, many researchers have done work in the development and use of Aluminium – Fly Ash Metal Matrix Composite. We have listed below some of the studies done by the researchers in the field of Aluminium and Fly Ash MMC. Aluminium - Fly Ash Metal Matrix Composite is strengthened composite with good wear resistance used in various applications such as aerospace, automotive and other fields [2]. Aluminium is widely used in industry as it is common material with various useful properties. Using Aluminium fly ash MMC decreases the demand for intensive energy by Aluminium, it results in energy savings [3]. Fly Ash is having low density and available in major quantities as it is a waste product of thermal power plant when coal combustion. It has been successfully added into aluminium to make alloys and composites [4]. Previously Metal Matrix Composite was concentrated along the preparation of only FRC. As the cost of production is high, the use of such useful composite material is less. In current days the MMCs with lighter reinforcement grabbing importance because of less cost and higher strength properties. The strengthen aluminium alloy can have better stiffness as it has high strength and low density [5]. The Aluminium with Fly Ash Metal Matrix Composites are prepared by Stir Casting. Wettability of the particles can increase by the addition of active elements such as Mg into liquid Aluminium. The conventional method of production of composites by casting route is the vortex method, in which the Aluminium with 2% to 4% Mg is added and stirred. Mg helps to reduce the surface tension and avoid the dispersion of particles from casting [6,7]. Machinability is also increased with addition of Fly Ash in Aluminium with effect of lesser weight [8].

3. Materials and Experimental Study

3.1. Materials

In this experiment, we have used pure Aluminium as it is one of the common metals used in the aerospace and automotive industry as well as many other industries. Aluminium is soft in nature and have wide applications in every sector of engineering. Pure Aluminium is used to form the Metal Matrix Composite. For the reinforcement, we have used Fly Ash which is collected from the thermal power plant. As Fly Ash is waste for many industries and thermal power plants, it is beneficial for society and nature to use it in such engineering applications.

3.2. Aluminium

Aluminium is one of the most common materials used in engineering applications. It is highly useful in the automobile and aerospace sector. Aluminium is known as the lighter material which is having wide applications in day to day life which needs to be strengthen and reduction in cost. So we have selected Aluminium for making the metal matrix which can replace the existing Aluminium material for having better results.

In this experiment, we have used the Aluminium A1100 blocks to make Metal Matrix Composite. The composition and properties of A1100 are listed below in table 1 and 2 respectively.

Table 1. Composition of Aluminium

Elements	Weight (%)
Al	99
Si	0.45
Cu	0.15
Mg	0.05
Fe	0.30
Zn	0.05

Table 2. Properties of Aluminium

Properties	Values	Units	Conditions (°C)
Density	2.72	g/cm ³	25
Poisson's Ratio	0.32	-	25
Melting Point	648	°C	25
Tensile Strength	108	MPa	25
Elastic Modulus	75	GPa	25
Yield Strength	106	MPa	25
Elongation	11	%	25
Hardness	30	HB500	25
Fatigue Strength	40	MPa	25
Shear Strength	70	MPa	25
Thermal Conductivity	210	W/m-K	25

3.3. Fly Ash

It is one of the cheapest industrial waste which is produced by thermal power plants and other manufacturing industries. Fly ash is easily available at any power plant or in our daily use. Fly ash is the cheapest industrial waste produced by the industry which can be used as reinforcement in our experiment. Fly Ash has two classes as Class F and Class C.

We have used Fly Ash of F class as a reinforcement for the MMC. The particle size of Fly Ash is less than 100 μm . Composition and properties of Fly Ash are given below in table 3 and 4 respectively.

Table 3. Composition of Fly Ash

Compounds	Weight (%)
SiO ₂	60.32
Al ₂ O ₃	20.41
Fe ₂ O ₃ + Fe ₃ O ₄	8.14
MgO + CaO + SO ₄	4.11
Other	7.02

Table 4. Properties of Fly Ash

Properties	Values	Units	Conditions (°C)
Density	0.61	g/cm ³	25
Poisson's Ratio	0.17	-	25
Melting Point	>1000	°C	25
Tensile Strength	140	MPa	25
Elastic Limit	145	MPa	25
Young's Modulus	71	GPa	25
Bulk Modulus	34.2	GPa	25
Hardness	6700	MPa	25
Compressive Strength	1300	MPa	25
Shear Modulus	30.2	GPa	25

3.4. Experimental Setup

Stir Casting method was used to form this composite of Aluminium and Fly Ash. Aluminium is in the chips where the Fly Ash is in powder form with size 0.1 to 100 μm . Stir Casting Setup includes the furnace with mild steel turbine stirrer. The furnace can achieve a maximum temperature of 1000°C which is sufficient for melting of Aluminium. Different percentage of Fly Ash is reinforced into the Metal Matrix to form a composite. We have taken Fly Ash at 0%, 5%, 10%, and 15%. Accordingly, we have made each sample with a different percentage of Fly Ash and Aluminium.

4. Methodology

- Form the different materials distribution for different percentage of Fly Ash.
- Heat the furnace up to 720°C i.e. more than melting temperature of Aluminium.
- To remove moisture, preheat the Fly Ash powder at 350°C for two hours.
- Insert chips of Aluminium setup of Stir Casting furnace for melting.
- At 720°C add the particles of Fly Ash in the furnace and start stirring process.
- Stir the melt with mild Steel turbine stirrer at an impeller speed of 250 rpm for 10 to 15 minutes.
- Pour the melt at a maintained temperature of 700°C into the mould.
- Allow melt to solidify in the mould in natural solidification.

5. Results and Discussion

The prepared Aluminium-Fly ash composite specimens were tested for different mechanical properties like hardness and tensile strength. Also it is tested for weight reduction. Hardness test is carried by using Rockwell cum Brinell Hardness Tester (Model-TRB250) and tensile strength is measured using (make-UTK 100E) of 100-ton capacity. Table 5 shows the measured hardness, tensile strength and weight reduction with variation in fly ash percentage.

Table 5. Test results of Aluminium Fly Ash Metal Matrix Composite

Variation of Fly Ash	Hardness (BHN)	Tensile Strength (MPa)	Weight (gm)
Al	55	108.20	810.04
Al + 5 % Fly Ash	62	119.85	791.5
Al + 10 % Fly Ash	68	131.23	773.04
Al + 15 % Fly Ash	66	127.25	754.56

5.1. Hardness Test

Hardness test is carried by using Rockwell cum Brinell Hardness Tester (Model-TRB250) for all the composites. The result of Brinell Hardness Test of each specimen respect to the various amount of Fly Ash is shown in Fig 1.

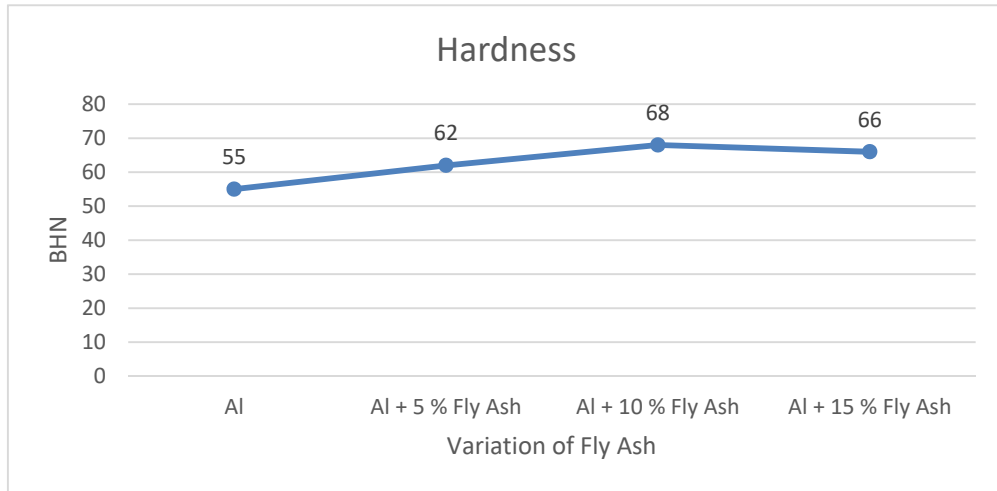


Figure 1. Hardness Test Results

The hardness of Al-Fly ash composite has been found to increase with increased fly ash percentage up to 10%. But further at 15% fly ash, the hardness found to reduce due to less wetting of fly ash particles and improper mixing.

5.2. Tensile Test

The tensile test is carried by using (make-UTK 100E) of 1000 KN capacity for all the composites. Following (Fig.2) is the result of tensile test of each specimen respect to the various percentage of Fly Ash.

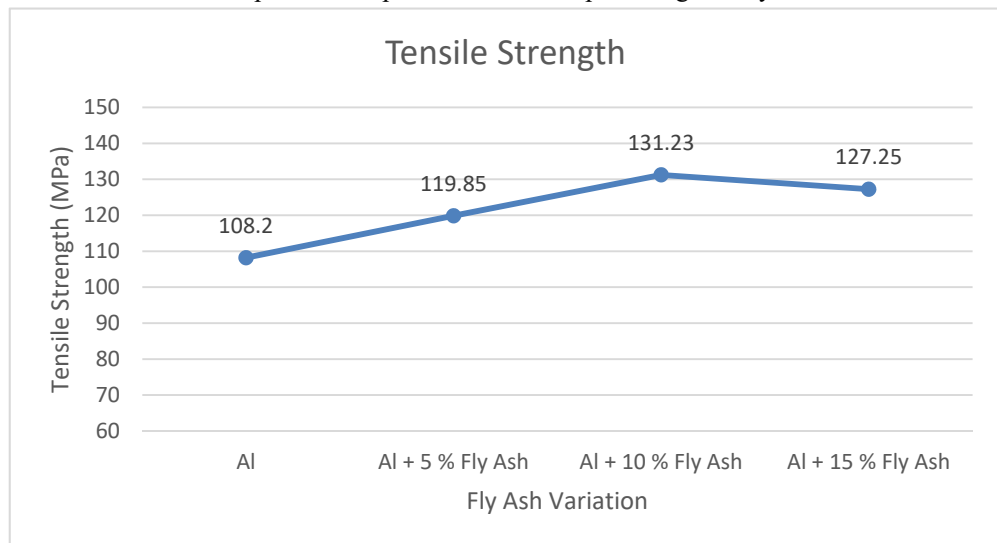


Figure 2. Tensile Test Results

The tensile strength of Aluminium-Fly ash composite has been found to increase with increased fly ash percentage up to 10%. But further at 15% fly ash, the hardness found to reduce due to less wetting of fly ash particles and improper mixing. The maximum tensile strength has been noted as 131.23 MPa at 10% fly ash percentage.

5.3. Weight Reduction Test

Fly Ash is lighter than commercially pure Aluminium hence the prepared composite is lighter than conventional material. For this testing, we have considered blocks of material with dimensions of length, width and thickness of 100 mm, 100 mm, 30 mm respectively.

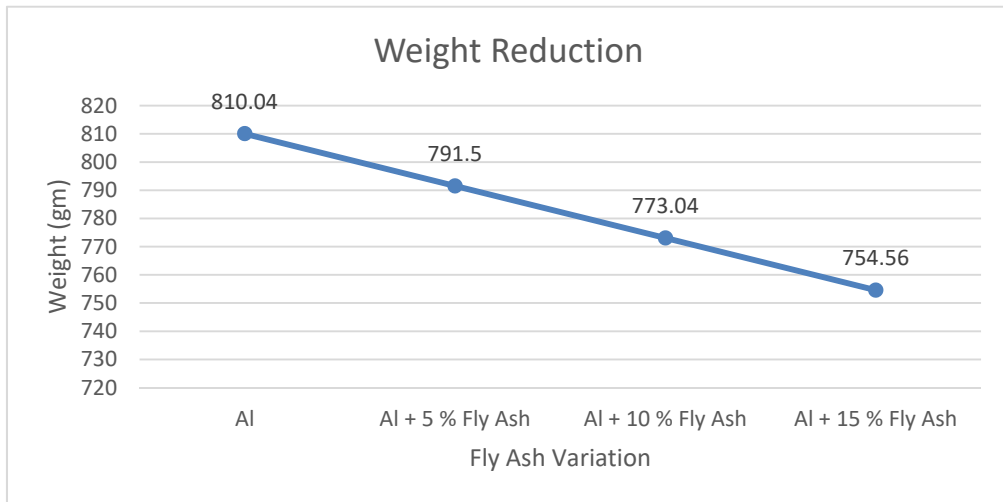


Figure 3. Weight Reduction Test Results

The weight of material gets decreased as the fly ash is added in it. As fly ash is lighter material, weight will be gradually decreased with addition of fly ash. The result is shown in fig 3.

6. Conclusion

- We have successfully added up to 15 % Fly Ash in commercially pure Aluminium to form Metal Matrix Composite which helps to turn industrial waste as industrial wealth.
- We have observed that Hardness and Tensile Strength of Aluminium Fly Ash MMC are more than commercially pure Aluminium.
- Fly Ash can be used in metals to improve strength to weight ratio of materials.
- This prepared composite may be used in Aerospace and Automotive applications instead of conventional materials.

Acknowledgements

The authors of this paper would like to thank Dr. S. G. Kulkarni, SKN COE Korti, for providing the setup of Stir Casting and necessary arrangements. We also thank Dr. N. D. Misal, COE Poly. Engineering, Pandharpur for providing necessary equipment for testing and analysis. Also, authors thanks to readers and investigators of this paper and would happy to receive any comments.

References

- [1]. P. Shanmugasundaram¹, R. Subramanian² “Some Studies on Aluminium-Fly Ash Composites Fabricated by Two Step Stir Casting Method”, *European Journal of Scientific Research* ISSN 1450-216X Vol.63 No.2 (2011), pp.204-218.
- [2]. Mahendra.K.V and Radhakrishna. K, Castable composites and their application in automobiles, *Proc. IMechE* Vol. 221 Part D: J. Automobile Engineering, (2007): pp. 135-140.
- [3]. P. K. Rohatgi, J. K. Kim, R. Q. Guo, D. P. Robertson and M. Gajdardziska-Josifovska, “Age Hardening Characteristics of Aluminium Alloy – Hollow Fly Ash Composites”, *Metallurgical & Materials Transaction A*, Vol. 33A, (2002).
- [4]. Lindroos V.K, Talvitie M.J, Recent advances in metal matrix composites, *J. Mater. Proc. Technol.* 53 (1995): pp. 273–284.
- [5]. Hung N. P, Boey,F.Y.C. Khor K.A, Phua Y.S. and Lee H.F, Machinability of Aluminium alloys reinforced with silicon carbide particulates, *Journal of Materials Processing Technology*,56 (1996): pp. 966-977.
- [6]. Rohatgi P.K, Asthana R, Das, S Solidification, structures, and properties of cast metal- ceramic particle composites, *International metals reviews*,31(1986): pp. 115-139.
- [7]. Sarkar S., Sen S. and Mishra S. C, Aluminum – fly ash composite produced by impeller mixing, *Journal of reinforced plastics and composites*, (2008): pp 1-6
- [8]. R. Elangovan and M. M. Ravikumar, Performance of Al – Fly Ash Metal Matrix Composites, *ARPN Journal of Engineering and Applied Sciences*, Vol. 10, No. 4, (2015)

ICMN-2K19

Comparative CFD Analysis of Mini Impeller Using Different Materials

Ashutosh.B.Deshmukh^{a*}, Aditya.A.Lotake^a, Hrushikesh.N.Paricharak^a,Subhash.V.Jadhav^a, Digambar.T.Kashid^a, Sandeep.S.Wangikar^a^a*Department of Mechanical Engineering, SVETI's College of Engineering, Pandharpur, Pandharpur-413304, Maharashtra, India*

Abstract

In this present era there is continuously increasing the use of centrifugal pump which is required to pump the various fluids like water, fuel, etc. from lower level to higher level. And in the field of research and development there is use of miniature centrifugal pump for different applications. So, there is need to design the miniature pump impeller by standard design procedure. The model is developed with the help of CATIA v5 R21 software. Then an analysis is carried out in the ANSYS Fluent for different materials and various parameters like wall shear stress and static pressure are analyzed.

© 2019 Elsevier Ltd. All rights reserved.

Selection and peer-review under responsibility of International Conference on Advances in Material Science & Nanotechnology, ICMN-2K19.

Keywords: centrifugal pump; mini impeller design; ANSYS Fluent; CFD; CATIA v5 R21

1. Introduction

The centrifugal pump is the device which lifts the water from lower level to higher level by utilizing centrifugal force. In this centrifugal pump the impeller is used to increase pressure and flow of fluid. It converts the mechanical energy into kinetic and pressure energy. An impeller is rotating component of pump which transfer energy from motor which pumps the fluid to outwards from the centre of rotation. An impeller is nothing but a small cylinder with an open inlet called as eye which accepts the incoming fluid. At the centre of impeller it produces the negative pressure at the inlet vanes to pushes the fluid radically. The prediction of performance of impeller with conventional trial and error method is very difficult and time consuming as well as costly. Using CFD approach one can easily

* Corresponding author. Tel.: +91-9503458956; fax: +91-2186-225082
E-mail address: ashu2051998@gmail.com

predict the complex flow inside the pump. Hence CFD analysis is efficient method for analysis of impeller. As very few researchers have made attempt in this area so the study is made for the analysis of mini impeller. Pierret and Braembussche [1] studied for satisfying the aerodynamic and mechanical requirements and shows the Navier - stokes computations is important. By using optimized algorithms depend upon simulating annealing will not trap in local minimum. Miguel Asuaje et al. [2] studied that design of centrifugal pump and optimization depends mainly on the 3D quasi-unsteady flow simulation using two methods which is CFX-TAS flow and CFX 5.5 codes. It causes the unsymmetrical flow distribution and cavitations appear on blades. Shang-liangchen and wen-Tsai Wang [3] studied the various computerized manufacturing processes for impeller. From this it states that the rough milling using cavity mill with three axis milling machine gives or improves the manufacturing efficiencies. Kim et al. [4] studied the CFD analysis of the volute of the impeller of centrifugal pump. And suggested that stepanoff theory is better for design of impeller and efficiency is decreases as there is increase of head. Gurupranesh et al. [5] studied the various parameters of impeller as static pressure and wall stress and it states that CFD analysis is so much important for analysis. Zhang et al. [6] studied the fatigue -failure analysis of impeller and founds that mistuning is the main causes of the fracture of the open impeller. The Vibration Stress of semi open impeller at the working speed is only 15.8 Mpa. Gamal et al. [7] studied the effect of number of impeller blades on pump performance. They took three different impellers with 5,7,9 blades and did numerical analysis and found that the optimum blade number at 2800 rpm and also found that the losses decreases by increasing blade number by numerical investigation were carried out to making reduction of secondary flow. Ragot et al. [8] analyze the flow field in a pump impeller and got efficiency 58.53% for circular method and 57.31% for the point method and circular method is much efficient for higher efficiency. Anagnostopoulis [9] studied flow in a centrifugal pump impeller by using Cartesian Grid. In this the numerical model is developed with the help of RANS Equation for finding the solution for impeller. Hazeri [10] studied the design of impeller for increasing the performance of pump and also optimized the design to give reduced energy consumption and prolonged component life. Zhou et al. [11] studied the wall shear stress and pressure distribution on the impeller of various models and he got uniform BVF distribution on the blade surface. Very less work has been reported on the analysis of mini centrifugal pump open impeller. Hence, an attempt is made to analyze the performance of a mini centrifugal pump by studying the different parameters like wall shear stress and static pressure for different materials like ABS, Steel and Aluminum. By comparing the results obtained after the analysis, the most suitable material for impeller is predicted.

2. Methodology

The methodology includes the design procedure of impeller which give the parameters and dimensions of the of impeller. The second part is the computational analysis. In computational analysis, the model is created in CATIA V5 software and then imported to ANSYS FLUENT software. Further, the mesh independence test is carried out and then the required simulations are performed in order to analyze the effect of speed and fluid flow direction on the wall shear stress, static pressure.

2.1 Design Procedure of Impeller:

In this impeller design, the discharge of 30 ml per sec and rpm of impeller is 5500 rpm with head of 30 cm is considered.

Specific speed :

$$N_s = N * \frac{\sqrt{Q}}{H^{\frac{3}{4}}}$$

Selection of vane number and discharge angle Assuming number of vanes is 6 and angle of discharge is 20°

Calculation of impeller dimension:

Head constant= $ku=1.18$

$$D_2 = \frac{1840 * ku * \sqrt{H}}{(N_s)}$$

Calculation of impeller width:

$$B_2 = 0.78(Ns/100)^{(1/2)} * (Q/N)^{(1/3)}$$

Eye Diameter of Impeller:

$$D_0 = K_0 * \sqrt[3]{Q/N}$$

Inlet Blade angle of the inlet:

$$\tan \beta = \frac{u_1}{V_{m1}}$$

Tangential velocity at inlet of impeller:

$$U_2 = \frac{\pi D_2 N}{60}$$

Inlet area of impeller:

$$A = [(\pi/4) * D_2^2]$$

Table 1. Parameters used for analysis

Specific speed	3700 rpm
Outer diameter of impeller	2cm
Width of impeller	0.6cm
Inlet angle	12°
Outlet angle	20°
Discharge	30ml/sec
Inlet velocity	3.87cm/sec
Area of impeller	3.14cm ²
Number of vanes	6

Table 2. Density of materials

Material	Steel	Aluminium	ABS
Density(kg/m ³)	7700	2700	1060

The parameters of impeller used for analysis and the densities of materials are presented in Table 1 and Table 2, respectively.

After design, the next stage is modelling using a suitable software. CATIA is widely used for modelling different kinds of 3D models. Therefore, for modelling of the mini impeller, the CATIA v5 R21 software is preferred and the prepared model is presented in Fig. 1.

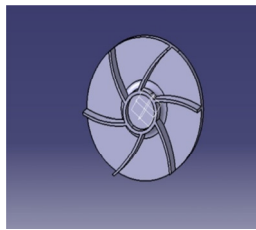


Fig.1. CATIA Model of impeller

There are softwares COMSOL Multiphysics, ANSYS Fluent, NASTRAN, etc. used by various researchers for analysing the performance of different devices like wind turbine, microchannels, micropumps, hydrodynamic bearings, etc. [12-14]. The computational analysis of mini impeller is carried out with the problems help of ANSYS Fluent. This works on the CFD theory. The ANSYS Fluent has ability to solve flow by providing complete mesh

flexibility. The interactive interface of ANSYS Fluent displays the results which are easily accessible. This impeller design CATIA file is converted in to .igs file. This file is imported into the ANSYS (fluent) software. After this, the mesh with coarse, medium and fine sizing and 100 relevance is generated. The volume of fluid is divided into three numbers of volumes such as rotating fluid volume, inlet fluid volume and inlet and outlet duct volume. The impeller wheel has given a constant rotating speed and setup referred as frozen rotor. Navier-Stokes equations is used for incompressible fluid. The details of input conditions and boundary condition are given below:

Input Material: ABS, Steel, Aluminium

Hydraulic Region: Water

Boundary Conditions: Specific speed =3700 rpm and Inlet velocity of 1.89 m/s

2.3 Mesh Independence Analysis:

In order to avoid the effect of enhanced meshing condition on the performance of mini impeller, the mesh or grid independence test is required to be performed. For Analysis of mini impeller, the unstructured mesh is used. The simulation is carried out for different mesh to improve computational the results. The different meshing conditions like coarse, medium, fine, and extra fine are applied to mini impeller and are depicted in Fig. 2. The result of the different meshing on the wall shear stress of the steel material is given below table 3. It has been observed that the results obtained for fine and extra fine be numbered with Arabic numerals. Every table should have a caption. Headings should be placed above tables, left justified. Only horizontal lines should be used within a table, to distinguish the column headings from the body of the table, and immediately above and below the table. Tables must be embedded into the text and not supplied separately. Below is an example which the authors may find useful. meshing for the wall shear stress pressure distribution are observed to be independent of the mesh (Fig. 3) beyond the fine meshing, therefore the extra fine meshing with meshing element 265706 has been found suitable to use for further computational analysis.

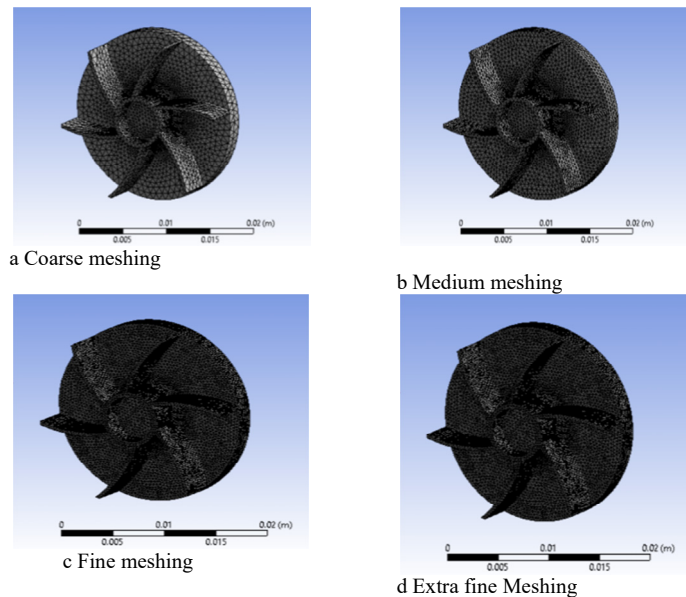


Fig.2. Different meshing conditions for mini impeller

Table 3. Mesh Independence Analysis

	Coarse	Medium	Fine	Extra fine
Nodes	25114	20771	51925	51945
Elements	130285	146249	264706	265706
Wall shear stress(Mpa)	4.31	3.34	2.97	2.97

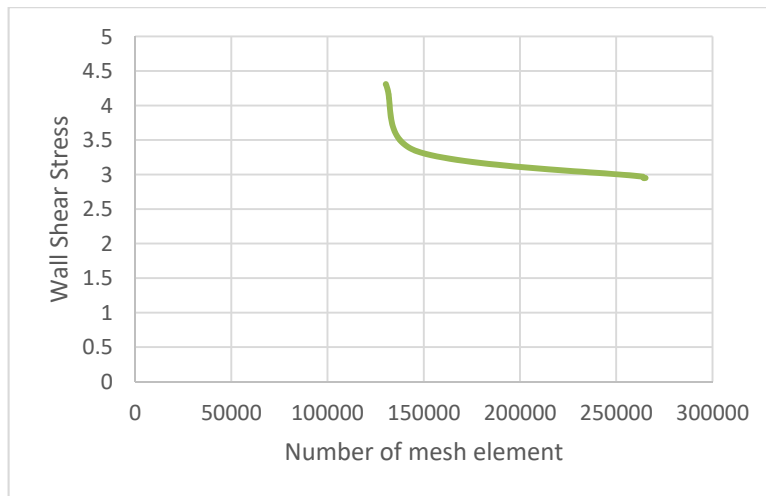


Fig. 3. Mesh independence test for wall shear stress

3. Results and Discussion:

The analysis has been carried out for studying the performance of mini impeller. The results are recorded for wall shear stress and static pressure. The results are taken when the convergence is obtained for solution where the numbers of iteration are 200.

3.1 Wall Shear Stress:

Wall shear stress is the shear stress in the layer of fluid next to the wall. Wall shear stress develops from the vector component parallel to the cross section of the material. Generally, the wall shear stress should be less for better performance. The Wall shear stresses developed in various materials is presented in below Fig. 4.

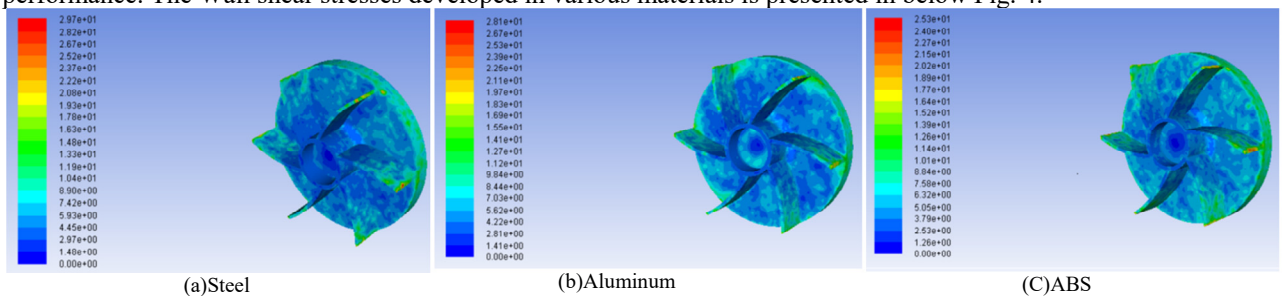


Fig. 4. Wall shear stresses for different materials

By performing numerical analysis on each material, the observed results are displayed in Table 4.

Table 4. Result of wall shear stress

Material	Wall shear stress (Mpa)
Steel	0.297
aluminium	0.281
ABS	0.253

From the results, it can be concluded that ABS material is good because it gives less wall shear stress which is of 0.253 MPa and maximum wall shear stress developed in steel material is 0.297 Mpa which is higher. The results states that the wall shear stress is increases gradually from all directions from leading edge of blade toward the trailing edge of blade. And the pressure gradient in axial direction is lesser than the radial direction and this is due to the centrifugal force acts on the trailing edges of the impeller blades. At the hub or centre low pressure is developed due negative suction pressure. So, the wall shear stress developed in ABS is less so it is preferable material for mini impeller. Due to this the low-pressure zone created at the hub side and gas blockage may be caused.

3.2 Static Pressure:

Static pressure is the pressure of fluid on a body when the latter is at rest relative to it. Static pressure developed on the impeller blades is negative at middle and increases toward the outside. Higher Static pressure will cause failure to the impeller. Static pressure contour of different material are shown Fig 5.

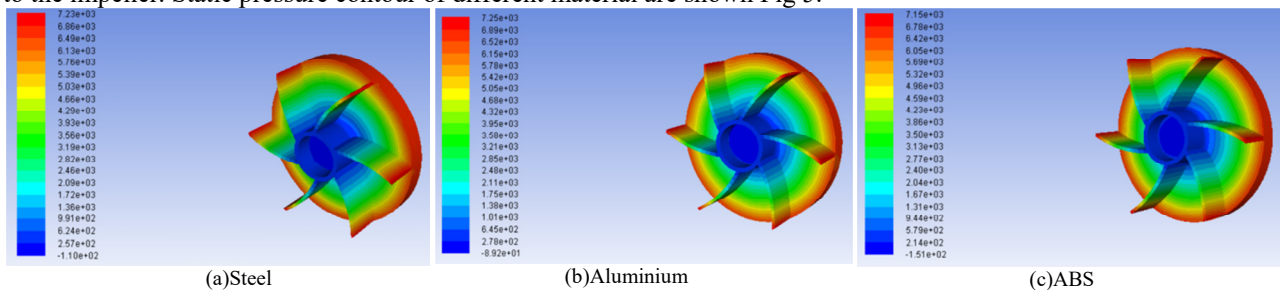


Fig. 5. Static pressure distribution for different materials

By performing the numerical analysis we have got the following results

Table 5. Result of static pressure

Material	Static Pressure(Mpa)
Steel	7.25
Aluminium	7.23
ABS	7.15

From the above the static pressure developed in various material like Steel, Aluminum and ABS in fig 5 (a), (b), and (c). In these materials the lowest static pressure is developed in ABS Material which is 7.15Mpa and highest pressure developed in steel which is 7.25 Mpa. The result says that the static pressure is increases gradually from all directions from leading edge of blade toward the trailing edge of blade. The pressure gradient in axial direction are

lesser than the radial direction. and this is due to the centrifugal force acts on the trailing edges of the impeller blades. At the hub or centre the low pressure is developed due negative suction pressure. The static pressure should be less as increase in static pressure velocity flow decreases So Static pressure developed is less in ABS material.

3.3) Validation:

Zhou et al. [5] studied the static pressure developed on various position of blades of impeller. The graph of pressure distribution vs. position on the blades is plotted and it shows similar trend as compared to the results of Xin Zhou et al. as demonstrated in Fig. 6.

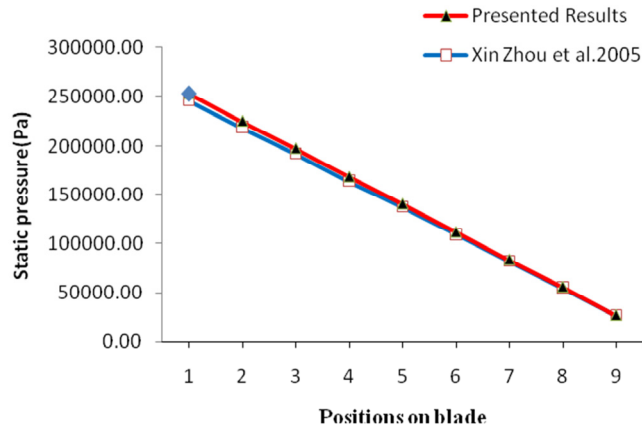


Fig. 6. Validation of Computational Results

4. Conclusion:

The computational analysis of mini impeller is performed using ANSYS Fluent Software in order to study the effect of speed and fluid flow condition on the wall shear stress and static pressure. The study has been carried out computationally on three different materials as steel, Aluminium and ABS. From the analysis of computational results, the static pressure and wall shear stress produced on impeller for ABS material are less as compared to steel and aluminum. So, it can be concluded that ABS material is most suitable for this type of impeller within the considered materials.

References:

- [1] S. Pierret and R. A. Van den Braembussche, "Turbomachinery Blade Design Using a Navier–Stokes Solver and Artificial Neural Network," *J. Turbomach.*, vol. 121, no. 2, p. 326, 2009.
- [2] S. L. Chen and W. T. Wang, "Computer aided manufacturing technologies for centrifugal compressor impellers," *J. Mater. Process. Technol.*, vol. 115, no. 3, pp. 284–293, 2001.
- [3] J. H. Kim, K. T. Oh, K. B. Pyun, C. K. Kim, Y. S. Choi, and J. Y. Yoon, "Design optimization of a centrifugal pump impeller and volute using computational fluid dynamics," *IOP Conf. Ser. Earth Environ. Sci.*, vol. 15, no. PART 3, 2012.
- [4] P. Guruprakash, P. Guruprakash, R. C. Radha, N. Karthikeyan, and N. Karthikeyan, "CFD Analysis of centrifugal pump impeller for performance enhancement," *IOSR J. Mech. Civ. Eng.*, pp. 33–41, 2010.
- [5] X. Zhou, Y. Zhang, Z. Ji, and H. Hou, "The Optimal Hydraulic Design of Centrifugal Impeller Using Genetic Algorithm with BVF," *Int. J. Rotating Mach.*, vol. 2014, pp. 1–14, 2014.
- [6] T. Report and I. Universiti, "Design and development of centrifugal pump impeller for performance enhancement," no. November, 2015.
- [7] J. S. Anagnostopoulos, "Numerical Calculation of the Flow in a Centrifugal Pump Impeller Using Cartesian Grid," *2nd WSEAS Int. Conf. Appl. Theor. Mech.*, pp. 124–129, 2006.
- [8] R. Ragoth Singh and M. Nataraj, "Design and analysis of pump impeller using SWFS," *World J. Model. Simul.*, vol. 10, no. 2, pp. 152–160, 2014.
- [9] G. R. H. Abo Elyamin, M. A. Bassily, K. Y. Khalil, and M. S. Gomaa, "Effect of impeller blades number on the performance of a centrifugal pump," *Alexandria Eng. J.*, 2019.

- [10] X. Zhang, W. Zhao, and Y. Xie, “Fatigue failure analysis of semi-open impeller with mistuning considered,” *Eng. Fail. Anal.*, vol. 95, no. September 2018, pp. 127–139, 2019.
- [11] M. Asuaje, F. Bakir, F. Kenyery, R. Rey, and S. Kouidri, “Numerical Modelization of the Flow in Centrifugal Pump: Volute Influence in Velocity and Pressure Fields,” *Int. J. Rotating Mach.*, vol. 2005, no. 3, pp. 244–255, 2005.
- [12] Shinde, A., Pawar, P., Shaikh, P., Wangikar, S., Salunkhe, S. and Dhamgaye, V., 2018. Experimental and Numerical Analysis of Conical Shape Hydrodynamic Journal Bearing With Partial Texturing. *Procedia Manufacturing*, 20, pp.300-310.
- [13] Das, S. S., Tilekar, S. D., Wangikar, S. S., & Patowari, P. K. (2017). Numerical and experimental study of passive fluids mixing in micro-channels of different configurations. *Microsystem Technologies*, 23(12), 5977-5988.
- [14] Wangikar, S. S., Patowari, P. K., & Misra, R. D. (2018). Numerical and experimental investigations on the performance of a serpentine microchannel with semicircular obstacles. *Microsystem Technologies*, 24:3307, 1-14.

Design of Mini Abrasive Vertical Belt Grinding Machine

**Rahul Khadtare¹, Pravin Chavan^{2,3}, Govind Wagh³,
Shubham Atkale⁴, Avinash K. Parkhe⁵**

*^{1, 2, 3, 4} UG Students, Mechanical Engineering Department,
SVRI's College of Engineering, Pandharpur*

*⁵Assistant Professor, Mechanical Engineering Department,
SVRI's College of Engineering, Pandharpur*

Abstract: Grinding is an abrasive machining process that uses a grinding wheel as the cutting tool. A wide variety of machines are used for grinding. Although mini belt grinding abrasive belt have stronger cutting ability than that on the grinding wheel. The main aim of this paper is to design vertical abrasive belts grinding machine to achieve good tolerance as well as better surface finish for various materials such as metal, glass, ceramic, rock and specified material. The abrasive belt grinding can reduce the surface roughness of work pieces and accuracy meanwhile Aluminium oxide belt with high stock removal cleaning and polishing is effectual. The abrasive belt grinding as compared to wheel grinding have more efficient with efficiency and parameter range. It is conclude that Aluminium oxide belt hardness makes it suitable for use as an abrasive and as a component in cutting tools with significant proportion. We have designed such Abrasive Belt vertical Grinding Machine having better advantages over wheel grinding machine.

Keywords: Aluminium oxide, abrasive belt, wheel grinding.

1. INTRODUCTION

Abrasive belt grinding is a common finishing process in the metal and wood working industries. Coated abrasive belts are used in the same speed range as bonded wheels, but they are not generally dressed when the abrasive becomes dull. Abrasive belt grinding is a kind of grinding tool with special form, which needs straining device and driving wheel and to make abrasive belt strained and moved at high speed, and under certain pressure, the contact between abrasive belt and work piece surface can help to realize the whole process of grinding and machining. Belt grinding is a rough machining procedure utilized on wood and different materials. It is commonly utilized as a completing procedure in industry. A belt, covered in rough material, is kept running over the surface to be handled so as to evacuate material or create the ideal finish. [6]

This Belt Grinder machine is designed using CATIA V5. It consists of 775 HP motor which is fundamentally rotates the pulley attached to it, along with a mini grinder, grinding paper and an abrasive belt grinder. The second pulley is attached to the wooden base vertically with the tensioner spring. Grinding paper is then fitted in pulley. To support the mini grinder a base frame is provided, it helps in grinding wooden material. Machine is designed using DC motor, spring, base Frame (support frame), abrasive grinder belt, coupling and a pulley. This machine helps to shape the material without putting much effort and getting better surface finish, and also getting larges area of belt for grinding operation than wheel grinding.

Grinding is an abrasive machining process that uses a grinding wheel as the cutting tool. A wide variety of machines are used for grinding. Although mini belt grinding abrasive belt have stronger cutting ability than that on the grinding wheel.

Yun Huang et al. presented the literature survey on belt grinding shows certain limited understanding of material removal, wear and grinding process. The importance of belt related parameters in grinding and finishing of work piece can be seen in the illustration on grinding. Compared to the grinding with wheels, involving non rigid wheel with belt grinding is another way to enhance the flexibility. In abrasive belt grinding Titanium alloy blade of aviation engine experiment, through the single factor experiment method, the influence of abrasive belt linear speed and work-piece feeding speed on the

grinding quantity is discussed. In abrasive belt grinding Titanium alloy blade of aviation engine experiment, through the single factor experiment method, the influence of abrasive belt linear speed and work-piece feeding speed on the grinding quantity is discussed. [1]

A. Robert Henry et al. studied Machining processing industries have continuously developed and improved technologies and processes to transform finished product to obtain better super finished product quality and thus increase products. Abrasive machining is one of the most important of these Processes and therefore merits special attention and study. Belt grinding is an abrasive machining process used on metals and other materials it is typically used as a finishing process in industry. The main objective of this project is to design and fabricate an abrasive belt grinding which can be used as versatile grinding machine, the work area can be rotated from 0 degree to 180 degree. The 0 degree work area can be used for bottom grinding of component, the 90 degree work area can be used for vertical grinding of component and The 180 degree work area can be used for top grinding of component. [2]

Huang presented the surface finishing and stock removal of complicated geometries is the principal objective for grinding with compliant abrasive tools. To understand and achieve optimum material removal in a tertiary finishing process such as Abrasive Belt Grinding, it is essential to look in more detail at the process parameters/variables that affect the stock removal rate. The process variables involved in a belt grinding process include the grit and abrasive type of grinding belt, belt speed, contact wheel hardness, serration, and grinding force. Changing these process variables will affect the performance of the process. [3] [4] [5]

2. Design of Belt Grinding Machine

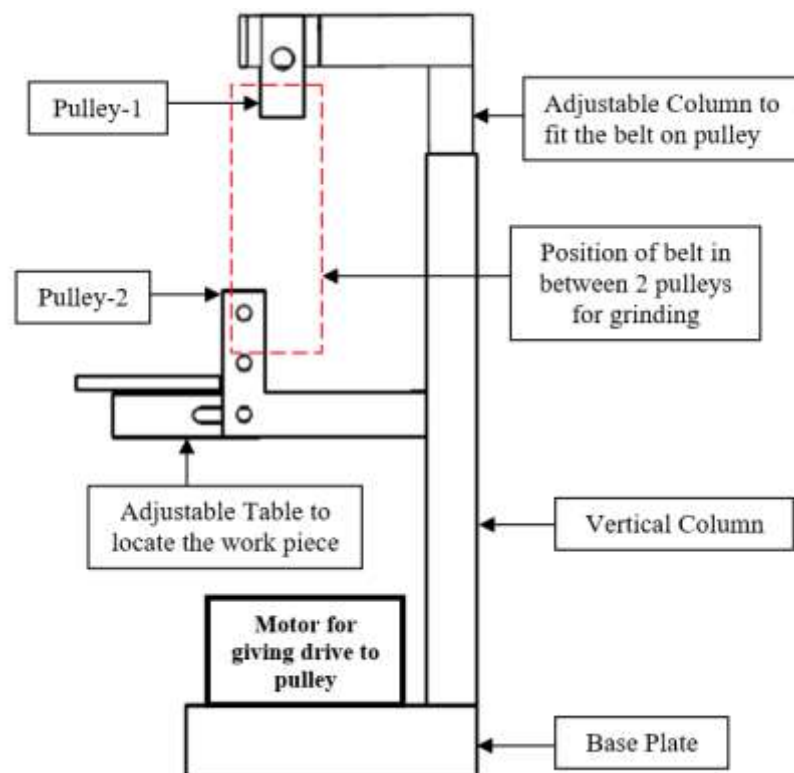


Figure 1. Front view of Belt Grinding Machine

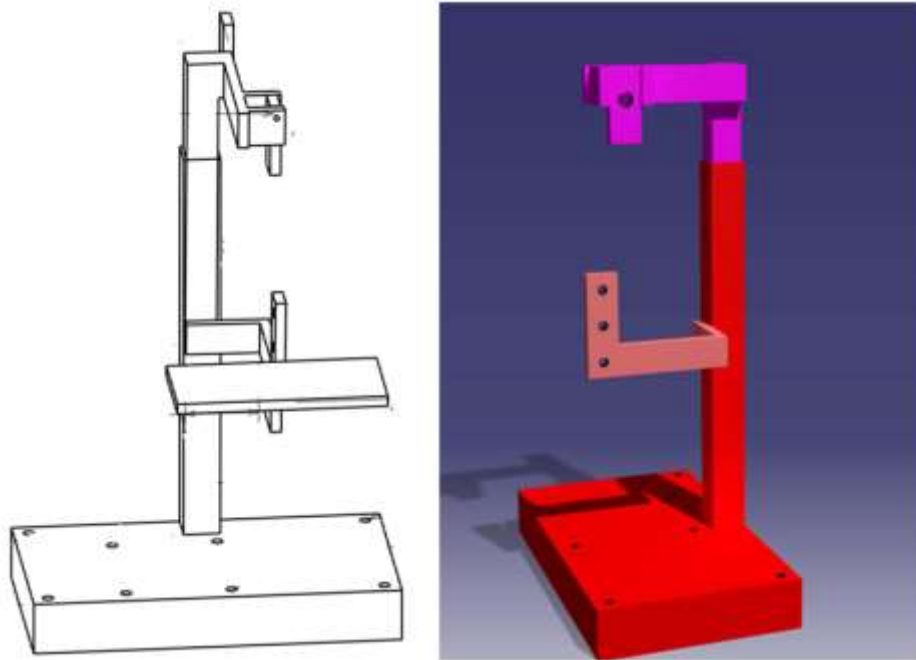


Figure 2. 3D modelling of Belt Grinding Machine in CATIA

2.1 Working Principal of Abrasive Belt Grinding Machine:

As you know that nowadays wheel grinding machines are mostly used for grinding operation. In most the workshops it is used for grinding, to remove the sharpen edges, sharpen the cutting tools by giving different angles. But in such wheel grinding machines there is one problem that very less area of wheel available to perform the grinding operation. Due to this area of contact in between grinding wheel and workpiece maximum time is required finish the surface or to grand the surface.

To avoid this major disadvantage we have developed this vertical abrasive belt grinding machine. The above figure 1 shows the front view of this machine with all important components. Figure 2 represents 3D modelling or 3D views of belt grinding machine which is designed using CATIA v5 software. The basic working principal of this machine is too grand or to finish the surface using abrasive belts which to be mounted on this designed machine. Due to this abrasive belts used maximum area of belt is comes in contact with workpiece due to which material removal rate or surface finish rate is more in less time as compared to wheel grinding machine.

2.2 Construction of Abrasive Belt Grinding Machine:

The above figure 1 represents the construction of abrasive belt grinding machine with all its important components. This machine is constructed on one base plate and is supported through vertical column shown in both figure 1 and figure 2. The motor is also mounted on base plate from which drive is given to grinding belts through pulleys shown in figure 1. One adjustable column is also provided to attach and remove the belts easily. The grinding belt rotates when motor starts and its movement used to grind or finish the surface similar to grinding wheel.

The table is also attached to vertical column to put the workpiece while performing the grinding operation shown in above figure 2. Due this vertical rotation of belts its maximum area is utilized for finish the surface due to which less time is required for grinding with maximum material removal rate than wheel grinding operation.

2.3 Abrasive Belts used in Belt Grinding Machine:

There are different abrasive materials which are used to manufacture the grinding wheels or belts. Sometimes abrasives materials used in wheel and belts are common sometimes it is different. But nowadays some special abrasives belts are available or manufactured to perform the grinding operation. The basic advantages of belts over wheels we have discussed above. Following figures represents the types of abrasive belts used in belts grinding machine having different dimensions manufactured for different applications.



Figure 3. Abrasive Belt (Ceramic and Nylon)

Table 2. Specifications of Ceramic and Nylon Belt

Material	Ceramic and Nylon
Size	25 mm width
Scope of Application	Metal processing industry, non-ferrous metal, rubber product, stone, black metal etc.

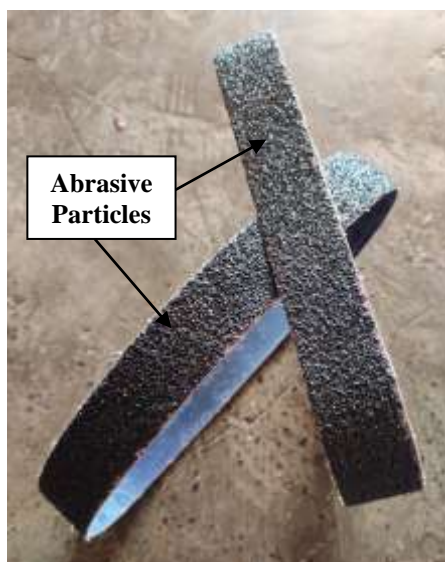


Figure 4. Abrasive Belt (Aluminium Oxide)

Table 2. Specifications of Aluminium Oxide Abrasive Belt

Brand	Drillpro
Material	Aluminium Oxide
Size	30 mm width
Scope of Application	Grinding of metal, wood, furniture, stone, steel other fields etc.

8. Conclusions

Grinding is an abrasive machining process that uses a grinding wheel as the cutting tool. A wide variety of machines are used for grinding. Although mini belt grinding abrasive belt have stronger cutting ability than that on the grinding wheel. But as wheel grinding is having some disadvantages in form of time required to finish the surface, material removal rate, surface finish obtained etc.

To over such disadvantages this vertical abrasive belt grinding machine is designed using CATIA v5 software to overcome disadvantages of wheel grinding machine. Also this machine helps too grand or to finish the surface using abrasive belts which to be mounted on this designed machine. Due to this abrasive belts used maximum area of belt is comes in contact with workpiece due to which material removal rate or surface finish rate is more in less time as compared to wheel grinding machine.

REFERENCES:

- [1] H. Huang, Z.M. Gong, X.Q. Chen, L. Zhou, "Robotic grinding and polishing for turbine-vane overhaul", *Journal of Materials Processing Technology*, 127, 140–145, 2002.
- [2] Yun Huang, Yun Zhao, and Xindong Zhang, Chongqing University, Chongqing, P.R. China, "Experiment research on the abrasive belt grinding titanium alloy blade of aviation engine", ISSN 1662-8985, Vol. 565, pp 64-69, China, 2012.
- [3] Huang Yun, Huang Zhi. *Modern belt grinding technology and engineering applications [M]*. Chongqing: Chongqing university press, (2009).
- [4] L. Yi, Y. Huang, G. H. Liu. *Experimental research on the electrochemical abrasive belt grinding 0Cr17Ni4Cu4Nb stainless steel [J]*. *Advances in Materials Manufacturing Science and Technology*, 2009, 626-627: 617-622.
- [5] X.Y. Re, K. Bernd. *Real time simulation and visualization of robotic belt grinding processes [J]*. *International Journal of Advanced Manufacturing Technology*, 2008, 35:1090-1099.
- [6] S. Mezghani, M. El Mansori, E. Sura. *Wear mechanism maps for the belt finishing of steel and cast iron [J]*. *Wear*, 2009, 267:132-144.

PERFORMANCE EVALUATION OF VCRS BY USING R134a AND R600a REFRIGERANTS: A STUDY

Mahesh Ghodake¹, Avinash Devmare², Chaitanya Kawale³,
Sachin Gosavi⁴, Milind Kulkarni⁵

^{1, 2, 3, 4} UG Students, Mechanical Engineering Department,
SVRI's College of Engineering, Pandharpur

⁵ Assistant Professor, Mechanical Engineering Department,
SVRI's College of Engineering, Pandharpur

ABSTRACT: The main aim of this paper is to comparatively analyze the performance of VCRS by using R134a (Tetrafluoroethane) and R600a (Isobutane) refrigerants. A domestic refrigerator was selected for performance. R134a is having zero ODP (Ozone Depletion Potential) but high GWP (Global Warming Potential approximately equal to 1200) where R600a having zero ODP (Ozone depletion potential) and negligible GWP (Global Warming Potential less than 20). The results of the performance analysis indicate that the amount of R600a refrigerant was the most effective parameter. The amount of R600a refrigerant required to produce the approximately same effect as that of R134a is approximately 50% less than the amount of R134a refrigerant. It is one of the economical advantage, also it reduces the flammability of hydrocarbon. All the results were compared. Based on the results, the coefficient of performance of R600a is better than R134a.

Keywords: R134a (Tetrafluoroethane), R600a (Isobutane), coefficient of performance (COP).

1. INTRODUCTION

The American Society of Refrigerating Engineers defines refrigeration as "the science of providing and maintaining a temperature below that of surrounding atmospheric Temperature". This implies the development of temperature differentials rather than the establishment of a given temperature level. The science of Refrigeration utilizes several methods of providing temperature differential. They vary from the simplicity of the spring house where cool water removes heat from fresh milk, to the complex machinery required for the manufacturing of ice-cream or production of considerably low temperature. In the olden days, natural ice was used for refrigeration purposes which were quite inconvenient and inadequate for large requirements. The different techniques are developed in the last 100 years and now there are numerous applications of refrigeration in our daily life as well as in many industries.

In different types of refrigeration systems, some physical property of matter is used for producing cold. Any substance capable of absorbing heat from another required substance can be used as the refrigerant, i.e., ice, water, air, or brine. The refrigerants which carry the heat in the form of latent heat and also dissipate in the form of latent heat are more efficient than the refrigerants which carry the heat in the form of sensible heat. The first refrigerant used was ether, employed by Perkins in his hand-operated vapor compression machine.

During the 1880s, ethyl chloride (C_2H_5Cl) was used as a refrigerant which soon gave way to ammonia, sulphur dioxide (SO_2), methyl chloride (CH_3Cl) and carbon dioxide (CO_2) found application as refrigerants. During 1910-30 many new refrigerants, such as N_2O_3 , CH_4 , C_2H_6 , C_2H_4 , C_3H_8 , were employed for medium and low-temperature refrigeration [1]. Hydrocarbons

were, however, found extremely inflammable. Dichloromethane (CH_2Cl_2), dichloroethylene ($\text{C}_2\text{H}_2\text{Cl}_2$) and monobromomethane (CH_3Br) were also used as refrigerants for centrifugal machines.

A great breakthrough occurred in the field of refrigeration with the development of Freon's (a trade name) in the 1930s by E.I. du Pont de Nemours and Co. Freon's are a series of fluorinated hydrocarbons, generally known as fluorocarbons, derived from methane, ethane, etc., as bases. Refrigerants like CFC's (eg. R11, R12, etc) and HCFC's (eg. R21, R22, etc) contain chlorine atoms, which is the main cause of the ozone layer deflation. Hence these are replaced by HFC's (eg. R134a, R404a, etc) type of refrigerants that have ODP value zero but causes Global Warming. Now a day's hydrocarbons (eg. R600a, R290, R600, etc.) are used as refrigerants, as they produces the same refrigeration effect with less charge and with less energy consumption.

1.1 DOMESTIC REFRIGERATOR:

The household refrigerator commonly used works on the VCRS principle. It contains the following processes,

1. Isentropic compression process in a compressor.
2. Isobaric heat rejection process in the condenser.
3. Isenthalpic expansion process in expansion device (In capillary tube).
4. Isobaric and Isothermal heat rejection process in the evaporator.

The schematic representation of VCRS is as shown below

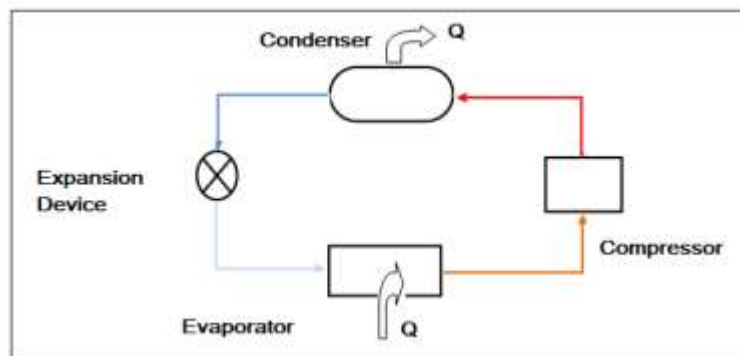


Fig.1: Schematic of the VCRS cycle.

The refrigerant vapor is compressed by means of the compressor to pressure at which temperatures obtained at the end of compression will be more than atmosphere so that at high temperature it will reject heat to the surrounding atmosphere and will then get condensed.

Capillary acts as an expansion device. Past expansion vapor is allowed to absorb the heat in the evaporator. After which it gets converted to vapor which will be further compressed in the compressor.

1.2 WORKING FLUIDS:

1. R134a (Tetrafluoro Ethane):

Table No.:1 Properties of R134a

Critical Temperature (°C)	101.06
Critical Pressure (bar)	40.56
Boiling point temperature (°C)	-26.15
Freezing point temperature (°C)	-96.6
Latent Heat Of Vaporization at NBP (kJ/kg)	222.5

2. R600a (Isobutane):

Table No.:2 Properties of R600a

Critical Temperature (°C)	135
Critical Pressure (bar)	36.45
Boiling point temperature (°C)	-11.67
Freezing point temperature (°C)	-159.6
Latent Heat Of Vaporization at NBP (kJ/kg)	367.7

2. LITERATURE REVIEW

- a) Shailesh Golabhavi and Vivekanand Navadagi, “Thermal and Performance analysis of R600a in vapor compression cycle”, published in IJERT-vol,7 Issue 01, January-2018
In this paper they have given the thermal performance analysis VCRS i.e. analysis of condenser and evaporator by using CFD. This analysis also shows the system effectiveness by using R600a is better than by using the R134a and other refrigerants.
- b) Dhanasi Sabari and Dr.Prasanthi, “Improvement in COP of domestic refrigeration with two refrigerants (R134a and R600a)”, published in IJESRT-vol,6(11), -(nov)2017
This gave us idea regarding the use same compressor of R600a for the refrigerant R134a without any effect. Also they used condenser with two different metals i.e. iron condenser and copper condenser.
- c) N Austin, “Experimental Performance Comparison of R134a and R600a in VCRS at steady state condition”, published in Journal of advances in mechanical engineering and sciences-vol,2(3)-2016
In this paper they showed us that same refrigerating effect is produced by using R600a as that of R134a but with approximately half quantity as that of R600a.

3. EXPERIMENTAL SETUP



Fig.2: Experimental Setup.

The experiment was carried out on a domestic Refrigerator of 170L capacity. Set up contains hermetically sealed compressor (230V, 50Hz, 1 Phase and 538BTU), naturally air-cooled condenser, capillary tube (diameter=0.7366cm and length=243.84cm) and evaporator. In addition to that two pressure gauges were fixed one at the inlet of the compressor (of range -30 psi to 250 psi) and another at the outlet of the compressor (of range 0 psi to 500 psi) respectively. They show the values of suction and delivery pressures in psi. A temperature drop of water was measured by LED Temperature meter (of range -50 to 99 °C), where condenser inlet temperature, condenser outlet temperature, evaporator inlet temperature, and evaporator outlet temperature were measured with the help of Digital Non-Contact IR Infrared Thermometer Temperature Gun (of HTC having a temperature range -30 to 550 °C). Single Phase Energy Meter (impulse type 240 V, 50 Hz) was used to measure the energy consumption of the compressor. The thermostat was detached for the continuous working of the compressor. The set up is as shown in the above figure.

4. EXPERIMENTAL PROCEDURE

1. Charge the complete system with the R134a.
2. Fill the evaporator with water.
3. Record the initial cabinet temperature and ambient temperature.
4. Switch on the 230 V, 50 Hz electric supply.
5. After half an hour record the - Condenser inlet temperature(T_2)

- Condenser outlet temperature(T_3)
- Evaporator inlet temperature(T_4)
- Evaporator outlet temperature (T_1).

6. Meanwhile, note down the time required for 10 blinkings of energy meter which is attached across the compressor to measure the load on the compressor.
7. Do the similar procedure at least for 3 times with sufficient time gap in between .
8. Remove the R134a from the system.
9. Charge the system with the R600a.
10. Repeat the similar procedure for the R600a.

5. OBSERVATION S AND CALCULATIONS

5.1- R134a

Suction Pressure = 1.1 bar

Delivery Pressure = 12 bar

Suction Temperature (T_1) = 20.2°C, $h_1 = 418$ kJ/kg

Delivery Temperature (T_2) = 85.8°C, $h_2 = 468$ kJ/kg

Condenser outlet Temperature (T_3) = 40.3°C, $h_3 = 258$ kJ/kg

Evaporator inlet Temperature (T_4) = -10.2 °C, $h_4 = 258$ kJ/kg

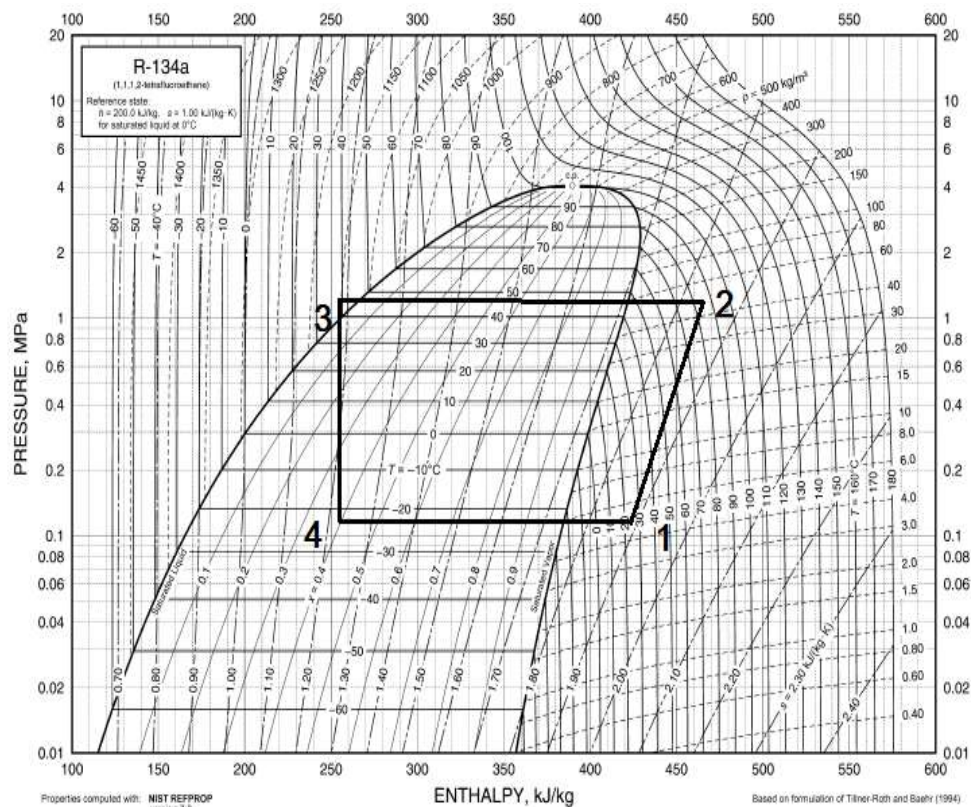


Fig. 3: Cycle representation of R134a

Hence, theoretical COP is

- $COP = (h_1 - h_4) / (h_2 - h_1)$
- $COP = (418-258) / (468-418)$
- $COP=3.2$

5.2 - R600a

Suction Pressure = 0.6 bar

Delivery Pressure = 7.9bar

Suction Temperature (T_1) = 10.1°C, $h_1 = 578$ kJ/kg

Delivery Temperature (T_2) = 65.3°C, $h_2 = 653$ kJ/kg

Condenser outlet Temperature (T_3) = 39.9°C, $h_3 = 300$ kJ/kg

Evaporator inlet Temperature (T_4) = -22.1°C, $h_4 = 300$ kJ/kg

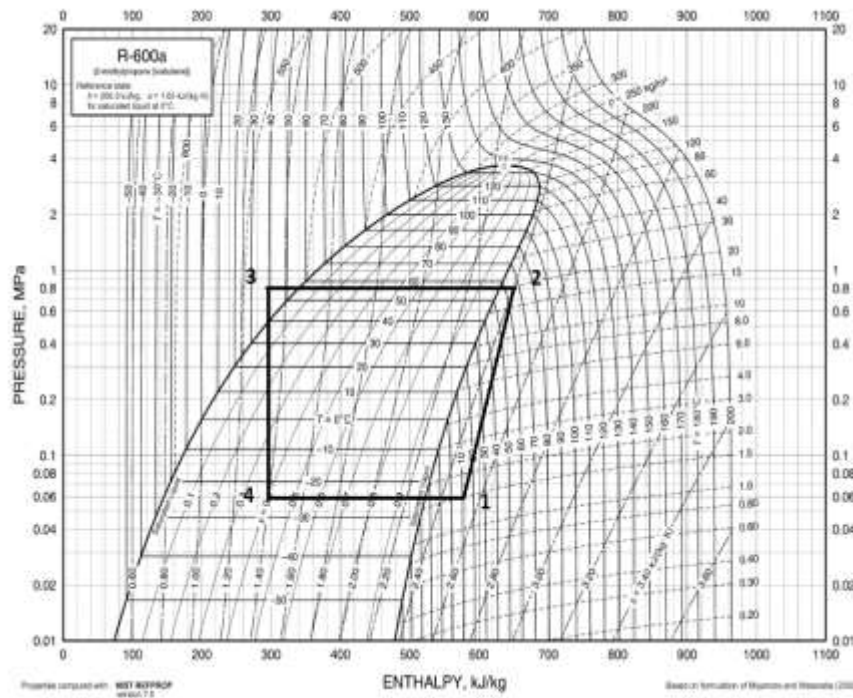


Fig. 5: Cycle representation of R600a

Hence, theoretical COP is

- $COP = (h_1 - h_4) / (h_2 - h_1)$
- $COP = (578-300) / (653-578)$
- $COP=3.7$

5. RESULTS AND DISCUSSION:

The theoretical COP of R600a is 3.7 where as the theoretical COP of R134a is 3.2. It means the theoretical COP of refrigerant R600a is greater than the theoretical COP of R134a. From these results it is clear that the refrigerant R600a is giving better performance than refrigerant R134a. Also the GWP of R600a is negligible which is one of the advantage. Compressor while working on refrigerant R600a consumes less energy as compared with refrigerant R13a. As the

latent heat of evaporation of R600a is more than R134a hence it gives better refrigeration effect than R134a and quantity of charge required to produce same refrigeration effect is also less. So use of R600a as a refrigerant is advantageous.

6. CONCLUSIONS

- The theoretical COP of R600a is 15.62% more than the theoretical COP of R134a, which is one of the economical advantages.
- The amount of R600a required to produce the same refrigeration effect as that of R134a is approximately 50% less. So accordingly the system can be designed.
- R600a is giving a better cooling effect as compared to R134a within less time.
- The load on the compressor while running on R600a is less as compared to R134a.
- The delivery temperature of R600a (65.3°C) is less than the delivery temperature of R134a (85.8°C).

REFERENCES:

- [1] C. P. ARORA, *Third Edition of Refrigeration and Air Conditioning*, Tata McGraw Hill Education Private Limited New Delhi.
- [2] Domkundwar and Arora, *Refrigeration and Air-Conditioning*, DHANPAT RAI & CO. (P) LTD.
- [3] Shalaka S. Hastak, Jagdeep M. Kshirsagar, *Comparative performance analysis of R600a and R463a as an alternative of R134a refrigerant in a domestic refrigerator*, International Conference on Mechanical, Materials and Renewable Energy, IOP Conf. Series: Materials Science and Engineering 377(2018)012047
- [4] ASHRAE Handbook-Fundamentals (SI)
- [5] M. Mohanraj, Jayaraj, C.Muraleedharan (2007), *Improved energy efficiency for HFC134a domestic refrigerator retrofitted with hydrocarbon mixture (HC290/HC600a) as drop-in substitute*, Energy for Sustainable Development, Volume XI No. 4
- [6] S. Uma maheswara Reddy, V. Dhana Raju & P. Tharun Sai, *Comparative Performance Analysis of Domestic Refrigerator using R12, R134a and R600a Refrigerants*, International Journal of Research and Analytical Review, VOLUME 5 | ISSUE 3/JULY-SEPT 2018.

Superiority of Graphene over Activated Carbon in terms of Adsorption Capacity, Proposed Mechanism and Interaction with Metal Ions and Biological Particulates

Debojeet Bhattacharjee¹ & Dr. Santosh B. Salunkhe²

¹UG Student, Mechanical Engineering Department
SVERI's College of Engineering Pandharpur, Maharashtra, India.

²Assistant Professor, Mechanical Engineering Department
SVERI's College of Engineering Pandharpur, Maharashtra, India.

Abstract: To tackle the on-going pollution and various contaminants in the ecosystem and to ensure availability of ambient conditions of natural resources like air and water, there is an alarming demand globally for developments in high performance purification materials/ devices. This paper is a review of performance of two of the most widely discussed carbonaceous materials often spoken about in the context of filtration and contamination - the conventional Activated Carbon (AC) along with its modified forms and the relatively new 2D counterpart Graphene. Our study describes how the 2D Graphene and its composite structures possess considerable superiority over AC in terms of adsorption capacity and efficiency in interacting with ions and pathogens like viruses and bacteria. The superiority in properties can be attributed to high surface area per unit mass, distribution of surface functionality, pH tolerance and higher multisite adsorption due to large number of surface functional groups. The review has a vital role in predicting possible areas of applications where Graphene has potential to replace AC.

Keywords: Graphene, activated carbon, oxide of graphene,

1. Introduction

The extend of industrialization and environmental pollution continue to increase at an unprecedented rapid pace. We also face a constant threat of being infected by pathogens which may sometimes even challenge our existence in this planet. Industrial discharges and fumes containing high concentration of toxins like pharmaceuticals, pesticides, dyes containing heavy metal ions like Pb, Cr, Cd, and Cu; when released into the environment are highly toxic and can bio-accumulate in human body, aquatic life, atmosphere and in soil [1]. In fact, metal contamination is found to be a major problem in disposing industrial and municipal wastewater [2]. These contaminants when present in atmosphere can cause great degree of health hazards, especially to the more vulnerable ones like children, pregnant women, elderly people and allergic people.

Pathogens like bacteria and viruses can also have significant health implications in humans as well as animals [3]. To tackle the situation, various chemistry based efforts have been devoted to feasibly control the impact on human health and environment, also to filter out these contaminants from the environment. Among various methods of treating the industrial effluents like electrochemical treatment, reverse osmosis filtration, evaporation recovery and electrocoagulation [4-6]. Among these all technologies, adsorption is relatively new and is found to be comparatively superior in terms of efficiency, rapidness, cost effectiveness and environment friendly method. Many papers have been published in the past few decades, confirming the carbonaceous materials are effective adsorbents for decontamination of metal ions and their complexes [7]. Activated carbon (AC) being one of the first material applied as adsorbent, has been utilized in numerous applications due to its excellent adsorption capabilities, attributing to its large specific surface area and highly porous internal structure.

Studies show successful role of AC in the adsorption of heavy metal ions [8]. Another research shows successful adsorption of polio virus and infectious hepatitis virus on AC [9]. Through introduction of different acidic/oxidative or basic surface functionality, AC can be modified to increase selectivity of certain species. However, this limits the adsorption of other contaminants, making AC more selective to specific species only.

This turns to be a major disadvantage in an environment where numerous species co-exist, as in water bodies and atmospheric air. Relatively low evidences of work have been found to prove an appropriate balance of selectivity on AC or to show the effect of competitive adsorption and any positive or negative effects that can arise from complex mixtures [10].

Talking of the newly developed counterpart Graphene, a fascinating new member of the carbon family, this hypothetical one-atom thick sheet has sp_2 hybridized carbon bonded to each other; forming a honeycomb 2D lattice. Graphene is one of the most fascinating nanostructure with unique physical, chemical, electrical and mechanical properties [14] which qualifies it as a promising nanomaterial in material science [11,12] and a wide range of technological applications like bioelectronics and bio sensing [13]. The oxide of Graphene, generally prepared by Hummer's method or modified Hummer's method [18] from Graphene, which is basically an acid treatment process, GO's specific surface area indicates it can be used as an efficient adsorbent. The topological variation can result in different interactions between the carbon substrate and a guest molecule and consequently, variation in adsorption behaviour [15]. Studies show that GO is more efficient than AC in adsorption of metal ions [15]. Destruction of peptidoglycan in bacteria(cytotoxicity)[16], inactivation of virus by destruction of capsid structure as well as lipid envelop[17], can be attributed to physicochemical interactions(like mechanical strength, magnetism, hydrophobicity etc) which could primarily ascribe hydrogen binding, electrostatic interaction and redox reaction.

Herein, we discussed the adsorption behaviour of AC and Graphene (oxides) for metal ions and pathogens like Bacteria and viruses based on the characterization of these two carbonaceous materials, analysis of adsorption isotherms, Buffer capacity (i.e. pH effect on adsorption) and effect of adsorption due to surface functionalities. We further extend our discussion to some of the crucial findings that highlight the fact that Graphene exhibit a clear superiority over AC, which can possibly open door for further studies to develop the next generation regenerative filtration and purification devices/mechanisms with enhanced functionality and stability.

2. Analysis and Discussion:

Adsorption being a surface phenomenon, higher specific surface area plays the most important role in determining the adsorption capacity of a material (table 1). 2D materials like Graphene possess high aspect ratio as compared to the 3D structure. Further, the presence of internal atoms in the lattice limits the adsorption capacity. The promising aspects of 2D nanostructures like Graphene and CNTs to be used in adsorption process is that they give higher adsorption for relatively low quantity of material.

Table 1: Physical properties of GO and AC [15]

	Specific surface Area(m^2/g)	Pore Volume(cm^3/g)
GO	148.34	0.091
AC	28.64	0.038

A detailed discussion of the interaction of these two carbonaceous materials with various contaminants mentioned earlier have been analysed in the following sections.

2.1 Adsorption analysis of metal ions on AC and GO:

Adsorption of methylene blue dye on GO was attributed to π - π electron donor acceptor interactions and electrostatic interactions, however while that on AC was due to large surface area [19]. Another study on the

suggests that AC materials have the capacity to form cation/ anion- π interaction with metal species, but this process is generally extremely poor, hence not considered.

A study on the adsorption of Cu ions suggest that AC has lower adsorption efficiency than GO under acidic condition [15]. The maximum adsorption capacity for GO was found to be 1.18×10^{-3} mol g⁻¹ and that for AC was much low, at around 2.31×10^{-4} mol g⁻¹; as found from the Langmuir's adsorption isotherm. The study also suggested Langmuir model to be more accurate for metal ions like Cu(II) as compared to the Freundlich model. Further, potentiometric acid-base titration experiment on these carbonaceous materials reveal that the buffer capacity of GO>AC. The buffer capacity can be assigned to the concentration of surface functional groups, that was found to be 6 times higher in GO than on AC. The affinity of Cu(II) ions towards GO and AC .

GO>AC. This can be correlated with the $\text{pH}_{\text{pzc}}(\text{GO}) < \text{pH}_{\text{pzc}}(\text{AC})$. pH_{pzc} controls the Coulombic interactions between carbonaceous surface and the aqueous metal ions and hence the metal ion uptake [20]. pH_{pzc} value depends upon the surface acidic functional groups[21] . The higher the concentration of surface acidic functional groups, lower the value of pH_{pzc} , suggesting the reason for higher efficiency of Cu(II) ions decontamination using GO. Another remarkable conclusion that can be drawn out from the pH_{pzc} discussion is the higher concentration of the surface acidic or oxidative functional groups in GO.

Other major heavy metal ion contaminants that are found to be highly toxic apart from Cu(II) are Pb(II), Cd(II),Cr(VI) [22] is also found to have a similar trend in adsorption as that of Cu(II) ion. The adsorption capacity of GO and AC for Pb(II) and Cd(II) metal ions is shown in Table 2.

Table 2: Adsorption of Pb and Cd ions on AC and GO [2]

	Adsorption capacity (mg/g)		
	AC		GO
	Native	Modified	
Pb(II)	66.23	95.24	447
Cd(II)	N/A	1.98	177

It is evident from this table that GO-composites possess tremendously high adsorption capacity for these ions as compared to even the modified acidic - functionalized AC.

2.2 Adsorption analysis of bacteria on AC and Graphene:

Using native AC in the application where bactericidal properties are needed is found to be a problem. Studies show that AC may adversely affect by favouring environment for the growth of microorganisms. Hence, an alternative that is being employed to produce AC with antimicrobial properties is its modification with silver nanoparticles (AgNPs) that are commonly used as microbial agents [28].

A study shows that some unique properties of graphene nano sheets are similar to the properties of CNTs. This is a vital implication of potential of graphene to be used in this field.

Earlier studies suggest, single wall CNTs present noticeable cytotoxicity to human and animal cells[32,33]. Also, toxicity of SWCNTs is greater than MWCNTs; which can be associated to oxidative stress[32,34] cutting off the intercellular metabolic routes [34] and rupture of cell membrane [35]. However, oxidative stress is rega Experiments performed to check interaction of gram (+) and gram (-) with metal impregnated AC [25, 26] especially AgNPs, CuNPs, ZnNPs and PbNPs had shown successful results in adsorption data when analysed by UV-Vis Spectroscopy and FT-IR Spectroscopy. Although these in-vitro results are limited by the high cost of manufacturing metallic nanoparticles and problems of aggregation of metal ions in the

dispersion due to interparticle surface attraction and release of metal ions from metallic nanoparticles which is attributed to the oxidation process[27].

Bacterial toxicity of the graphene nanosheets in the form of graphene nanowalls [16]; capture of bacterial species and particulates which cause severe nosocomial infection in patients and health care workers by a porous conductive graphene material called Laser Induced Graphene(LIG) obtained from CO₂ laser cutting of simple polyamide film[29] which employs periodic Joule heating (>300°C) that only destroys bacteria but any other microorganisms that possess potential to cause adverse biological reactions and diseases (like pyrogens, allergens, exotoxins, endotoxins, mycotoxins, nucleic acid and prions); studies made on the graphene materials and composite for neutralizing microorganisms function through different mechanism including penetration and compromise of the bacteria membrane, generation of reactive oxygen species(ROS) and envelopment of microbes[30,31] are few critical studies mentioned among the large number of other successful studies implying the use of graphene and it's composites for antibacterial action.

Hence, we postulate that Graphene is far superior to AC and it's modified forms in terms of effectiveness of bacteriocidal effect and in general, cytotoxicity considered as the most acceptable mechanism. Extending this subject to graphene nanosheets with extreme high aspect ratio can be proposed as one of the excellent and ideal nanostructure for the application. Further, a study shows that the graphene oxide nanowalls(GONWs) obtained by Electrophoretic deposition (EPD) process good cytotoxicity to bacterial cell [16].

However, on reducing GONWs with Hydrazine as reducing agent in the suspension, reduced graphene nanowalled structure (RGNWs) were produced. RGNWs possess higher toxicity than GONWs. To determine the bacterial toxicity of both GONWs and RGNWs their effect on a gram (-)ve bacteria (E.coli) and a gram (+)ve bacteria (S.Aureus) was analysed. The result of the experiment after 1 hour is tabulated below[Table 3].

Table 3: Antibacterial activity of GONWs and RGNWs [16]

Sample	Antibacterial Activity (in 1 hour)	
	{Survival Bacteria (%)}	
	E.coli	S.aureus
GONWs	41(±8)	26(±5)
RGNWs	16(± 3)	5(± 1)

These result shows that RGNWs works better for antibacterial applications. Further extension in the time of experiment to upto 2 days showed 100% antibacterial activity, proving RGNW to be one of the most efficient nanostructure for the application. This can be attributed to stronger interaction between more sharpened edges of reduced nanowalls with the cell membrane and/or better charge transfer between the bacteria and edges of RGNWs.

Further, the reason for the relatively low inactivity of gram (-ve) bacteria E.Coli as compared to the gram(+)ve S.Aureus may be attributed to the pressure of thin peptidoglycan layer in E.Coli, this inhibiting the interaction of bacteria to the lateral plane of RGNWs. Reverse is the case for gram (+)ve S.Aureus which possesses a much thicker peptydoglycan layer resulting in higher affinity to graphene nanowalled structures.

2.3 Adsorption analysis of viruses on AC and Graphene:

Considered to be the mo.st mischievous pathogen to humans, animals as well as plants; wide range of viruses have infected the human race in various ways time-to-time and continue to do so. A study by John T. Cookson Jr.[36] describes in his study, how the virus can be adsorbed by Activated Carbon and possible mechanism behind it. It is worth mentioning here, that even earlier, activated carbon has successfully adsorbed Polio virus and infectious Hepatitis virus [9].

In this study[36], Coliform bacteriophage was used; as the knowledge of phage properties are advanced for bacterial cell (E. coli B cells were used in this study). In spite of using a bacteriophage, adsorption

characteristics of human-infecting viruses can be concluded from the study, as bacterial virus exhibit similar adsorption characteristics. Adsorption of virus on AC is greatly dependent on the pH of the solution or atmosphere, in which adsorption takes place. A decrease in pH from the optimum of 7 is found to decrease in pH the rate of adsorption, probably due to inability of carboxyl group surface functionality of AC to get ionized at low pH. However, at higher pH, positively charged amino acid groups of viruses protein shell interact with the negatively charged carboxyl groups of carbon. Such high dependency of virus and AC on the surrounding pH is a limitation for its application, which can also be attributed to the low Buffer capacity of the AC[15]. Moreover, esterifying of carboxyl groups may lead to blockage of adsorption sites[36] resulting in drastic decrease in the adsorption capacity. However, there is no evidence of lipid enveloped viruses being adsorbed on AC.

Graphene's capability to interact efficiently with bacterial membranes by direct inorganic biomolecule interaction have been discussed earlier in this paper. The interplay between GO and microbes have been demonstrated, attributing to the bioreduction of oxygen containing functionalities via bacterial respiration. Considering the versatile GO biomolecule interactions, we can reach to a conclusion that GO materials could potentially serve as a novel nanostructure for virus prevention.

This can be associated to the multiplex biological interaction between GO nanosheets and viruses. To get an insight of the answer to the question of why Graphene can act superior to AC in virus capture; we discuss the results of a study conducted on two enteric viruses, namely EV71 and H9N2[17].

In this study, the viruses were exposed directly to GO suspension (50 µm/ml) at different temperatures for about 30 mins. The disinfectant effect of GO was found to be weak at room temperature (25°C). However, increase in the temperature marked as adsorption enhancement. This dependency of adsorption to elevated temperature and prolonged exposure time is being explained by another study[38]. The analysis of GO-Virus interaction can be studied from the results of UV-Vis spectroscopy. It shows strong protein adsorption capacity of GO. This unique physicochemical interactions can be attributed to Hydrogen binding, electrostatic interactions and redox reaction.

The FT-IR spectroscopy analysis of the interaction suggests some major deductions, which is extremely useful for reasoning of GO to be highly effective nanostructure over virus adsorption. The results suggest that GO relatively bioreduced in the presence of these viruses (i.e. EV71 and H9N2) to reduced GO (rGO). The viruses were found to thermally reduce GO[39].

Hence, the capture of virus Particles may be explained as the physicochemical interaction between various oxygenated group on the GO surface and the viruses. Further, evidences of general disruption effect of GO have been observed successfully in various studies, siting disrupted virus particles both on the edge as well as the basal plane, implying effective destruction of both capsid(protein) coated viruses and lipid coated (enveloped) viruses.

3. Conclusion and Future Perspectives

The discussions made in this review points towards a quite clear picture of why the title of this paper is "Superiority of Graphene over AC". Be it in terms of larger specific surface area or multiplex trapping of the pathogens. One of the promising aspects of Graphene-based material over AC is its capability to regenerate its surface function groups, which is likely to be of use in next generation purification devices. The size-exclusion properties of graphene Nano mesh and tuneable size of Nano pores are the contributions which would help in achieving ultrafiltration and water desalination in the next few decades.

Activated carbon, due to its current cost of manufacture, remains the most prominent carbon – based adsorbent, and used in a wide spectrum of applications. However, the potentials of Graphene realized by researchers and nano- scientists cannot be neglected.

Though technical problems exist in taking out the laboratory finding on Graphene to an actually usable scale; the developments in the high precision Nanoprocessing promises that Graphene would soon take over, marking as the start of a new era in material science, probably calling it Graphene Era!

References:

1. Mathur N., Bhatnagar P. and Bakre P., "Assessing mutagenicity of textile dyes from Pali(Rajasthan) using Ames bioassay", *Applied Ecology and Environmental Research*, Vol.4, No.1, 2006.
2. J. Gracia-Martin, R. Lopez-Garzon, M. L. Godino-Salido, M. D. Gutierrez-Valero, P. Arranz-Mascards, R. Cuesta and F. Carrasco-Marin, "Ligand adsorption on an activated carbon for the removal of Chromate ions from aqueous solutions", *Langmuir*, Vol.21, 15, 2005.
3. Cabral J.P.S., "Water microbiology, Bacterial pathogens and water", *International journal of Environmental Res. Public Health*, Vol.7, 2010.
4. M. A. Amer, F.I. Khaili and A.M. Awwad, "Adsorption of Lead, Zinc and Cadmium ions on polyphosphate-modified Kaolinite clay", *Journal of environmental chemistry and Ecotoxicology*, Vol.2, No.1, 2010.
5. V. J. Inglezakis, M. D. Loizidov and H. P. Grigoropoulou, "Ion exchange of Pb^{2+} , Cu^{2+} , Fe^{3+} and Cr^{3+} on natural clinoptilolite: selectivity determination and influence of acidity on metal uptake", *Journal of colloid and interface science*, Vol.2, 2003.
6. P.T. Bolger and D.C. Szlag, "Electrochemical treatment and reuse of Nickel plating rinse waters", *Environmental Progress*, Vol.21, 2002.
7. G.P. Rao, C. Lu and F. Su, "Sorption of divalent metal ions from aqueous solution by carbon nanotubes: A review", *Sep. Purif. Technology*, Vol.58, 2007.
8. K. Pyrzynski, "Sorption of Cd(II) onto carbon-based material-a comparative study", *Microchimica Acta*, 169, 2010.
9. Black A.P. & Smith A.L., "Determination of mobility of colloidal particles by micro electrophoresis", *Jours AWWA*, Vol.54, 1962.
10. Pelekani C, Snoeyink V.L., "Competitive Adsorption in natural water: Role of activated carbon pore size", *Water Res.*, Vol. 33, 1999.
11. Wu Z.S., Pei S, Ren A, Tang D, Gao L, Lui B, Li F, Liu C, Cheng H.M., "Field emission of single layer graphene films prepared by Electrophoretic Deposition", *Adv. Materials*, Vol.21, p2009.
12. Hai J, Zhong X, Jiang S, Huang Y, Duan X, "Graphene Nanomesh", *Nat. Nanotechnology*, Vol.5, 2010.
13. Hong W, Hai H, Xu Y, Yao Z, Hu Z, Shi G, "Preparation of gold nanoparticles/ graphene composites with controlled weight contents and their application in Biosensors", *J. Phys. Chan. C*, Vol.114, 2010.
14. Samantara A.K. Ratha S & Raj S, "Functionalized Graphene Nanocomposites in Air Filtration Applications", *Functionalized Nanocomposites and their derivatives*, chap.4, pp.65-89.
15. Dheksi Ren, Jiaxing Li, Xiaomi Tan and Dianne Wang, "Comparative study of graphene oxide, activated carbon and carbon nanotubes as absorbents for copper decontamination", *Dalton Trans*, Vol.42, 2013.
16. Akhavan O., Ghaderi E, "Toxicity of Graphene & Graphene Oxide Nanowalls against Bacteria", *ACS Nano*, 4(10), 2010.
17. Zhigond S, Xiaogu W, Vending Z, Clinggong N., Hangyu Z., Dong Y., Chengfeng Q. and Ruikang Tang, "Virus capture and destruction by Label – Free Graphene Oxide detection and disinfection applications", *Small*, 2014.
18. Han Y., Xu Z, Gao C, "Ultrathin graphene nanofiltration membrane for water purification", *Adv Funct Material*, Vol. 23, 2013.
19. Li Y, Du Q, Liu T, Peng X, Wang J, Sun J, Wang Y, Wu S, Wang Z, Xia Y and Xia L., "Comparative study of methylene Blue dye adsorption onto activated carbon, Graphene Oxide and Carbon nanotubes". *Chemical Eng. Res. Des.*, Vol.91, 2013.
20. Alvarez- Merino M.A., Fontecha-Camara M.A, Lopez- Ramon M.V. and Moreno Castilla C., "Temp. dep. Of the point of zero charge of oxidized and non-oxidized activated carbons", *Carbon*, Vol.46, 2008.
21. Borah D., Satokawa S., Kato S. and Kojima T, "Sorption of As(V) from aqueous solution using acid modified carbon black" *J. Hazard Mater*, Vol.162, 2009.
22. Mulu Bethe Desta, "Batch Sorption experiments : Langmuir and Freundlich Isotherm studies for the adsorption of textile metal ions onto Teff Straw (*Exagrostis tef*) agricultural waste", *Jour. of Thermodynamics*, 2013.

23. M.J. Swectman, S. May, N. Mebbersson, P. Pendleton, K. Vasilev, S.E. Plush, J.D. Hayball, "Activated carbon, carbon nanotubes and Graphene: Materials and composites for advanced water purification", *Jour. Of Carbon research*, 2017.
24. Yao S, Zhang J, Shen D, Xiao R, Gu S, Zhao M, Liang J, "Removal of Pb(II) from water by activated carbon modified by nitric acid under microwave heating", *J. Colloid interface sci.*, 2016.
25. Ihsanullah, Al-Khaldi F.A., Abusharkh B, Khaled M, Stich M.A., Nasser M.S., Laboni T., Saleh T.A., Agarwal S., Tyagi I, et al, "Adsorption removal of Cd(II) ions from liquid phase using acid modified carbon based adsorbents", *J.Mol.Liq.*, Vol.204,2015.
26. Saravan A, Kumar P.S., Karthiga Devi G.,Aromugam T., "Synthesis and Characterization of Metallic Nanoparticles impregnated onto activated carbon using leaf extract of *Mulia Madarasapatna* : Evaluation of antimicrobial activities", *Microbial Pathogens*, Vol. 97,2016.Surely Patrica C.Gonsalves, Mathias Strauss, Fabricio S.Xelite, Zaira Clemente, Vera
27. L. Castro, Diego Stefani T.Martinez, "Activated Carbon from pyrolysed sugarcane bagasse : Silver Nanoparticle Modification and exotoxicity assessment".
28. Ma R., Lerard C., Cheng Y.M, Lio J., Michel F.M., Brown G.E., Lowry G.V., " Size- controlled dissolution of organic-crated silver nanoparticles", *Environ.Sci.Tech.*,Vol. 46, 2012.
29. Zhang F., Tai Y., Chen S., Lu Y, "Preparation and Properties of Silver loaded AC fibers", *Fiber Polyn*, Vol. 16,2015.
30. Stanford M.G., Li J.T., Chen Y, McHugh E.A., Liopo A., Xiao H. and Tour M.James, "Self Sterilizing Laser induced Graphene bacterial Air filter", *ACS Nano*, Vol.13, 2019.
31. Hu W., Peng C., Luo W., LvM., Li D, Huang Q., Fan C., "Graphene -based antibacterial paper", *ACS Nano*,Vol.4,2010.
32. Chen J., Peng H , Wang X., Shao F., Yuan Z., Han H., "Graphene oxide exhibits broad- spectrum antimicrobial activity against bacterial phytopathogens and fungal conidia by intertwining and membrane perturbation", *Nanoscale*, Vol.6,2014.
33. Shvedova A.A., Castronova V., Kisin E.R.Schmegler Berry D., Murray A.R., Gandelsman V.Z., Maynard A., Baron P., " Exposure to carbon nanotube material : Assessment of Nanotube Cytotoxicity using Human Keratinocyte cells", *J. Toxicol Environ Health, Part A*, Vol.66,2003.
34. Chen X., Tam U.C., Czapinski J.L., Les G.S., Rabuka D., Zettl A., Bertozzi C.R., "Interfacing carbon Nanotubes with Living Cells", *Journal of Am.Chem.Soc.*, Vol. 128,2006.
35. Nel A, Cia T, Madler L, Li N, "Toxic -Potential of materials at Nanolevel", *Science*, Vol. 311,2006.
36. Kang S., Herzberg M., Rodrigues D.F., Elimelach M., "Antibacterial effects of carbon nanotubes : size does matters", *Langmuir*, Vol.24, 2008.
37. John T. Cookson Jr., "Mechanism of virus absorption on activated carbon", *Amer.Water Works Ass.*,61.
38. Stent G.S., "Molecular Biology of Bacterial viruses, W.H.Freeman and company, San Francisco, California,1963.
39. Lee Y.M., Jung B., Kim Y.H., Park A.R., Han S., Choe W.S., Woo P.J., "Nanomesh-structured ultrathin membranes harnessing the unidirectional alignment of viruses on a Graphene-Oxide film",*Adv. Materials*,Vol.26,2014.
40. Lui J., Fu S. Yuan B., Li Y., Deng Z., "Toward a universal ""Adhesive Nanosheet"" for the assembly of multiple nanoparticles based on a Protein-Induced Reduction/Decoration of Graphene Oxide", *Journal of American Chem. Soc.*, Vol.132, 2010.

Design of an Earth Air Heat Exchanger System for Space Cooling in Hot and Dry Climate of Pandharpur, India

Digvijay Ronge¹, Vishal Kadam², Suraj Shende³, Pankaj Kate⁴,
Vishal Waghmare⁵ & Onkar Patil⁶

^{1,2,3,4,5,6}SVERI's College of Engineering Pandharpur, Maharashtra, India.
¹ddronge@coe.sveri.ac.in, ²vishaljkadam@coep.sveri.ac.in

Abstract: Earth Air Heat Exchanger (EAHE) system is a promising passive cooling technique which uses earth's potential to maintain constant temperature at certain depths throughout year to cool air during summer and vice versa in winter for space air-conditioning. EAHE systems are best suited in hot and dry climatic conditions because EAHE systems in humid areas face challenges of condensation of water and contamination by microorganisms. Commercial Heating, Ventilation and Air Conditioning (HVAC) systems are now installed everywhere because of various standards and guidelines in their installation. EAHE systems lack such standards, installations guidelines and hence have less commercialization, being in their early stages. An effort is made in this paper to design an EAHE system for a lab of SVERI's College of Engineering (Polytechnic) in hot and dry climate of Pandharpur City, India. Heat exchanger calculations are made based on NTU method and a piping layout is created for optimum space utilisation. This system is expected to reduce energy demands for space cooling in educational institutes.

Keywords: Earth-air Heat Exchanger, Earth's Undisturbed Temperature, NTU, Nusselt number.

1. Introduction

Heat Exchangers are used in Air conditioning systems worldwide for space cooling or heating in both industrial and residential buildings. It is mainly achieved efficiently by vapour compression machines. Various heat transfer enhancement involve the use of surface vibration, change of geometry, various inserts and use of nanofluids [2,3]. Air conditioning systems are worldwide employed for space cooling or heating in both industrial and residential buildings. An earth to air heat exchanger draws ventilation supply air through buried tube. The incoming air being heated in the winter and cooled in the summer by means of earth coupling. System can be driven by natural sack ventilation, but usually require mechanical ventilation. Earth to air heat exchangers are suitable to mechanically ventilated buildings with a moderate cooling demand, located in climates with a large temperature difference between summer and winter and between day and night [4]. Earth tubes are often a viable and economical alternative to conventional central heating or air conditioning systems since there are no compressors, chemicals or burners and only blower are required to move air. These are used for either partial or full cooling and /or heating of facility ventilation air. Their use can help building meet passive house standards. Passive Cooling techniques are gaining importance being pollutant free and low cost which use natural sources and Earth–Air Heat Exchanger (EAHE) system is one of them. Uses of EAHE can contribute to reduction in energy consumption, maintenance cost and toxic pollutants

Earth's undisturbed temperature (EUT) is the temperature of earth at a depth of 3 to 4 m that remains fairly constant throughout the year. The EUT remains higher than ambient air temperature in winter and lower than ambient air temperature in summer. As shown in figure 1, the ambient air is drawn through the pipes of the EAHE buried at a particular depth, moderated to EUT, and gets heated in winter and vice versa in summer. In this way, the heating and cooling load of building can be reduced passively. EAHE require low maintenance and low operating cost.

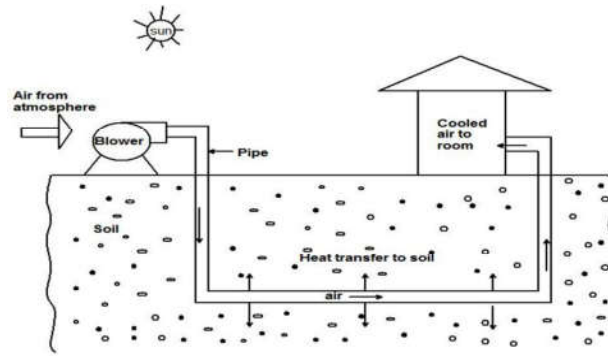


Figure 1: Two-dimensional EAHE model

Bordoloia [5] presented an apprehensible summary of the previous works on EAHE and describes of the analytical and experimental studies on the different combination of EAHE in different locations such as the hot and humid climate of Sahara, cold climate of Australia, tropical climate of Brazil, Mediterranean climate, moderate climate of India etc. EAHE systems in conjunction with the ventilation system and other cooling technique, i.e. hybrid EAHE has become very prominent in today's research as it promotes more energy saving.

Carslaw and Jaeger [6] provided analytical solutions for heat transfer through infinite hollow cylinder and infinite line sources, respectively. The temperature field on the ground can be written as a function depending on time (t) and radius r around a line source with a constant heat injection rate (q) from a line along the vertical axis of the borehole in an infinite solid.

$$\Delta T = - \frac{Q}{4\pi k} \text{Ei} \left(\frac{-r^2}{4\alpha t} \right) \quad (1)$$

The model does not account for ground surface interaction, does not readily account for initial ground temperature gradients, and the line source is also variable along the length of the pipe due to the fluid temperature changing, so this method cannot suitably predict the behaviour along the pipe. An effort is made in studying the behaviour of soil under constant heat flux conditions beneath the ground by DigvijayRongel[1]. Soil is observed to be thermally saturated after a period of time and there is no further heat transfer in soil.

De Paepe and Janssens [7] put forwarded one-dimensional analytical method for parametric analysis of thermo-hydraulic performance of Earth-Air heat exchanger. They considered design parameters like tube length, tube diameter, and number of parallel tubes. The purpose of this model is to evaluate the balance between pressure drop and heat transfer by developing an ε -NTU correlation for the earth tube heat exchanger. A 'specific pressure drop' term was used to allow a designer to then calculate required lengths of parallel tubes. The specific pressure drop J can be defined as a measure for the pressure drop necessary to realize one unit of NTU.

$$J = \frac{\Delta P}{NTU} \quad (2)$$

De Paepe suggested that multiple smaller diameter tubes in parallel both would lower pressure drop and raise thermal performance. Al-Ajmi et al. [8] developed a theoretical model to predict the outlet air temperature and cooling potential of an EATHE in a hot and arid climate by. It was concluded that if EAHE system is used in conjunction with an air-conditioning system, the energy demands can be reduced. A transient, numerical model was presented by Mihalakakou et al. [9] that predicts the ground temperature at various depths. Kusuda et al. [10] have mathematically modelled the annual sub-surface soil temperature based on heat conduction theory applied to a semi-infinite homogenous solid. Predictions of soil temperature exhibit a sinusoidal pattern due to the annual temperature fluctuation above as shown in eq. 3.

$$T_{z,t} = T_m - A_s * \exp \left[\frac{z}{z_o} \right] * \cos \left(\omega(t - t_o) - \frac{z}{z_o} \right) \quad (3)$$

Liu [11] had established an experimental setup of EAHE in Changsha, a hot summer and cold winter area of China. The effect of different variables, including inlet air temperature, pipe length, operation time on the performance and the influence of EAHE on underground soil temperature were analysed. Thermal saturation time of five days was observed, after which the system was disabled and allowed for self-recovery.

Yusof [12] presented the performance of EAHE based on experimental studies using a laboratory simulator. The simulator system has considered inlet temperatures of air from 31°C to 35°C, ground temperatures from 23°C to 25 °C and the air flow rate ranging from 0.03 to 0.07 kg/s. This concept of design for EAHE simulator in analysing the performance of EAHE has the advantages like no excavation cost involve in digging the soil, quick respond time in changing the variable and high repeatability of the experiment at constant variable.

Bansal et al. [13] developed a new concept of “derating factor” that could relate decline in thermal performance of EATHE under transient operating conditions with respect to steady state conditions in predominantly hot and dry climate of Ajmer, India. CFD-model with experimental results, in FLUENT software were validated. Derating Factor ($DF_{L,t}$) is defined as the ratio of the deterioration in thermal performance of EATHE under transient condition to the thermal performance under steady state condition.

$$DF_{L,t} = 1 - \frac{(T_i - T_o)_{L,t}}{(T_i - T_o)_{L,s}} \quad (4)$$

RohitMisra[14] investigated the thermal performance of EATHE system with dry and wet soil for the climatic conditions of Ajmer (India). A parametric study was carried out to examine the influence of soil moisture variation on the thermal performance of wet soil EATHE system. The thermal performance of EATHE was improved with wet soil during the experimentation as compared to dry soil.

Łukasz [15] validate the EAHE flow performance numerical model prepared by means of CFD software Ansys Fluent by using experimentally obtained flow characteristics of multi-pipe earth-to-air heat exchangers (EAHEs). CFD model of multi-pipe EAHE validated in this paper can be used for simulation of the flow performance of multi-pipe earth-to-air heat exchangers in the process of designing and optimization of the EAHE structures.

N. Rosa [16] numerically assessed the influence of three parameters on the overall thermal performance of an EAHE system for residential buildings in warm-summer Mediterranean climate: spacing between pipes, pipes diameter and air velocity. ANSYS-CFX® was used to simulate the EAHE transient behaviour during heating and cooling operation modes. A validated numerical model was used to perform a parametric study on the effect of three different pipe diameters operating with different air velocities, and the effect of three distances between adjacent pipes, operating with different air velocities and pipe diameters.

Thermal saturation and self-recovery ability of soil under continuous and intermittent operation modes was compared by A. Mathur et al. [17]. Campbell [18] measured thermal conductivity of nine soil minerals samples and studied variation in thermal conductivity caused by temperature, bulk density and soil moisture content. The thermal conductivities increased with increase in temperature, moisture content and bulk density and decrease in porosity. A laboratory experiment was conducted by P. Pramanik and P. Aggarwal[19] with three texturally different soils, compared the thermal properties as influenced by texture, compaction and mineralogical composition of soils. As revealed from their study, thermal properties were highest for black soil followed by alluvial soil and lowest for red soil.

Review of literature shows the experimental and numerical models have proven the EAHE system to be reducing energy requirements for space cooling. Unlike HVAC design process, these reviewed literatures lack design procedure which will guide architectures for including an EAHE system in Building planning and installation of the same. The effect of increased temperature of soil, surrounding the pipes, on EAHE performance is not considered in design calculations which are crucial in determining number of working

hours and distance between adjacent pipes. Standard installation guidelines are needed for commercial success of EAHE systems which will help the contractors.

2. Problem Definition

For the present study, the Power Plant Engineering lab of floor area (9.8*6.6) 64.68m² and ceiling height 3m, generally occupied by 30 people in SVERI's College of Engineering (Polytechnic) at ground level is selected. The college is situated in Pandharpur city, Maharashtra, India where summer temperatures reach up to 43 °C and 16% relative humidity. The physical and thermal properties for different materials in this study are as illustrated in table 1[13, 19].

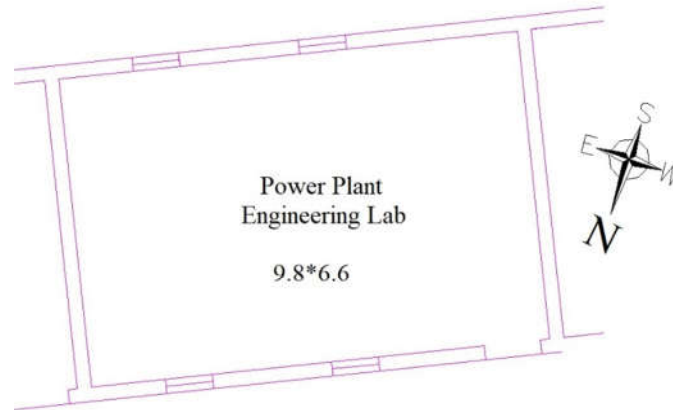


Figure 2: Classroom sketch under EAHE analysis

Table 1. Thermo-physical properties of materials

Material	Density (kg/m ³)	Specific heat capacity (J/kgK)	Thermal conductivity(W/mK)
Air	1.225	1006	0.024
Soil (SL3)	2050	1840	4
PVC	1380	900	1.16

2.1 Calculation of Parameters:

From ASHRAE climate data 2017 [23], for mean Temperature, $T_{\text{mean}} = 28^{\circ}\text{C}$ and design conditions (for 1% Peak condition) DBT = 40°C, MCWB = 22.8°C, a room condition of DBT = 30°C is selected.

A pipe of diameter 150mm and thickness 7mm (STD schedule of pipes for 6in) is selected for carrying air at velocity of 4 m/s. The other parameters such as heat transfer coefficient (h), length of pipe (L), etc. are calculated with NTU method for heat exchangers [7, 21].

2.2 Selection of Pitch (P):

The distance between centers of two adjacent pipes, as we've referred as Pitch (P), is taken 1 meter with reference to the EAHE model of R. Mishra [12].

2.3 Selection of depth:

Temperature variation with depth (z) underground is given by [10]

$$T_{z,t} = T_m - A_s * \exp\left[\frac{z}{z_o}\right] * \cos\left(\omega(t - t_o) - \frac{z}{z_o}\right) \quad (5)$$

Where:

- i. $T_m = T_{\text{mean}}$ = Mean surface temperature = 28°C (ASHRAE climate data [19])
- ii. A_s = Maximum Annual Amplitude of surface temperature = 8°C (Average temp in the month of May = 33.1°C [])
- iii. α_s = Thermal diffusivity of the ground (soil) = 0.203 m²/day
- iv. Day of min temperature, t_o = 10th Jan
- v. t = current time (day) in hours = 141 (21th March 2017)
- vi. Angular frequency, $\omega = \frac{2\pi}{365}$; Damping depth, $z_o = \sqrt{\frac{2\alpha_s}{\omega}}$

With given parameters, following table 3 illustrates temperature variation with depth for the selected date of the year in Pandharpur city.

Table 2. Temperature variation with depth

Depth (m)	Underground Temperature (°C)
1	30.3
2	28.7
3	27.6
4	26.8
5	26.3

As we have assumed $T_{\text{wall}} = T_{\text{mean}}$, a depth of 3 - 4meters can be selected.

2.4 Calculation for Length (L) based on NTU method [8][9]:

- i. Design conditions:

$T_{\text{air,out}}$ = Room DBT= 30°C; $T_{\text{air,in}}$ = Outdoor DBT= 40°C; $T_{\text{wall}} = T_{\text{mean}} = 28^\circ\text{C}$
 $D = 150 \text{ mm}$, $v = 4 \text{ m/s}$

Here, the kinematic viscosity of air (ν) is calculated [8] using Eq. (8):

$$\nu = 10^{-4}(0.1335 + 0.000925T_a) \quad (6)$$

Here, $\nu = 1.7\text{e-}5 \text{ m}^2/\text{s}$

- ii. Reynolds's no.,

$$Re = \frac{VD}{\nu_{\text{air}}} \quad (7)$$

$$= 35294.11$$

Friction factor,

$$f = (1.82 \cdot \log Re - 1.64)^{-2} \quad (8)$$

$$= 0.0227$$

- iii. Nusselt number

$$Nu = \frac{\frac{f}{8}(Re - 1000) \cdot Pr}{1 + 12.7 \cdot \sqrt{\frac{f}{8}} \cdot (Pr^{\frac{2}{3}} - 1)} \quad (9)$$

$$= 69.60 \quad \text{for } Pr = 0.71$$

- iv. Heat transfer coefficient (h):

$$Nu = \frac{hD}{k_{air}} \quad (10)$$

$$\rightarrow h = 11.13 \text{ W/m}^2\text{K}$$

- v. NTU calculation:

$$\varepsilon = 1 - e^{(-NTU)} = \frac{T_{air,out} - T_{air,in}}{T_{wall} - T_{air,in}} \quad (11)$$

$$= 0.833$$

$$\text{Therefore, } NTU = 1.79$$

- vi. Calculation for overall heat transfer coefficient (U):

Radius of soil domain (r_2) is assumed as twice of radius of pipe [8] and pipe thickness is neglected.

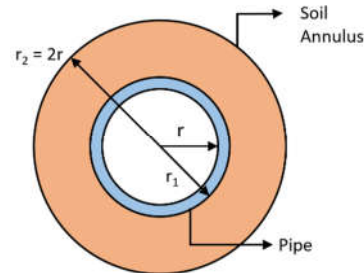


Figure 3: Earth-air heat exchanger (EAHE) system with the layers is shown in cross-section.

$$\text{Thermal resistance, } R_{th} = \frac{1}{h} + \frac{r \ln\left(\frac{r_1}{r}\right)}{k_{pipe}} + \frac{r_1 \ln\left(\frac{r_2}{r_1}\right)}{k_{soil}} \quad (12)$$

$$= 0.1053$$

$$U = \frac{1}{R_{th}} = 9.49 \text{ W/m}^2\text{K}$$

- vii. Calculation of Length

$$NTU = \frac{U \cdot A_s}{\dot{m}_{air} \cdot c_{p,air}}; \quad (13)$$

$$\text{Surface area, } A_s = \pi D L \quad (14)$$

$$\text{Mass flow rate, } \dot{m}_{air} = \rho_{air} \cdot A \cdot V \quad (15)$$

$$\text{Therefore } L = 34.86 \sim 35 \text{ m}$$

2.5 Pressure drop (Δp)

The pressure difference and the power required to pump the air through the earth air heat exchanger is given by [20]

$$\Delta p = f \cdot \left(\frac{\dot{m}_{air}}{\rho_{air}}\right) \cdot \left(\frac{L}{D}\right)^3 \quad (16)$$

$$= 20383.96 \text{ Pa}$$

This pressure drop often increases due to contamination of dust and other particles, pipe bends, fittings, blower outlet, filters, supply diffuser outlet, etc.

Considering all these losses as 15% of Δp , Total $\Delta p_{\text{tot}} \sim 23441.5 \text{ Pa}$

2.6 Air Fan Power (AFV)

The fan energy consumed in blowing air through a pipe is additional energy expenditure in the EAHE system. The fan air power is given by [20]

$$P_f = \frac{\Delta p_{\text{tot}} \cdot q}{\eta_{\text{fan}}} \quad (17)$$

Where Δp_{tot} is the fan total pressure difference, q is volumetric flow rate and η_{fan} is fan total efficiency which may be expressed as the ratio of total air power to the shaft power input.

Assuming 85% fan efficiency (η_{fan}), $P_f = 1949.39 \text{ W} \approx 2 \text{ kW}$

This power will be consumed to overcome pressure losses. Hence Fresh air blower for introducing fresh air into EAHE system is selected for flow rate of 148 CFM and power of 2kW. A Variable Frequency Drive (VFD) can be installed along with blower for controlling air flow according to requirement.

2.8 Trench sizing:

For a given length of pipes and pitch value and with allowance for installation, a trench of (6x6)m size and 4m deep underground should be made nearer to the lab for ease of installation.

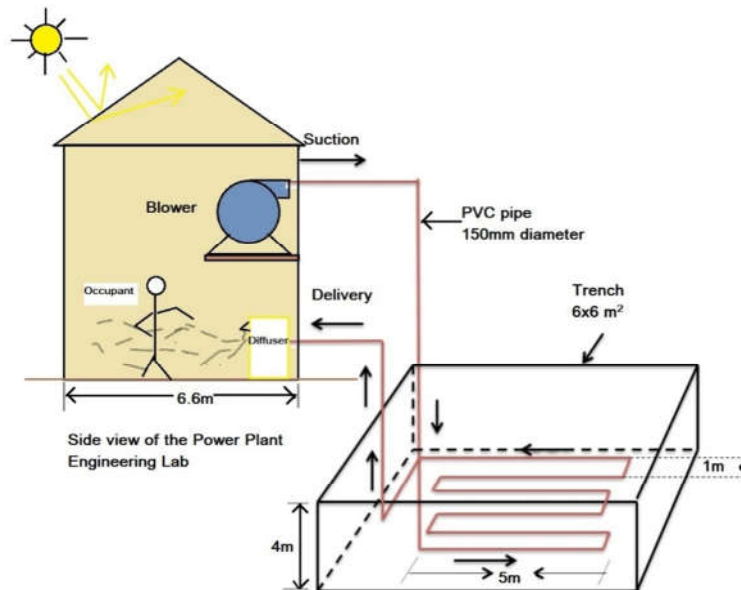


Figure 4: Planned schematic of EAHE system for the lab

3. Conclusion

In this paper the authors have reported the design parameters and the calculations useful for design of EAHE systems. These calculations are applied to hot and dry climate of Pandharpur city. With assessment of ASHRAE weather data and NTU method of heat exchangers, we were successful in designing the system of PVC pipe of 100 mm diameter of 35 m length placed in serpentine manner and air blown at 4m/s. The same system can work in winter conditions space heating, when the T_{mean} will be greater than $T_{\text{air,in}}$. Such

EAHE systems will provide alternative to commercial HVAC systems and make most of natural resources for space cooling.

References:

- [1] Digvijay Ronge and R Maurya, "Experimental and numerical investigation of soil under different constant heat flux conditions," *ICTF Phuket (Thailand)*, no. ISBN No. 978-605-9546-05-8, pp. 75–83, 2017.
- [2] Divyesh Prafulla Ubale, "Heat Transfer Enhancement in Heat Exchanger using Twisted Tape Inserts: A Review", *International Journal on Recent and Innovation Trends in Computing and Communication*, Vol. 5, No. 6, June 2017, pp. 425-428.
- [3] Divyesh Ubale, P.V Ubale, "Heat Transfer and Numerical Analysis in Microchannel Heat Exchanger Using Nanofluids : A Review", *International Journal of Scientific Research in Science, Engineering and Technology(IJSRSET)*, Print ISSN : 2395-1990, Online ISSN : 2394-4099, Vol. 4, No. 9, pp.198-203, July-August-2018.
- [4] T. S. Bisoniya, A. Kumar, and P. Baredar, "Study on Calculation Models of Earth-Air Heat Exchanger Systems," *J. Energy*, vol. 2014, pp. 1–15, 2014, doi: 10.1155/2014/859286.
- [5] N. Bordoloi, A. Sharma, H. Nautiyal, and V. Goel, "An intense review on the latest advancements of Earth Air Heat Exchangers," *Renew. Sustain. Energy Rev.*, vol. 89, no. March, pp. 261–280, 2018, doi: 10.1016/j.rser.2018.03.056.
- [6] Carslaw H. S. and Jaeger J. C. *Conduction of Heat in Solids*. Oxford Univ. Press, Oxford (1959).
- [7] M. De Paepe and A. Janssens, "Thermo-hydraulic design of earth-air heat exchangers," *Energy Build.*, vol. 35, no. 4, pp. 389–397, 2003, doi: 10.1016/s0378-7788(02)00113-5.
- [8] F. Al-Ajmi, D. L. Loveday, and V. I. Hanby, "The cooling potential of earth-air heat exchangers for domestic buildings in a desert climate," *Build. Environ.*, vol. 41, no. 3, pp. 235–244, 2006, doi: 10.1016/j.buildenv.2005.01.027.
- [9] G. Mihalakakou, M. Santamouris, D. Asimakopoulos, and A. Argiriou, "On the ground temperature below buildings," *Sol. Energy*, vol. 55, no. 5, pp. 355–362, 1995, doi: 10.1016/0038-092X(95)00060-5.
- [10] Kusuda T., Piet O. and Bean J. W. "Annual variation of temperature field and heat transfer under heated ground surface: slab-on-grade floor heat loss calculations", *National Bureau of Standards, Building Science Series*, p. 156 (1983).
- [11] J. Liu, Z. Yu, Z. Liu, D. Qin, J. Zhou, and G. Zhang, "Performance Analysis of Earth-air Heat Exchangers in Hot Summer and Cold Winter Areas," *Procedia Eng.*, vol. 205, pp. 1672–1677, 2017, doi: 10.1016/j.proeng.2017.10.342.
- [12] T. M. Yusof, H. Ibrahim, W. H. Azmi, and M. R. M. Rejab, "Thermal analysis of earth-to-air heat exchanger using laboratory simulator," *Appl. Therm. Eng.*, vol. 134, pp. 130–140, 2018, doi: 10.1016/j.applthermaleng.2018.01.124.
- [13] R. Misra, V. Bansal, G. Das Agrawal, J. Mathur, and T. K. Aseri, "CFD analysis based parametric study of derating factor for Earth Air Tunnel Heat Exchanger," *Appl. Energy*, vol. 103, pp. 266–277, 2013, doi: 10.1016/j.apenergy.2012.09.041.
- [14] R. Misra et al., "Energy & Buildings Field investigations to determine the thermal performance of earth air tunnel heat exchanger with dry and wet soil : Energy and exergetic analysis," *Energy Build.*, vol. 171, pp. 107–115, 2018, doi: 10.1016/j.enbuild.2018.04.026.
- [15] Ł. Amanowicz and J. Wojtkowiak, "Validation of CFD model for simulation of multi-pipe earth-to-air heat exchangers (EAHEs) flow performance," *Therm. Sci. Eng. Prog.*, vol. 5, no. October 2017, pp. 44–49, 2018, doi: 10.1016/j.tsep.2017.10.018.
- [16] N. Rosa, N. Soares, J. J. Costa, P. Santos, and H. Gervásio, "Assessment of an earth-air heat exchanger (EAHE) system for residential buildings in warm-summer Mediterranean climate," *Sustain. Energy Technol. Assessments*, vol. 38, no. January, p. 100649, 2020, doi: 10.1016/j.seta.2020.100649.
- [17] A. Mathur, A. K. Surana, P. Verma, S. Mathur, G. D. Agrawal, and J. Mathur, "Investigation of soil thermal saturation and recovery under intermittent and continuous operation of EATHE," *Energy*

- Build.*, vol. 109, pp. 291–303, 2015
- [18] G. S. Campbell, J. D. Jungbauer Jr, W. R. Bidlake, and R. D. Hungerford, “Predicting the effect of temperature on soil thermal conductivity,” *Soil Science*, vol. 158, no. 5, pp. 307–313, 1994, doi:
- [19] P. Pramanik and P. Aggarwal, “Comparison of thermal properties of three texturally different soils under two compaction levels,” *African J. Agric. Res.*, vol. 8, no. 28, pp. 3679–3687, 2013. [8] G. N. Tiwari et al., “Design of an earth air heat exchanger (EAHE) for climatic condition of Chennai, India,” *Open Environ. Sci.*, vol. 8, no. 1, pp. 24–34, 2014.
- [20] G. N. Tiwari et al., “Design of an earth air heat exchanger (EAHE) for climatic condition of Chennai, India,” *Open Environ. Sci.*, vol. 8, no. 1, pp. 24–34, 2014.
- [21] D. Ronge and D. Ubale, “Design of an Earth-Air Heat Exchanger System for Space Cooling in Climatic Conditions of Nagpur, India,” *Techno-Societal 2018*, pp. 479–488, 2020, doi: 10.1007/978-3-030-16848-3_44.
- [22] ASHRAE standard 62.2-2013 ‘Ventilation for Acceptable IOQ’
- [23] ASHRAE climatic design conditions 2009/2013 (<http://ashrae-meteo.info/>)

Study of Etchant Concentration Effect on the Edge Deviation for Photochemical Machining of Copper

Rushikesh M.Bhagwat¹, Suraj S.Gaikwad¹, Shivam S.Shete¹, Nikhil V.Chavan¹ and Sandeep S.Wangikar²

¹UG Students, Department of Mechanical Engineering, SVERI's College of Engineering, Pandharpur, M.S., India

²Associate Professor, Department of Mechanical Engineering, SVERI's College of Engineering, Pandharpur, M.S., India

rushikeshmbhagwat@coep.sveri.ac.in, surajsgaikwad@coep.sveri.ac.in, shivamsshete@coep.sveri.ac.in, nikhilvchavan@coep.sveri.ac.in, sswangikar@coe.sveri.ac.in

Abstract—Photochemical machining is one of the least explored non-conventional machining processes. Various components fabricated by photochemical machining having application in different fields like medical, electronics, biological, microelectronics, etc. Copper is a material which has various applications like heat sinks, microchannel molds for lithography, electronics, decorative items, etc. Edge deviation is one of the governing factors for predicting the accuracy of machining for any product. In this paper the parametric effect of etchant concentration on the edge deviation for photochemical machining is reported. The etchant concentration is varied as 300 g/L, 400 g/L, 500 g/L, 600 g/L, and 700 g/L and other parameters like temperature and etching time of ferric chloride etchant are kept constant. The edge deviation analysis was carried out with RAPID I Vision 5 microscope. It is observed that the edge deviation is increasing with increase in etchant concentration and noted maximum at concentration of 700 g/L.

Index Terms—Photochemical machining, etchant concentration, edge deviation, copper, parametric effect.

I. INTRODUCTION

The one of the widely used non-conventional machining process is the Photochemical machining (PCM) which is also called as photo etching or photochemical milling or photo fabrication. PCM employs chemical milling process for fabricating the components of sheet metals using a photoresist and etchants (solvents) to machine away selected areas corrosively [1].

The Process:

The photochemical machining process is briefed below [3-6]:

1. The procedure begins by printing the state of the part onto optically clear and dimensionally stable photographic film, known as photo tool. Simultaneously, cutting of the material into required size followed by cleaning of the material, is performed.
2. Then photoresist is plied to the metal or prepared specimen. Photoresist may be positive or negative.
3. Further, the specimen is exposed to source of UV (ultra violet) light.

4. After UV light exposure, the specimen is dipped in developer for specific time period. Developing will happen and the required area will be made open for etching in this stage.
5. Now, the specimen is subjected to etching where the material removal takes place through corrosion phenomenon. The etchants used are generally ferric chloride or cupric chloride.
6. Then, after achieving the required etching, the specimens are cleaned. The photoresist is stripped off from the specimens. Here, the required component is ready by using photochemical machining.

Related Work:

Various researchers have contributed in photochemical machining investigation for different materials and their parametric study. Ferric chloride (FeCl_3) is reported as the most widely used etchant for copper and its alloys in photochemical machining. The analysis for effect of control parameters on the performance parameters like material removal rate, undercut, surface roughness has been reported by researchers for the copper and its alloys like brass, german silver, etc. [3-6]. The photochemical machining study for the hard to cut materials like Inconel has been also reported [7-8]. The photochemical machining process has been applied for fabrication of components like microchannels, heat sinks, etc. [9-14]. In this paper, the analysis of photochemical machining for copper material is presented.

II. METHODOLOGY

Material:

Copper material has wide range of application in fabrication of micro components like micro heat exchangers, microchannels, molds for microchannels, etc. Therefore, Copper is selected as the material for analysis. The size of the copper specimen was 20mmx20mmx1mm thk.

Experimental Set-up:

The experimental set up for photochemical machining is presented in Figure 1. Ferric chloride was used as the etchant. The etching temperature was kept constant as 50 °C (+/- 0.5 °C). The etching time was also kept constant as 15 minutes. The photo tool was prepared by taking print out on a transparent paper. The size of the component to be etched was 6.8 mm by 6.8 mm.



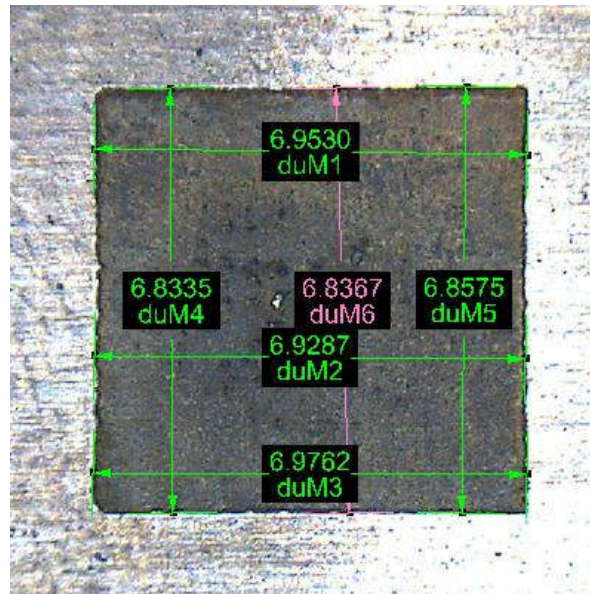
Figure 1: Experimental set up for PCM

The experimentation was carried out for analyzing the effect of concentration of etchant. The concentrations are varied from 300 g/L. to 700 g/L. with an interval of 100 g/L. The performance parameter was the edge deviation.

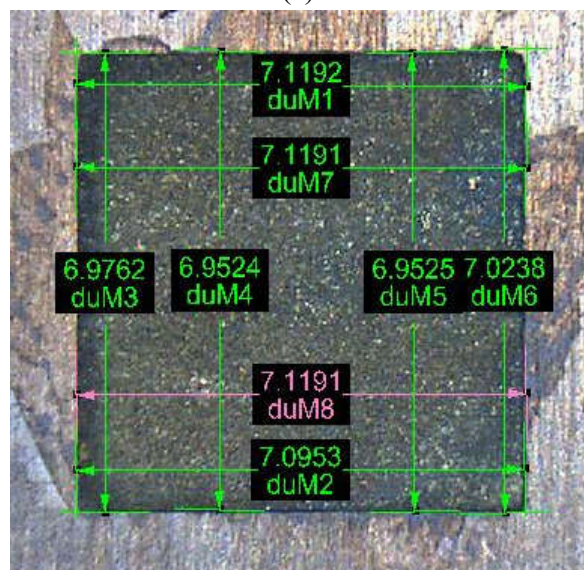
III. RESULTS AND DISCUSSION

The photochemical machining has been carried out on copper specimen at different concentrations of ferric chloride i.e. 300 g/L, 400 g/L, 500 g/L, 600 g/L, and 700 g/L. The dimensional analysis has been performed using RAPID I Vision 5 microscope. The specimen images for concentration 500 g/L and 700 g/L are depicted in Figure 2 (a) and (b), respectively. It is observed from the images that there is increase in dimensions (size of the specimen) and it is increasing with increase in concentration of the etchant. This is due to the formation of undercut during photochemical machining.

The deviation of edge from the required is one of the significant factors for the fabrication of micro components. Therefore, edge deviation always desired to be minimum. The analysis for the edge deviation has also been performed by using the RAPID I Vision 5 microscope. The sample images for the edges (one edge) at different concentrations as 300 g/L, 400 g/L, 500 g/L, 600 g/L, and 700 g/L are presented in Figures 3 (a), (b), (c), (d), and (e), respectively. The average edge deviation is observed to be minimum at concentration level 300 g/L. The edge is noted to be increasing with increase in concentration and found to be maximum at concentration 700g/L. This may be due to lesser attack of molecules on the edges of specimen at lesser concentration. As the concentration increases, the molecules present in the etchant increases. The greater number of molecules will attack on the edge for the fixed temperature and time. The material will be removed abruptly through diffusion at the edges and in turn, the edge deviation increases with increase in concentration.

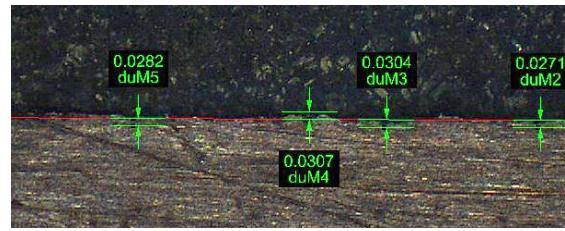


(a)

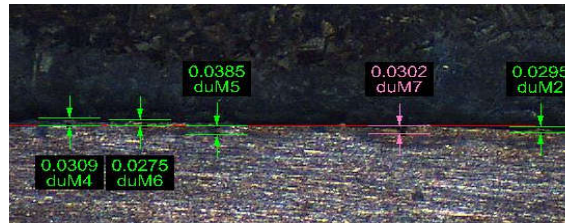


(b)

Figure 2: Dimensions of photochemically machined components at different concentrations (a) 500 g/L.(b) 700 g/L.



(a)



(b)



(c)



(d)



(e)

Figure 2: Edge deviation for photochemically machined components at different concentrations (a) 300 g/L, (b) 400 g/L, (c) 500 g/L., (d) 600 g/L., (e) 700 g/L.

IV. CONCLUSIONS

The photochemical machining study for analysis of edge deviation for copper material performed. Ferric chloride is used as the etchant and effect of concentration on the edge

deviation has been analyzed by keeping the other factors like temperature and etching time as constant. It is found that the dimensions of the photochemically machined component are greater than the desired dimensions of photo tool. The edge deviation is observed to be minimum for concentration of 300 g/L and increases with increase in concentration up to 700 g/L and noted maximum at concentration of 700 g/L.

REFERENCES

- [1]. Allen DM (2004) Photochemical machining: from ‘manufacturing’s best kept secret’ to a \$6 billion per annum, rapid manufacture process. CIRP Ann—Manuf Technol 53(2):559–572. Doi : 10. 1016/S0007-8506(07)60029-8
- [2]. Yadav, R. P., &Teli, S. N. (2014). A Review of issues in photochemical machining. International Journal of Modern Engineering Research, 4(7), 49–53.
- [3]. Wangikar, S. S., Patowari, P. K., & Misra, R. D. (2017). Effect of process parameters and optimization for photochemical machining of brass and german silver. Materials and Manufacturing Processes, 32(15), 1747-1755.
- [4]. Wangikar, S. S., Patowari, P. K., & Misra, R. D. (2016, December). Parametric Optimization for Photochemical Machining of Copper Using Grey Relational Method. In Techno-Societal 2016, International Conference on Advanced Technologies for Societal Applications (pp. 933-943). Springer.
- [5]. Wangikar, S.S., Patowari, P.K., & Misra, R.D. (2018). Parametric Optimization for Photochemical Machining of Copper using Overall Evaluation Criteria. Materials Today Proceedings. 5(2), 4736-4742, Doi :10.1016/j.matpr.2017.12.046
- [6]. Wangikar, S. S., Patowari, P. K., Misra, R. D., &Misal, N. D. (2019). Photochemical Machining: A Less Explored Non-Conventional Machining Process. In Non-Conventional Machining in Modern Manufacturing Systems (pp. 188-201). IGI Global.
- [7]. Misal, N. D., &Sadaiah, M. (2017). Investigation on Surface Roughness of Inconel 718 in Photochemical Machining. Advances in Materials Science and Engineering, 2017.
- [8]. Misal, N. D., Saraf, A. R., &Sadaiah, M. (2017). Experimental investigation of surface topography in photochemical machining of Inconel 718. Materials and Manufacturing Processes, 32(15), 1756-1763.
- [9]. Wangikar, S. S., Patowari, P. K., & Misra, R. D. (2018). Numerical and experimental investigations on the performance of a serpentine microchannel with semicircular obstacles. Microsystem Technologies. 24(8), 3307-3320.
- [10]. Das, S. S., Tilekar, S. D., Wangikar, S. S., & Patowari, P. K. (2017). Numerical and experimental study of passive fluids mixing in micro-channels of different configurations. Microsystem Technologies, 23(12), 5977-5988.
- [11]. Chavan, N. V., Bhagwat, R. M., Gaikwad, S. S., Shete, S. S., Kashid, D. T., & Wangikar, S. S. (2019). Fabrication & Characterization of Microfeatures on PMMA Using CO2 Laser Machining. International Journal for Trends in Engineering and Technology. 36(1), 39-32.

- [12]. Kulkarni, H. D., Rasal, A. B., Bidkar, O. H., Mali, V. H., Atkale, S. A., Wangikar, S. S., & Shinde, A. B. (2019). Fabrication of Micro-Textures on Conical Shape Hydrodynamic Journal Bearing. *International Journal for Trends in Engineering and Technology*. 36(1), 37-41.
- [13]. Raut, M. A., Kale, S. S., Pangavkar, P. V., Shinde, S. J., Wangikar, S. S., Jadhav, S. V., & Kashid, D. T. (2019) Fabrication of Micro Channel Heat Sink by using Photo Chemical Machining. *International Journal of New Technology and Research*. 5(4), 72-75.
- [14]. Patil P. K., Kulkarni A. M., Bansode A. A., Patil M. K., Mulani A. A., Wangikar S. S. (2020) Fabrication of Logos on Copper Material Employing Photochemical Machining. *NOVYI MIR Research Journal*, 5(6), 70-73.

Number of students filed/published Patents

A.Y. – 2019-20

Sr. No.	Title of Patent	Name of Applicant/Inventors	Status
1.	A Low cost Semi-Automatic Metallurgical specimen Grinding and Polishing Machine to Develop specimen for Microscopic Analysis	Akash Rakate, Indrajit Wadgave, Sachin Ingale, Nitin Tele, Pranav Ippanpalli	Filed

**Application Filing Receipt****Government of India
Patent Office**

Intellectual Property Office Building,
S.M. Road, Antop Hill,
Mumbai-400037

Phone- 022-24137701,24142026

Fax: 022-24130387

e-mail: mumbai-patent@nic.in

CBR Number : 1920

CBR date: 24-01-2020

Application Type: ORDINARY APPLICATION

Priority Number:

Priority Date:

Priority Country: Not Selected

To,

Sachin Mahadev Khomane

SVERI's College of Engineering, Pandharpur P.B. No. 54, Gopalpur -Ranjani Road, Gopalpur Rd, Pandharpur, Solapur 413304

Received documents purporting to be an application for patent numbered 202021003381 dated 24-01-2020 by Sachin Mahadev Khomane of SVERI's College of Engineering, Pandharpur P.B. No. 54, Gopalpur -Ranjani Road, Gopalpur Rd, Pandharpur, Solapur relating to A LOW-COST SEMI-AUTOMATIC METALLURGICAL SPECIMEN GRINDING AND POLISHING MACHINE TO DEVELOP SPECIMEN FOR MICROSCOPIC ANALYSIS together with the Provisional and fee(s) of ₹1600 (One Thousand Six Hundred only).

Note:

1. In case of Patent Application accompanied by a Provisional Specification, a complete Specification should be filed within 12 months from the date of filing of the Provisional Specification, failing which the application will be deemed to be abandoned under Section 9(1) of the Patent Act, 1970.
2. You may withdraw the application at any time before the grant of patent, if you wish so. If, in addition to withdrawal, you also wish to prevent the publication of application in the Patent Office Journal, the application should be withdrawn within fifteen months from the date of priority of date of filing, whichever is earlier.
3. If not withdrawn, your application will be published in the Patent Office Journal after eighteen months from the date of priority of date of filing, whichever is earlier.
4. If you wish to get your application examined, you should file a request for examination in Form-18 within 48 months from the date of priority or date of filing, whichever is earlier, failing which the application will be treated as withdrawn by the applicant under Section 11(B)(4) of the Patent Act, 1970.

(For Controller of Patents)

Number of students participated in Project Exhibition

A.Y. – 2019-20

Sr. No.	Name of Students	Name of Project Exhibition	Name of Award
1.	Gund Omkar S., Kakade Shubham M., Ghuge Hrushikesh R.	DIPEX-2020 (State Level Project Exhibition cum Competition of Working Mdels)	Best Degree Project
2.	Gund Omkar S., Kakade Shubham M., Ghuge Hrushikesh R.	TECHNO-THON 2k20 (A National Level Socio-Technofest on Hi-Tech Farming)	3 rd rank in Agrofest event



सम्मानपत्र

श्री. विठ्ठल एज्युकेशन ग्रुन्ड रिसर्च महाविद्यालय के
श्री./शु. भोकार शाहाजी भुंड ने दि. ६ से ९ मार्च २०२०,
सोलापूर में आयोजित राज्यस्तरीय अभियांत्रिकी चलप्रतिकृति प्रतियोगिता एवं प्रदर्शन

डिपेक्स २०२०

के A2 (मेकॅनिकल) विभाग में मोनियन कोरिंग
मशीन चलप्रतिकृति को 'सर्वोत्तम'
तंत्रनिकेतन/ अभियांत्रिकी प्रकल्प पुरस्कार से सम्मानित किया जाता है। अतैव यह
सम्मानपत्र आपको प्रदान किया जाता है।

आपका वर्धमान कर्तृत्व भारतमाता के चरणों में समर्पित हो।

डॉ. अंकार राय
हायवेक्टर जपान,
एच.टी.सी. आय.

श्री. सारंग जोशी
ग्रैंड अथल,
अनांचि महागण्ट

श्री. राम मोगले
अथल,
गुजरा

श्री. अशिलेश भारतीय
विभाग,
डिपेक्स २०२०



सम्मानपत्र

श्री विठ्ठल एज्युकेशन अँड रिसर्च महाविद्यालय के
श्री./कु. ऋषिकेश रविंद्र चुगे ने दि. ६ से ९ मार्च २०२०,
सोलापूर में आयोजित राज्यस्तरीय अभियांत्रिकी चलप्रतिकृति प्रतियोगिता एवं प्रदर्शन

डिपेक्स २०२०

के ए-२ (मेकॅनिकल) विभाग में ओनिशन बोरींग
मशीन चलप्रतिकृति को 'सर्वोत्तम'
संयोजक/ अभियांत्रिकी प्रकल्प पुरस्कार से सम्मानित किया जाता है। अतैव यह
सम्मानपत्र आपको प्रदान किया जाता है।

आपका वर्धमान कर्तृत्व भारतमाता के चरणों में समर्पित हो।

डॉ. आँकार राय
हायरैक्टर जनरल,
एन.टी.पी. आय.

प्रा. सारंग जोशी
प्रदेश अध्यक्ष,
अभ्यास महाराष्ट्र

श्री. राम मोगले
अध्यक्ष,
शुनर

श्री. अश्विनेश भारतीय
निर्देशक,
डिपेक्स २०२०



सम्मानपत्र

श्री. विठ्ठल एज्युकेशन अँड रिसर्च इन्स्टिट्यूट महाविद्यालय के
श्री./शु. शुभम मधुकर काकडे ने दि. ६ से ९ मार्च २०२०,
सोलापूर में आयोजित राज्यस्तरीय अभियांत्रिकी चलप्रतिकृति प्रतियोगिता एवं प्रदर्शन

डिपेक्स २०२०

के ए-२ (मेकैनिकल) विभाग में ओनियन बोरिंग
मशीन चलप्रतिकृति को 'सर्वोत्तम'
तंत्रनिकेतन / अभियांत्रिकी प्रकल्प पुरस्कार से सम्मानित किया जाता है। अतैव यह
सम्मानपत्र आपको प्रदान किया जाता है।

आपका वर्धमान कर्तृत्व भारतमाता के चरणों में समर्पित हो।

डॉ. आंकार राय
डायरेक्टर जनरल,
एम.टी.पी.आय.

प्रा. सारंग जोशी
प्रदेश अध्यक्ष,
अभ्यास महासंघ

श्री. राम भोगले
अध्यक्ष,
गुवन

श्री. अश्विनी भारती
निर्माता,
डिपेक्स २०२०



Best Degree Project

REDMI NOTE 5 PRO
MI DUAL CAMERA

2020/3/9 20:21



JSPM & TSSM Group of Institute

**PADMASHOOSHAN VASANTDADA PATIL
INSTITUTE OF TECHNOLOGY, BAYDHAN**

Pune-21 | NAAC 'A' Graded Institute | pvpitssm.edu.in



TECHNOTHON

2K20

A National Level
Socio-Technofest on
"Hi-Tech Farming"

Taking India to Next Decade

Certificate

This is to certify that Mr. / Ms. Omkar. S. Gund has

~~Coordinated~~ / ~~Participated~~ / ~~Secured~~ First / ~~Second~~ / Third Position in the event AGRO FEST

of TECHNOTHON 2K20 - A National Level Socio-Technofest

Organized by TSSM's PVPIT, Baydhan, Pune during 29th and 30th January, 2020.

Dr. B. K. Sarkar / Dr. R. R. Sorate
Co-Convenor

Dr. C. M. Sedani
Principal

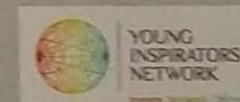
Prof. S. R. Thite
Director, PVPIT Pune

Mr. G. T. Sawant
Secretary, TSSM, Pune

Our Sponsors



Youth Forum Partner





JSPM & TSSM Group of Institute

**PADMABHOOSHAN VASANTDADA PATIL
INSTITUTE OF TECHNOLOGY, BAVDHAN**

Pune - 21 | NAAC 'A' Graded Institute | pvpittssm.edu.in



TECHNOTHON

2K20

**A National Level
Socio-Technofest on
"Hi-Tech Farming"**

Taking India to Next Decade

Certificate

This is to certify that Mr. / Ms. Hrushikesh R. Ghuge has

~~Coordinated~~ / ~~Participated~~ / ~~Secured~~ ~~First~~ / ~~Second~~ / Third Position in the event AGROFEST

_____ of TECHNOTHON 2K20 - A National Level Socio-Technofest

Organized by TSSM's PVPIT, Bavdhan, Pune during 29th and 30th January, 2020

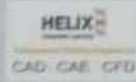
Dr. B. K. Sarkar / Dr. R. R. Sorate
Co-Convener

Dr. C. M. Sedani
Principal

Prof. S. R. Thite
Director, PVPIT Pune

Mr. G. T. Sawant
Secretary, TSSM, Pune

Our Sponsors



Youth Forum Partner



**YOUNG
INSPIRATORS
NETWORK**



JSPM & TSSM Group of Institute

PADMABHOOSHAN VASANTDADA PATIL INSTITUTE OF TECHNOLOGY, BAVDHAN

Pune - 21 | NAAC 'A' Graded Institute | pvpittssm.edu.in



TECHNOTHON

A National Level
Socio-Technofest on
"Agro Tech Farming"

Taking India Forward

Certificate

This is to certify that Mr. / Ms. Shubham . M. Karkade

~~Coordinated~~ / ~~Participated~~ / ~~Secure~~ - First / ~~Second~~ / Third Position in the event AGROFEST

_____ of TECHNOTHON 2K20 - A National Level Socio-Technofest

Organized by TSSM's PVPIT, Bavdhan, Pune during 29th and 30th January, 2020.

B.K. Sarkar

Dr. B. K. Sarkar / Dr. R. R. Sorate
Co-Convenor

R.R. Sorate

M. Sedani

Dr. C. M. Sedani
Principal

S. R. Thite

Prof. S. R. Thite
Director, PVPIT Pune

G. T. Sawant

Mr. G. T. Sawant
Secretary, TSSM, Pune

Our Sponsors



Youth Forum Partner

